Ketil Svinning

Design and manufacture of Portland cement Application of statistical analysis

Thesis for the degree of Dr.philos

Trondheim, September 2011

Norwegian University of Science and Technology
Faculty of Natural Sciences and Technology

NTNU – Trondheim
Norwegian University of
Science and Technology

NTNU
Norwegian University of Science and Technology

Thesis for the degree of Doctor Philosophiae

Faculty of Natural Sciences and Technology

Norcem AS, HeidelbergCement
Setrevegen 2
3950 Brevik

ISBN 978-82-471-2944-9 (printed ver.)
ISBN 978-82-471-2945-6 (electronic ver.)
ISSN 1503-8181

Doctoral theses at NTNU, 2011:196

Printed by NTNU-trykk

Table of contents

Preface

This thesis is submitted to the Faculty of Natural Sciences and Technology , Norwegian University of Science and Technology, Norway, for the degree of Doctor philosophiae. My employer Norcem AS, HeidelbergCement has supported my work and let my activities be an integrated part of the research and development of the company. The thesis consists of nine papers presenting an investigation on the influences of cement characteristics and production conditions on the cement properties using multivariate data analysis, sensitivity analysis and optimization. The papers were published in the period 2000-2010.

Realizing that production and performance of cement are complex matters, I became interested in applying statistical methods and tools for the examination of correlation and influence mentioned above. In 1988, I was introduced to various types of multivariate data analysis, like principal component analysis, principal component regression and partial least square regression. Multivariate data analysis is much used in predicting component composition and material characteristics in process mass flows and in chemical processes from spectral data from different types of spectroscopy measurements. Combined with experimental design as factorial design the multivariate data analysis was applied in the design of the optimization of material properties and chemical processes.

A great challenge in the manufacture is controlling the processes where adjustments of some the process variables influence the variation in others. Therefore, developing a program for model-based optimisation of the response variable constrained by latent variables was started. From my experience with development and application of a program for raw meal composition control optimizing the cost of the raw meal, the idea of model based optimizing based on linear programming was formed.

In the course of the investigations and the development of program and in the research, communication with other cement manufacturers and research institutions has been important. Some of the communications has been in the form of publications presented at conferences. 10 years ago I became aware that publications to be included in theses should preferably be published in peer review magazines. Focusing and questioning the originality of the publications contributed to this thesis, they differ from those in the same fields by other authors by the application of partial least square regression analysis in the prediction of cement properties. They also differ by the inclusion of spectral variables from the characterization of the mineralogy and superficial microstructure in the investigations, and the application of sensitivity analysis to examine influences. The same publications differ from those of the same author published in conference proceedings and commercial magazines. The main differences are the use of model-based optimization in the examinations of influences and the application of multi-block methods and the thoroughness of the presentations.

Acknowledgements

I would like to thank people at Norcem AS, HeidelbergCement for their support and encouragement during this long period of work and studies. Especially, I want to thank Kjell Skjeggerud, technical director of Heidelberg Cement, North Europe, David Verdu, manager of the Brevik Plant, and Dr. Terje Rønning, manager R&D, Norcem AS. A very important co-worker in the investigations and co-author of some of the papers (unfortunately not included in the thesis) has been S. K. Bremseth. Her main contribution to the investigation has been microscopy examination of clinkers and a good knowledge of the influence of the burning conditions in the kiln on the clinker quality.

The very skillful and experienced programmers Øystein Ingerøyen, Norcem AS, and Kjell Dalsveen, an external consultant, participated in the development of the program for model-based optimization, OptPilot. They are co-authors of the paper introducing the method. In the further development Professor emeritus Agnar Høskuldsson at the Danish Technical University contributed with a modelling part to OptPilot. He is an interesting discussion partner and is the co-author of seven of the papers included in the thesis. His main contribution in our collaboration is introduction and application of multi-block methods in the cement technology. Besides, he has been encouraging me much to write a doctoral thesis. Professor Terje Hertzberg contributed a program code for simplex optimization to OptPilot.

Profesor Harald Justnes, NTNU, and I have been cooperating and participated in co-projects concerning cement reactivity. He is the co-author of two of my papers. He has encouraged me much to keep on with my research on the interaction between cement characteristics and properties. Professor Harald Martens, Norwegian University of Life sciences, Ås, and Professor emeritus Rolf Ergon, Telemark University College, have inspired me much in my study and application of the multivariate method. Dr. Donald H. Campbell and the rest of the people at the International Cement Microscopy Association (ICMA) arranging The International Conference on Cement Microscopy, have motivated me much in my study of the microstructure of clinker. Thorleif Nodeland has been working hard with improving my English.
Finally – but not least - I wish to thank my wife Eva Nodeland and my children Ingvild and Audun for their patience with me and their encouragement during my work.

I would like to thank everybody involved with my work in any way, for their support and enthusiasm.

Brevik, September 2010

Ketil Svinning

Abstracts

The purpose of the work is to enable design and manufacture of cement with emphasis on the quality and the properties of cement. Data used in the design and manufacture were collected from predictions of properties and characteristics of cement. The properties of cement were predicted from its characteristics and from the production conditions in cement kiln and mill. The cement characteristics were in some investigations predicted from the production conditions. The design was based on sensitivity analysis focusing the influence of the characteristics and production variables, **x,** on the properties, **y**. The influence was analyzed by predictions of **y** from the simulated variation in **x**. In cases there were correlation within observation matrix **X**, the simulations were constrained by the latent structure of **X**. The simulations were in the form of optimization of the function for prediction of **y**. The optimal solutions of the production variables were then implemented in the manufacture of cement.

The prediction models were evaluated by multivariate data analysis by using partial least square regression (PLS). PLS is a member of the bilinear class of methods. The method compresses the observation matrix **X** to its most relevant factors and using these compressed variables as regressors for **y**. In the thesis the compressed variables were sometimes called PLS-components and sometimes latent variables.

Two types of sensitivity analysis for the examination of influences of the *x*-variables on *y* were applied. The first is based on comparison of the size and certainty of the regression coefficient from PLS on scaled and weighted **x**. The second was based on predictions of *y* from simulated variation in **x**. The influence of a single *x*-variable or a latent variable was valued or ranged from the variation of predicted *y* relative to the confidence intervals of *y*. The development of a program for optimization was an important part of work presented in the thesis. The optimization was in the form of linear programming where the regression function of *y* was optimized but constrained by the latent variables and upper and lower limits of at least one of the *x*-variables.

The purpose was not to focus only on the methods but also to apply the methods on real data from production and characterization of cement for prediction of the quality and the properties of cement. Two investigations were performed on pure observations of **X** and **Y**. In the first investigation three PLS-models were evaluated for prediction of the three properties; amount of water required to achieve standard consistency, setting time and compressive strength at 1 day from production conditions in a cement mill. In the second investigation, a PLS-model was evaluated for predictions of compressive strength up to 28 days from characteristics of the cement. The observation **X** was made up by four sub-matrices representing three different types of characteristics, the first one representing the mineralogy of the clinker part of the cement, the second the particle size distribution and the third and fourth superficial microstructure of cement. The mineralogy characterized by X-ray diffraction (XRD) analysis could be related to the production conditions in the cement kiln. The particle size distribution and superficial microstructure, the latter characterized by thermogravimetric analysis, could be related to the production conditions in a cement mill.

From the observation **X** matrix an artificial observation matrix was made for predicting potential compressive strength of clinker from the mineralogy. The original variation in the mineralogy in the new artificial matrix was maintained, while the other variables were kept constant and equal to their mean values. The mineralogy was represented by XRD-curves, which are characterized as spectral data, in two selected 2 θ ranges. Further, the spectral data were optimized to min and max potential compressive strength. In addition, they were interpreted qualitatively with respect to the variation in the mineralogy. The spectral data from thermogravimetric analysis included in PLS, were the differential form of a mass loss curve recorded during the analysis.

In addition to examining the influence of submatrices or blocks to on the properties by sensitivity analysis, multi-block regression methods were applied. By application of multi-block methods, the part of the characteristics or the microstructure that influences the properties could be found directly from the regression analysis.

Finally, the production conditions in a cement mill and a cement kiln were optimized to achieve optimal cement properties. Amount of water required to achieve standard consistency and setting time were predicted from production conditions in a cement mill, and potential compressive strength of clinker up to 28 days were predicted from production conditions in a cement kiln. The production conditions were optimized to achieve min and max values of the properties. The microstructure or the characteristics were predicted from the optimal production conditions to explain the influence of the production conditions on the properties mechanistically and chemically.

The main contributions in the form of papers in this thesis are (the roman numerals refer to the list of papers at the end to this chapter):

1. Developing methods for model-based optimization based on PLS, sensitivity analysis, prediction and linear programming. A case of demonstration was optimizing compressive strength of cement from variation of particle size distribution of cement [I-III]
2. Modelling compressive strength up to 28 days of cement on the characteristics of cement, predicting and optimizing potential compressive strength from the mineralogy of clinker [IV-V]
3. Presenting the principles and application of multi-block methods in cement production [VI-VII]
4. Optimizing production conditions to achieve optimal cement properties [VIII-IX]

The use of multivariate data analysis, sensitivity analysis and model-based optimization is very useful in the design and manufacture of cement. The methods enabled tailoring of cement aiming at target values of properties like compressive strength, setting time and initial flow properties. The tailoring can be based on the variables representing the characteristics of cement as well as the variables representing the production conditions in the cement kiln and the cement mill. The max values of the compressive strength at 1 and 28 days were achieved by optimizing the production conditions in the kiln giving the

optimal mineralogy for achieving max strengths. Optimal values of cement properties at early ages were achieved by optimizing the production conditions in the cement mill giving the optimal superficial microstructure.

List of papers

I Svinning, K., Ingerøyen, Ø., Dalsveen, K., Optimization of a response variable *y* constrained by principal directions of variations in the observation **X**-matrix, *J. Chemometrics*, 14(2000) 699-709

II Svinning, K., "Design and manufacture of Portland cement – application of sensitivity analysis in exploration and optimization, Part I: Exploration", *Journal of Chemometrics and Intelligent Laboratory Systems* 84 (2006) 177-187

III Svinning, K., Høskuldsson, A. "Design and manufacture of Portland cement – application of sensitivity analysis in exploration and optimization, Part II: Optimization", *Journal of Chemometrics and Intelligent Laboratory Systems* 84 (2006) 188-194

IV Svinning K., Høskuldsson, A., Justnes, H., "Prediction of compressive strength up to 28 days from microstructure of Portland cement", *Cement and Concrete Composites* 30(2008) 138-151

V Svinning, K., Høskuldsson, A., Justnes, H., "Prediction of potential compressive strength of clinker" *Cement and Concrete composites* 32 (2010) 300-311

VI Höskuldsson A., K. Svinning: Modelling of multi-block data, *J. Chemometrics* 21 (2007) 1–10

VII Svinning, K., Høskuldsson, A., Application of multi-block methods in cement production, *J. Chemometrics* 22 (2008) 587-593

VIII Svinning, K., Høskuldsson, A., Optimization of production conditions in cement mill to achieve optimal cement properties at early ages, *Journal of ASTM International*, 7(2010)3 pp 18

IX Svinning, K., Høskuldsson, A., Prediction of potential compressive strength of Portland clinker from production conditions in cement kiln, *Journal of ASTM International*, 7(2010)3 pp 18

1. INTRODUCTION

1.1 Background

In the design and manufacture of cement, the knowledge of how the characteristics of the cement influence the cement properties, like setting and strength build-up during hydration is of great importance. Knowing how the production conditions influence the characteristics and the properties is equally important.

Cement is a material that binds together solid bodies by hardening from a plastic state. When mixed with water, cement forms a plastic paste that develops rigidity (sets), and then steadily increases in compressive strength (hardens) by chemical reaction with water (hydration). *Cement* will be used here as a synonym to Portland cement. *Concrete* is a composite material produced by using cement to bind fine and coarse material into a dense coherent mass. *Mortar* is a more plastic material using a fine sand and cement mix [1]. The characteristics of cement are defined in the thesis as the parameters representing the microstructure and the mineralogy of cement in dry or prehydrated conditions before mixing it with water. Due to the hydraulic character of cement, it easily prehydrates when exposed to moisture during production and storage. The properties are defined as parameters describing different types of behaviour during hydration. Important properties could be compressive strength, setting time, and initial flow behaviour.

In short, cement is made by heating a mixture of calcareous and argillaceous materials to a temperature of about 1450 °C. In the process, partial fusion occurs and nodules of so-called clinkers are formed. The cooled clinker is mixed with a few percent of gypsum, acting as a hydration modifier, and sometimes other additives, and is then ground to cement [2].

Design and development of cement are usually described in a quality assurance manual made by the manufacturer [3]. Cement design for product development should be initiated from:

1. Changes in wishes and needs from the customers and the market, new knowledge of the products
2. New process technology implemented
3. New raw materials and fuels introduced
4. Change in the product standards
5. Change in the body of laws

Changes in wishes and needs from the customers and market are closely related to the standard properties of cement like strength build-up and setting. Over the recent years there has been a rapid development in concrete technology. New production techniques require more proper specifications of the fresh concrete properties [4]. During production and manufacture of concrete it is important to control the concrete properties, for instance workability.

New knowledge about the products, i.e. cement, could be discovering new characteristics which influence the cement properties, and new ways of characterizing the mineralogy and superficial microstructure. New knowledge could also be obtained by applying new methods of correlating the properties with the characteristics [5, 6]. Methods for statistical modelling of correlation could be multiple multivariable linear regression (MLR) and multivariate data analysis like partial least square regression (PLS) [7]. Keeping control of the fresh concrete involves a need for characterization and documentation of workability [4]. How cement interacts with new fillers and additives like retarders, plasticizers and accelerators is important for design and product development. The realization of optimal engineering properties in concrete depends on the efficient use of the characteristics of cement [1].

The design of a cement kiln and the process for burning clinker may have a major impact on the mineralogy. The mineralogy is much influenced by the chemical composition in the raw feed, the temperature profile in the rotary kiln [8] and the efficiency of the cooler, which in turn influence the temperature profile in the kiln. An example of the introduction of new process technology is the modification of the grate cooler supported to the kiln by replacing reciprocating grates in the cooler inlet with a stationary stepped grate [9]. Two-chamber ball mills are much used in grinding clinker to cement. The energy demand is high, however. Less than 10 % of total grinding energy is used for comminution. Applying high-pressure grinding rolls, pre-grinding and finishing the cement grinding in a single chamber ball mill, reduces the energy consumption by 20-40 % compared with a standard ball mill system. In addition, the particle size distribution can be better designed and the cement performance can be improved [10].

In many plants coal used in the cement kiln burning is partly replaced by alternative fuels as refuse derived fuels, car tires and plastic [2, 11]. The alternative fuels may deviate from coal in heating value, shape and size and the amount of ash. Examination of the influence of the alternative fuels could therefore be a part of the design [12, 13]. Reduction of the emission of gaseous pollutants per unit clinker produced may be obtained through two methods; to increase the use of alternative fuels (completely or partly CO_2 neutral), or to increase the use of pozzolans in order to reduce the amount of clinker in cement [14].

The two last points on the list of initiating design and development of cement are more related to standards, safety policy and juridical regulation than to design and manufacture and will not be treated or referred to further in this thesis.

In the current quality control in the manufacture of cement at the Brevik Plant, Norway, the component composition of the raw materials and clinkers is determined by X-ray fluorescence analysis (XRFA). The mineral composition is estimated from the component composition by Bogue's calculation. During the grinding, the quality of cement is controlled by measurement of fineness, sieve residues, amount of tri-sulphur oxide and loss on ignition. Some of the cement samples from the cement mills are tested with respect to setting and strength, and component composition is analyzed. In all

samples of delivered cement, component composition, loss on ignition, the amounts of tri-sulphur oxide and free lime, and specific fineness are analyzed. The properties being tested in the same samples are compressive strength up to 28 days, amount of water required to achieve standard consistency and setting time.

To enable design and tailoring of cement aiming at target values of a wide range of properties, a more thorough characterization of the cement should be done. In addition to chemical component composition, information about the mineralogy of cement, analyzed by X-ray diffraction analysis (XRDA) could be very useful [1]. The particle size distribution will further explain the variation in properties at early ages compared to a simple measurement of specific surface by Blaine's method [II]. The degree of dehydration of gypsum can in some cases better explain the variation in the rheological properties than the amount of gypsum or tri-sulphate alone [15]. The amounts of di- and hemihydrate of gypsum could be determined by differential scanning calorimetric analysis (DSCA) or thermogravimetric analysis (TGA) [16].

Some methods for the characterization of microstructure and mineralogy of cement are two-step operations. In the first step, a spectrum is recorded and in the second step, the mineral or the chemical composition is determined from the spectrum. Using XRDA, a diffractogram is recorded and the mineral composition can be determined by multi-component Rietveld analysis [17]. From integrating the curve or the thermogram from DSCA of cement to obtain the enthalpy of dehydration in two steps of gypsum, the amounts of di- and hemihydrate of $CaSO_4$ can be calculated [16].

Due to uncertainties in the determinations of the mineral composition, the raw data, the XRD intensities or the XRD-profiles, could represent the mineralogy in the examination of influences of the mineralogy on the properties. There are disadvantages using XRD-profiles here, in that they are presenting fingerprints of the mineralogy, and the number of variables needed to present the mineralogy is often higher. To compare the results with previous ones predicted from the real mineralogy as it were [6, IV] and to understand the influence more mechanistically, adding a more qualitative interpretation of XRD-curves could be appropriate. For the same reason**,** thermograms from DTGA (the differential form of TGA) and DSCA instead of the chemical compounds calculated from the respective thermograms could be included in the examination of influence [5, 15]. Thermograms from TGA or DTGA of cement describe the variation in the superficial microstructure of cement, giving important information about the degrees of dehydration of gypsum and prehydration and carbonation of clinker.

In the investigations of influence or the correlation, the x-variables are describing the process conditions and the characteristics of the cement, and the y-variables are describing the cement properties**,** and in some cases the characteristics are included. The many variables complicate the analysis of statistical correlations between $\mathbf{x}$ and y or $\mathbf{y}$. In cases where there is intercorrelation within the observation matrices $\mathbf{X}$ and $\mathbf{Y}$, the correlation analysis should be carried out by applying multivariate rather than multivariable data analysis. Using spectral data to present the mineralogy and the superficial microstructure, intercorrelation is likely to occur. The variation in an

observation matrix could then be explained by variation in principle components or latent variables rather than variation in the original variables. The complexity of multivariate data analysis with respect to the form in which the results are presented makes it appropriate to apply sensitivity analysis and model-based optimization in the implementation of the results in the design and manufacture of cement.

1.2 Objectives of the work

The objectives of the work have been to investigate correlation between production conditions, characteristics and properties of cement to enable design and manufacture of cement. Important parts of the investigation have been examination of different methods for characterisation of cement, multivariate data analysis, sensitivity analysis and development and application of methods for model-based optimization.

1.3 Outline of the thesis

The thesis is an article-based thesis in the form of a collection of papers together with a summary of the papers. Altogether 9 papers are included in the thesis. Two of the main parts of the summary are chapter 2 covering principle and state of art and chapter 3 the contribution referring to the publications of the author. Principles and state of art are not clearly separated in chapter 2 but are mentioned along with the principles in a way so that the reader can compare alternative methods of analysis applied in previous works and relate them to characteristics and properties of cement. Principles and state of art comprise characterization of mineralogy, superficial microstructure and particle size distribution of cement, as well as previous investigations on the influence of the characteristics of cement on the cement properties. Selected parts of the results presented in the papers are presented in the Contributions. A more thorough description of the program OptPilot is presented (in Norwegian) in Appendix.

2. PRINCIPLES AND STATE OF ART

2.1 Composition and mineralogy of cement

The major components of Portland cement are tri- and di-calcium silicates (Ca_3SiO_5 and Ca_2SiO_4), tri-calcium aluminates ($Ca_3Al_2O_6$) and tetra-calcium aluminates ferrates ($Ca_4Al_2Fe_2O_{10}$) [1]. Cement chemists use the shorthand notation C = CaO, S = SiO_2, A = Al_2O_3, F = Fe_2O_3, $\overline{S}$ = SO_3, N = Na_2O, K = K_2O, H = H_2O etc. In accordance with this notation the main mineral in cement, Ca_3SiO_5, should be written C_3S for simplicity. Cement microstructure can be described as composite grains from ground clinker consisting of domains of crystalline alite (C_3S) and belite (C_2S) partly embedded in frozen melt phase (interstitials) from where they are grown while in the kiln. The interstitials consist basically of C_3A and C_4AF. These minerals can attain several crystalline modifications. Alite is usually in the monocline form due to lattice

contaminations like magnesium and aluminium and rapid cooling. Alkalis like potassium and sodium are present in the clinker in the order of 0.5-1.0 % Na_2O equivalents and will end up as contaminants stabilizing different crystal modifications of other compounds (e.g. potassium in β-C_2S or sodium in C_3A) or as sulphates like aphthitalite, $K_3N\overline{S}_2$. Gypsum is ground together with clinker to form cement with controlled setting time. However, the temperature in the mill can be so high that gypsum ($C\overline{S}H_2$) may dehydrate to hemihydrate ($C\overline{S}H_{½}$). The distribution of main minerals in a neat portland cement (i.e. without any other mineral additions than calcium sulphate) may typically be of the order 60% C_3S, 20% C_2S, 10% C_4AF, 5% C_3A and 5% $C\overline{S}H_2$.

Portland cement can, according to US standard ASTM C150-07 [18], be classified into five types of neat cement (clinker + gypsum). The types of cement may differ in chemical composition and/or fineness. The European standard EN197-1 [19] defines 5 classes of common cement that comprise Portland cement as a main constituent. These classes differ from the ASTM classes by their content of additional constituents. Portland cement blends may contain blast furnace slag, fly ash or other pozzolans, microsilica or limestone filler among other additional constituents.

2.2 Hydration of Portland cement

Hydration of Portland cement is a sequence of overlapping chemical reactions between clinker components, calcium sulphate and water, leading to continuous cement paste stiffening and hardening [20]. The hydrating cement paste consists of unhydrated particles in a matrix of reaction products and pores. The matrix comprises a composition of near amorphous calcium silicate hydrates (C-S-H) of variable composition and structure, well-crystallized calcium hydroxide (CH), aluminate and ferrite compounds (mainly sulfoaliminates) in addition to a number of minor constituents [21]. The subsequent decrease in porosity and formation of a complex elastic and brittle material is called hardening.

The hydration reactions [20] of the two calcium silicates, as described in equations 1 and 2, are stoichiometrically very similar, differing only in the amount of $Ca(OH)_2$ or CH formed. The measured heats of hydration, ΔH, are considerably different.

$$2C_3S + 7H \rightarrow C_3S_2H_4 + 3CH \qquad \Delta H = -1114\,\text{KJ/mole}$$

$$2C_2S + 5H \rightarrow C_3S_2H_4 + CH \qquad \Delta H = -43\,\text{KJ/mole}$$

The primary initial reaction of C_3A with water in the presence of an excess supply of gypsum is:

$$C_3A + 3C\overline{S}H_2 + 26H \rightarrow C_6A\overline{S}_3H_{32} \text{ (ettringite)}$$

Ettringite (AFt phases) is a stable hydration product only while there is a sufficient amount of sulphate available. The impermeable coating on the reacting C_3A retards the hydration reaction. If the concentration of SO_4^{2-} in solution drops, then ettringite becomes unstable and converts to monosulphate (AFm phases):

$$2C_3A + C_6A\overline{S}_3H_{32} + 4H \rightarrow 3C_4A\overline{S}H_{12} \quad \text{(monosulphate)}$$

The conversion from ettringite to monosulphate causes the protective ettringite coating of C_3A to disrupt and results in a renewed hydration of C_3A.

The assumption that the cement compounds are hydrating independently is not entirely true. An example compound interaction is a faster hydration of C_2S in the presence of C_3S due to changes in the concentrations of Ca^{2+} and OH^- in solution, which also will affect the hydration of C_3A and C_4AF. The more reactive C_3A is expected to consume more sulphate ions than C_4AF, increasing the reactivity of C_4AF by formation of less ettringite than expected. The initial hydration of C_3A contributes to the activation of the hydrations of the other clinker minerals [20]. An increase in the amount of free lime may shorten the dormant period due to earlier precipitation of $Ca(OH)_2$.

The hydration reactions related to cement properties are summarised in Table 1.

Table 1: Meaning of basic Portland cement hydration reactions [20]

Reaction stage	Chemical processes	Physical processes	Relevance to mechanical properties
First minutes	Rapid initial dissolution of alkali, sulphates and aluminates; initial hydration of C_3S; formation of AFt	High rate of heat evolution	Changes in liquid phase composition may influence the subsequent setting
First hours (induction period)	Decrease in silicate but increase in Ca^{2+} ion concentration; formation of CH and C-S-H nuclei begins; Ca^{2+} concentration reaches a supersaturation level	Formation of early hydration products; low rate of heat evolution	Formation of AFt and AFm phases may influence setting and workability. Hydration of calcium silicates determines initial set and end of induction period
Approximately 3-12h (acceleration stage)	Rapid chemical reaction of C_3S to form C-S-H and CH; decrease of Ca^{2+} supersaturation	Rapid formation of hydrates leads to solidification and decrease in porosity; high rate of heat evolution	Change from plastic to rigid consistency (initial and final set); early strength development
Post-acceleration stage	Diffusion-controlled formation of C-S-H and CH; recrystallisation of ettringite to monsulphate and some polymerisation	Decrease in heat evolution. Continuous decrease in porosity. Particle-to-particle and paste-to-aggregate bond	Continuous strength development, diminishing rate. Decrease in creep. Porosity and

	of silicates possible. Hydration of C_2S becomes significant	formation	morphology of hydrated system determine ultimate strength, volume stability and durability

2.3 Manufacture of cement

2.3.1 General

A brief description of the manufacture of cement is given in Chapter 1.1. The main components in clinker are CaO, SiO_2, Al_2O_3 and Fe_2O_3. The oxides occur in varying amounts in different mineral compounds, such as limestone, marl and clay usually found in nature as deposits. The manufacturing process is schematically presented in figure 1. The additives mentioned in the figure are more or less synonymous with gypsum.

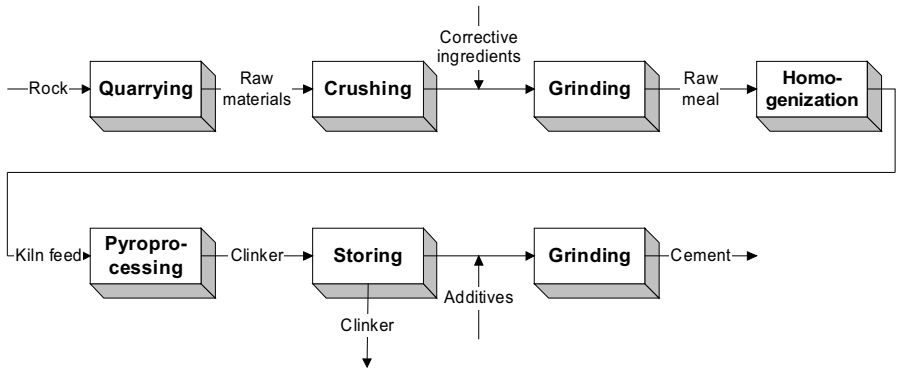

Figure 1. (from Tokheim [2])

2.3.2 Pyroprocessing

Clinker burning processes take place in rotary kilns. However, different types of processes and type kilns are used. A typical modern kiln is a short rotary kiln with feed of already pyroprocessed meal before it enters the kiln. The pyroprocessing often takes place in a suspension preheater equipped with a precalciner which is supplied with more than a half of the total fuel energy [22].

Schematically and according to Roy [22], the following reactions between the compounds in the meal and the intermediate compounds formed during burning occur in the rotary kiln:

1. Evaporation of water; takes place in the drying zone (< 100°C).
2. Release of water from the clay component of the mix and formation of a reactive mixture of oxides; preheating zone (100-750°C). In the case of presence of kaolinite, the following reactions will occur:

$$Al_4[(OH)_8Si_4O_{10}] \rightarrow 2(Al_2O_3 \cdot 2SiO_2) + 4H_2O$$
$$Al_2O_3 \cdot 2SiO_2 \rightarrow Al_2O_3 + 2SiO_2$$

3. Dissociation of carbonate phases (mainly $CaCO_3$, $MgCO_3$ to a minor extent only); formation of CaO; calcining zone (750-1000°C).
4. Partial fusion of the mix, formation of C_3S (alite) and C_2S (belite); the powdery materials form nodules, called clinker in cement terminology; burning zone (1000-1450°C).
5. Crystallization of melt, forming calcium aluminates and calcium aluminate ferrites; cooling zone (1450-1300°C).

The overall clinker formation reaction may be written according to the idealized scheme:

$$CaO + (Al,Fe)_2O_3 \cdot xSiO_2 \rightarrow 3CaO \cdot SiO_2 + 2CaO \cdot SiO_2$$
$$+ 3CaO \cdot Al_2O_3 + 4CaO \cdot Al_2O_3 \cdot Fe_2O_3$$

or

$$\text{lime} + \text{"meta"–clay} \rightarrow C_3S + C_2S + C_3A + C_4AF$$

Figure 2 shows variations in contents in typical phases during the clinker formation [23]

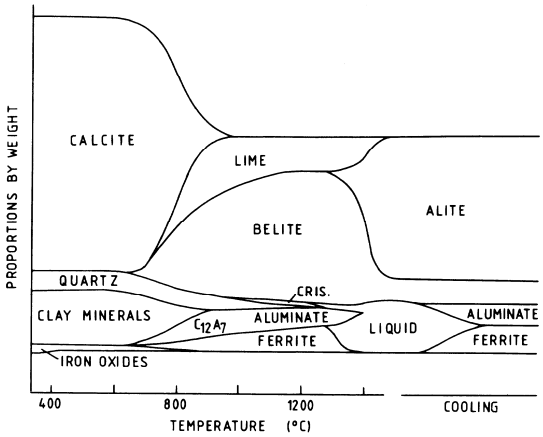

Figure 2. Variations of contents in typical phases during the clinker formation (from Taylor [23]

The type of cement kiln process studied in this work is a precalciner kiln process. A principle drawing of rotary cement kiln suspension preheater, precalciner and clinker cooler is shown in figure 3. The kiln being focused is located at Brevik Plant, Norway. The kiln was equipped with a grate cooler, an in-line precalciner and a double 4 stage

cyclone preheater system in the period of the studies and observation. The two cyclone strings in the tower were linked to the kiln and the tertiary air channel by a common riser duct. A thorough description of the kiln system focusing the impact of staged combustion on the operation of the kiln is given by Tokheim [2]. The correlation between NOx emissions and production conditions in the kiln was statistically analyzed by Svinning et al [11]. Svinning et al [24] studied the variations in mineralogy of Portland clinker, analyzed by X-ray diffraction, correlated to the variations in production conditions in the kiln at the Brevik Plant. Points of sampling and measuring process variables included in the examinations in Ref. [24] are marked in Fig 4.

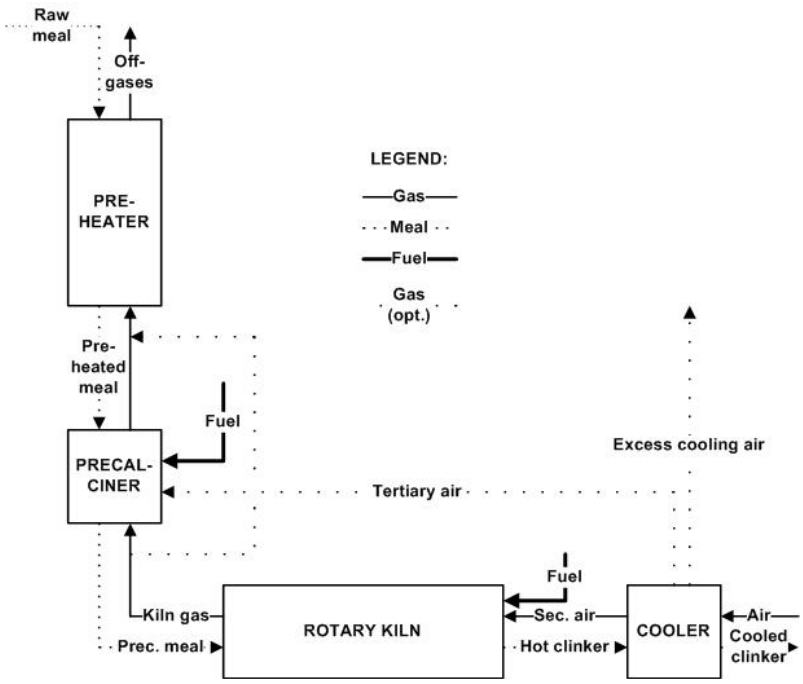

Fig 3. Principle drawing of rotary cement kiln suspension preheater, precalciner and clinker cooler. (from Tokheim [2])

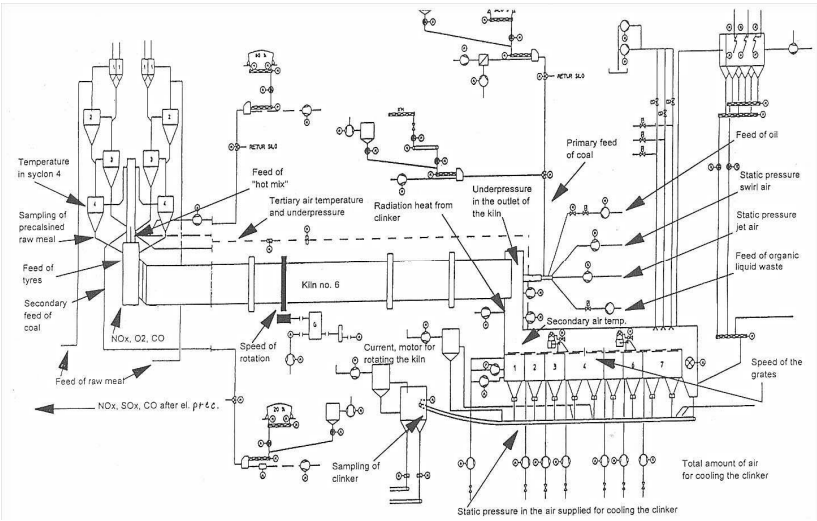

Figure 4. Schematic figure of kiln No. 6 at the Brevik Plant, except for the conditioner towers and electrostatic precipitators. Points of sampling and measuring process variables are marked (from Svinning et al [24]).

2.3.3 Grinding of cement

Grinding is commonly done in ball mills with closed or open-circuit system options; although roller mills and ring mills are frequently used. A ball mill can be described as tubular mills partly filled with hard steel balls. Cooled clinker is usually ground with either natural gypsum or chemical by-product gypsum. The charge of grinding media (bulk volume) is one-third of the total volume of the mill. The material being ground is held within the media at about the level needed to fill the voids among the balls. Cement mills are often divided into two chambers by slotted diaphragms [25].

In an open-circuit mill, the clinker and additives are fed into the mill at a speed which gives a sufficient retention time to grind the materials to the required fineness. In a closed-circuit mill, the mill discharge is segregated into a fine fraction that becomes the final product and a coarse fraction being returned to the mill for regrinding. For Blaine fineness up to 200 m^2/kg, there is no difference in the grinding efficiency between the two types of mills. The relation between the energy consumption and the fineness achieved is almost linear. Increasing the fineness further, the grinding efficiencies of both mill systems decrease. Simultaneously, the energy saving benefits of closed-circuits operation increase with increasing fineness [26].

The particle size distribution of cement depends mainly on: (a) The components of the cement, and (b) The type of grinding circuit and the operation of it. Usually, an open-circuit grinding gives a broader size distribution than what a closed-circuit grinding does [27, 28]. Theisen [29] has studied the influence of the components of clinker on the

grindability. The grindability of clinker was determined by grinding clinker and gypsum in a laboratory mill to a certain fineness while measuring the power consumption. The power consumption was correlated to the component composition and the microstructure of clinker characterized by optical microscopy. The results showed a strong correlation between the grindability and the Bogue calculated belite content and the crystal size of alite. In Ref. [14], an overview is given of similar examinations as Theisen's of the grindability of clinker, and what mineralogical factors are influencing grindability.

The cement mill examined in this work is located at the Brevik Plant, Norway [5]. The closed-circuit mill is of the type two-chamber Combidan ball mill. The mill system with a classifier, dust filter and the silos and feeding system is shown in figure 3. The classifier is an FLS-SEPAX® separator type 400-2s. The finished product leaves the separator at the top and is deposited in a set of four cyclones. During the production it is possible to intergrind iron(II)sulphate for dechromatising or reduction of Cr^{6+} in clinker, and limestone as a supply of filler, in addition to clinker and gypsum. The limestone filler that was fed into the mill had a sieve residue of approximately 14 % at 90 µm. Internal water sprays can be used at both the inlet and outlet ends of the mill. The location of sampling of the cement is right after the cement cooler. A schematic figure of the cement mill is presented in figure 2. The grinding aid used was of the type Technochem TC-84 N, which contains aliphatic amine acetate diluted in water (21 % conc).

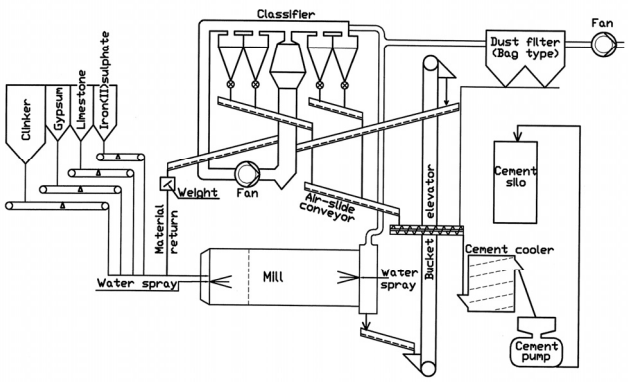

Figure 5. A schematic figure of the CM5 at Brevik Plant, Norway (from Svinning and Datu [5])

In order to minimize the risk of producing false setting cement, the milling should not be carried out at temperatures that are too high [1]. The false setting can be related to dehydration of gypsum, which also influences the workability of mortar and concrete [30]. The dehydration can be prevented by cooling the clinker and spraying water into the mill at the inlet [31, 5]. The amount of water at the inlet should be less that what can be evaporated, or else the clinker minerals would be prehydrated. Rehydrating already

dehydrated gypsum by spraying water into the mill at the outlet seems to be prevented by prehydration of free lime [31]. The water spray at the outlet is mainly used for preventing further dehydration of gypsum during storage in silos. The flow is controlled by monitoring the temperature of the cement leaving the mill and the loss on ignition of the final product [1].

Grinding aids such as aliphatic amine acetate (mentioned above), glycols and triethanol amine [1] have been found to reduce the energy needed in milling to reach a given fineness. They are considered to improve the flow of cement in the mill [1] and the efficiency of the classifier [15]. Water vapour could also function as a grinding aid by adsorption on freshly formed surface of cement, reducing the surface energy, reducing the interparticle adhesion and preventing re-agglomeration [25].

Environmentally friendly cement could be manufactured by inter-grinding clinker + gypsum and, for example, fly ash and/or limestone. The location of feeding the constituents, their particle size distribution and their grindability will influence the characteristics and the properties of the product [14].

2.4 Characterisation of cement

2.4.1 General

As mentioned in chapter 2.1, the purpose of characterisation of cement is to enable quality control ofcement during production and design of new types of cement. The characteristics of cement could be defined to consist of two parts. The first part contains information about the mineralogy and microstructure of clinker. These can be related to the production conditions in the kiln. The second part contains information about the superficial microstructure and the fineness or the particle size distribution of cement and can be related to the production conditions in the cement mill.

2.4.2 Characterisation of the mineralogy and microstructure of clinker

The mineralogy and microstructure of clinker can be characterized by optical microscopy (OM) and scanning electron microscopy (SEM), X-ray diffraction analysis (XRDA), nuclear magnetic resonance (NMR) spectroscopy and differential thermal analysis (DTA) among others. Only the three first methods will be described in detail.

Campbell [8] gives a thorough presentation of microscopical examination of Portland cement and clinker. The aim of his presentation is to improve economical production and quality control of Portland cement and the purposes are

1. To describe the methods of sample preparation for microscopical study and to recommend the use of certain methods of analysis and microchemical techniques

2. To describe the common phases in Portland cement clinker
3. To present a set of microscopical observations with corresponding genetic interpretation drawn from published sources.

Further, according to Ref. [8], some of the aspects of cement production in which microscopy can play an analytical and quality-controlling role, especially in clinker and cement examination are as follows:

1. Phase changes and phase concentration at various stages in the pyroprocessing system
2. Temperature profile – burning efficiency relationships in the calcining and burning zones of the kiln.
3. Grinding and storage of which prediction of clinker grindability is an important aspect
4. Prediction of cement performance as strength build-up

Microscopical methods applied in the examinations presented in Ref. [8], are OM and SEM. An important part of the microscopical examination by OM is the preparation of the clinker samples. An frequently used technique of preparation is embedding either the whole or crushed nodules of clinker in epoxy resin. After that, the samples are cut, ground, polished and etched. Etching is a technique of imparting colour to various crystalline phases in clinker. Certain phases are dissolved in the reflected light.

When using SEM, the electrons of the high-energy beam scanning the sample interact with the atoms of the sample, thus producing signals that contain information about the topography of the surface of the sample. The signals produced include secondary electrons, back-scattered electrons and characteristic X-rays [32]. Etching the sample before the SEM examination with nital, the silicate phases, alite and belite can be differentiated morphologically from interstitial phases containing aluminate and ferrite, from the signals of the secondary electrons. Aluminate and ferrite phases can be dissolved from the signals of back-scattering electrons. Heavy elements (high atomic number) backscatter electrons more strongly than light elements (low atomic number) and thus appear brighter in the image. By using energy dispersive X-ray analysis (EDX) component or element composition of an area (cross section > 10 μm) can be identified.

The types of characterization performed on clinker by OM and SEM can be the quantification of the amounts of alite, belite and the melting phase, and the crystal size distribution of alite. Qualitative characterization could be the reactivity of alite indicated by colour (nital etching, OM), the shape of the clinker phases and satellites around alite, indicating cooling conditions and back reaction [8]. Examples of characterisation are presented in Refs. [6, 33]. Another important characteristic that can be analyzed by OM is the birefringence of alite. The parameter indicates changes in the structure of alite and subsequently, changes in the reactivity of alite [8].

Powder XRDA is used to characterize the crystallographic structure of the minerals in clinker and identify them as well. The X-ray diffraction of powder samples results in a

pattern characterized by reflexes as peaks in intensity at certain positions. The height, width and position of these reflections can be used to determine many aspects of the material structure. Interpretations of the XRD-patterns are presented in Refs. [1, 23, 34]. According to [Taylor], the potential use of XRD powder diffraction in the study of clinker or anhydrous cement includes the qualitative and quantitative determination of polymorphic modification, state of crystallinity and other features of individual phases. Due to the lack of adequate reference data, Taylor [23] considers XRD to be generally less satisfactory for examining the clinker phases than X-ray microanalysis as applied in SEM. Certification of phase composition of three reference clinkers by Stutzman and Leigh [35] was based on two independent methods; OM and XRD analyses, the latter on powder. The XRD data agreed with the OM data with the exception of aluminate. The XRD data showed greater precision than replicate measurements by microscopy.

The Rietveld method is used for characterisation of crystalline materials from powder diffraction data. A least squares approach is used to refine a theoretical pattern until it matches the measured pattern. The method is able to deal reliably with strongly overlapping reflections [17]. Examples of structure refinements of clinker minerals are presented in Refs [36, 37, 38, 39].

The XRD analysis was performed on both ground clinker and cement [6]. The XRD-profiles consisted of intensities at every 0.02°. The scaling of the intensities and adjustment of the 2θ-position of the diffraction peaks were based on normalization of the area and adjusting the 2θ-axis to match the diffraction peak at d = 3.52 Å for anatase (TiO_2), which was intermixed in an amount of 10 wt% of the total sample. Examples of diffractograms including the peak of the reference are shown in Fig 6. The brand of the diffractometer used was Philips X'pert.

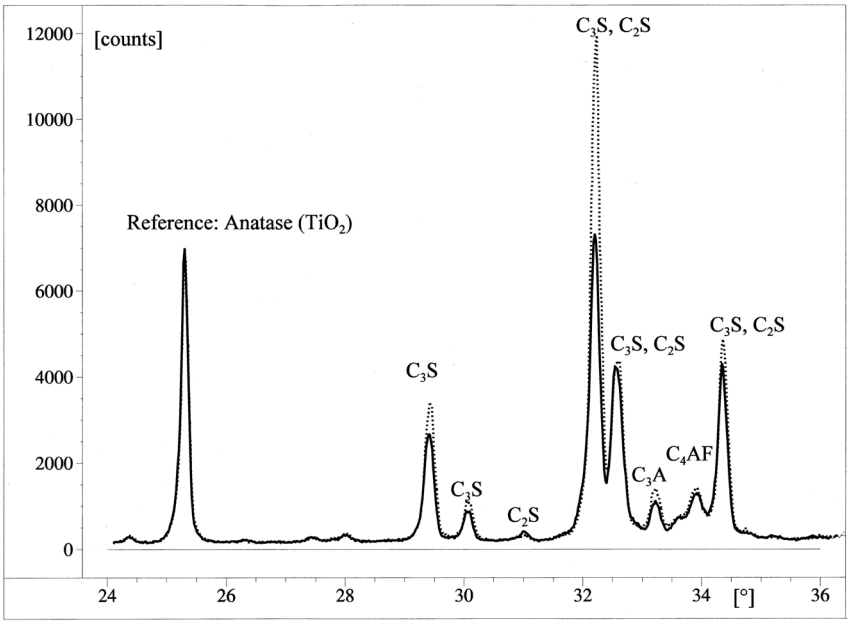

Fig 6. Examples of X-ray diffractograms of two neat cements in the 2θ range 24-36 ° (using CuK_{α} - radiation) [IV]

As mentioned in chapter 1.2, the mineral composition from XRD-curves determined by Rietvelds method, could be included when examining the influence of the mineralogy on the properties. Alternatively, the raw data, XRD-curves or intensities, could represent the mineralogy in the examinations. The relative inaccuracy of the amount of a mineral determined by Rietveld's, increases with decreasing amount of the mineral. The benefit of including the XRD-profiles in the examinations directly is that no information will be lost and error propagation through a two-step process of characterization can be avoided [IV].

The 2θ-ranges of the diffractogram, 29.88 – 30.70° and 32.90 – 34.10° were selected to be included in the examination of the influence of the mineralogy on the properties. The selection is based on the experience that the XRD-profiles of clinker and cement produced from this clinker, respectively; coincide to a high extent [6]. Neither gypsum nor lime stone filler gives rise to any reflections in the selected ranges. The minerals giving rise to reflections in the two selected ranges of diffraction angles are listed in Tables 5 and 6. For predicting the potential strength of clinker, only the variables describing the mineralogy were varied [6, V]. By comparing the studies and results from Ono [40] and Maki [41], a shift in the position of the peak at approximately 32.6 º due to a change in the structure of alite, could be related to the change in the birefringence of alite. For diagnosis of the production conditions in the cement kiln from the mineralogy, the second 2θ-range of 32.90 – 34.10° should be expanded to 32.42 – 34.10º [IX]. In the 2θ-range of 30.70 – 32.42°, there is strong alite reflection at d = 2.778 Å. The reflection

has pseudo-hexagonal indices < 009 >, which may have an increased intensity for flaky crystals due to preferred orientation [24]. Due to the high possibility of preferred orientation the pattern of the peak was not included in the investigations [III, IV, VIII].

Table 2. Major phases within the range 2θ = 29.88–30.70° (d = 2.990-2.912 Å) (from Svinning et al [6])

Phase	2θ (°)	d (Å)	Indices, hkl	Intensity (rel)
Alite (M3)	30.04 30.09	2.975 2.970	804 620	10 20
Aphthitalite	30.38	2.940	102	75

Table 3. Major phases within the range 2θ = 32.90-34.10° (d = 2.722-2.629 Å) (from [Svinning et al [6])

Phase	2θ (°)	d (Å)	Indices, hkl	Intensity (rel)
Belite, β-C_2S	32.98	2.716	121	38
α'- C_2S	33.65	2.663	260	100
C3A, cubic	33.26	2.694	044	100
C_3A, orthorhombic	33.27 33.04 32.93	2.693 2.711 2.720	224 040 400	100 25 31
$C_{12}A_7$	33.41	2.680	420	100
C_4AF	33.84 33.64	2.649 2.664	141 002	100 47
Gypsum	33.35	2.684	150,220	50

2.4.3 Characterisation of the superficial microstructure

A change in the superficial microstructure of cement could be in the form of dehydration of gypsum, prehydration and carbonation of clinker minerals [5]. The superficial microstructure can be analyzed by thermogravimetric analysis (TGA), differential scanning calorimetric analysis (DSC), differential thermal analysis (DTA), Fourier transform infrared – attenuated total reflectance spectroscopy (FTIR-ATR) [42] and X-ray photoelectron spectroscopy (XPS) [43] among others. TGA and DSC will be described more in detail.

Thermogravimetric analysis (TGA) is performed on samples to determine changes in weight in relation to change in temperature. The analysis relies on a high degree in of precision in measuring weight and temperature. To differentiate between two similar weight loss curves before interpretation, derivation of the curves (DTGA) should be performed. The next modification could be deconvolution of overlapping peaks. A physical/chemical way of separating the peaks is to provide the sample crucible with a lid with a small aperture in the middle. Increasing the pressure of an inert gas or building the

partial pressure of H_2O and CO_2 from the dehydration and the decarbonation of cement during the analysis, the trough resolution will increase [44].

The apparatus applied in this work and in the previous examinations was Netzsch STA – Apparatur 409 V/3/C® [5, 15]. A dynamic mode of thermogravimetry was used, in which the sample was heated in an environment whose temperature was changing in a predetermined manner, preferably at a linear rate. The weights of the analysed samples were 4.2 g and the heating rate was 2 K/min. No gas was purged through the furnace during the analysis. Limited space in the furnace and the large amounts of samples restricted the measurement of temperature to that of the sample only. Ideally, the temperatures to which the mass losses refer, should be those measured in an inert reference object lying next to the sample in the furnace. Due to the large volume of samples being analysed, the reaction involving mass loss of larger quantities of H_2O and CO_2 is partly diffusion controlled. The position [ºC] of a respective DTGA–trough will be at a higher temperature with an increase in the amount of the compound being dehydrated or decarbonised. The position of a trough also depends on the fineness of the compound. Figure 7 shows two examples of thermograms from DTGA of neat cement and cement with limestone used as filler, respectively. The thermograms are interpreted with respect to the most common reactions occurring during the heating.

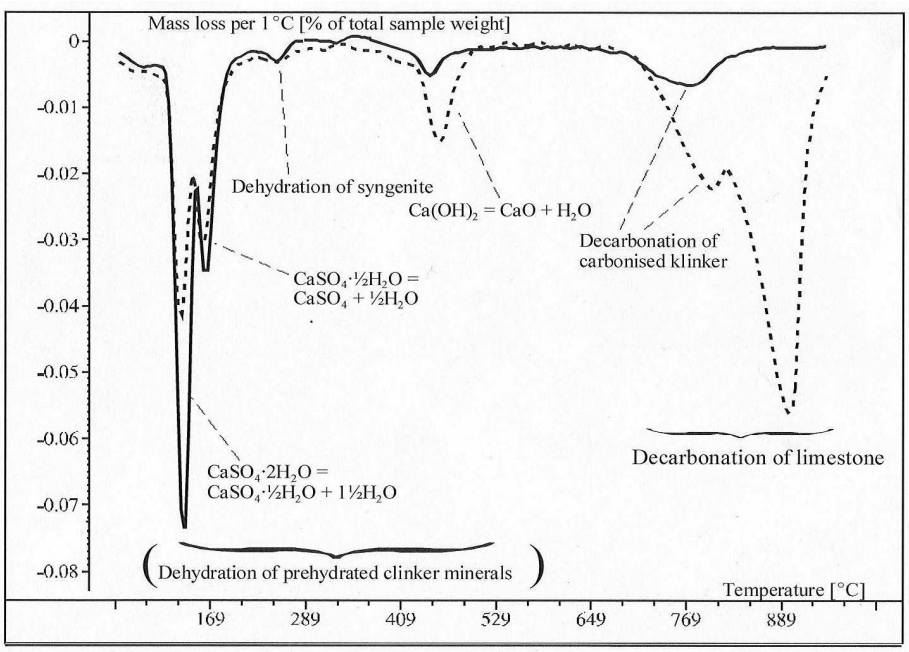

Fig 7. Two examples of curves from differential thermogravimetric analysis (DTGA) of neat cement and cement with limestone filler (dashed line) (from Svinning and Datu [5])

Differential scanning calorimetry (DSC) is a thermoanalytical technique in which the difference in the amount of heat required to increase the temperature of a sample and a reference are measured as a function of temperature. Both the sample and reference are maintained at nearly the same temperature throughout the experiment. The temperature program for a DSC analysis is designed in such a way that the sample holder temperature increases linearly as a function of time. The reference sample should have a well-defined heat capacity over the range of temperatures to be scanned [45].

The DSC curve obtained is a recording of heat flow as a function of temperature. The area enclosed by a DSC peak is directly proportional to the enthalpy change [44]. Knowing the enthalpy of the reaction and the calorimetric constant, the mass being converted during the reaction can be calculated. An example of application of the method in cement technology is determination of the amounts of di- and hemihydrate of $CaSO_4$ in cement [16]. In Fig 8 a curve from DSC analysis of cement is depicted. The ranges of integration (the peaks at 151 and 189˚C) are marked in the figure. Separation of the peaks was made by creating a suitable water pressure by closing the aluminium crucibles with a small pin hole of 40-50 µm. The amount dihydrate was calculated to 2.5 % and the amount of hemihydrate to 1.8 %.

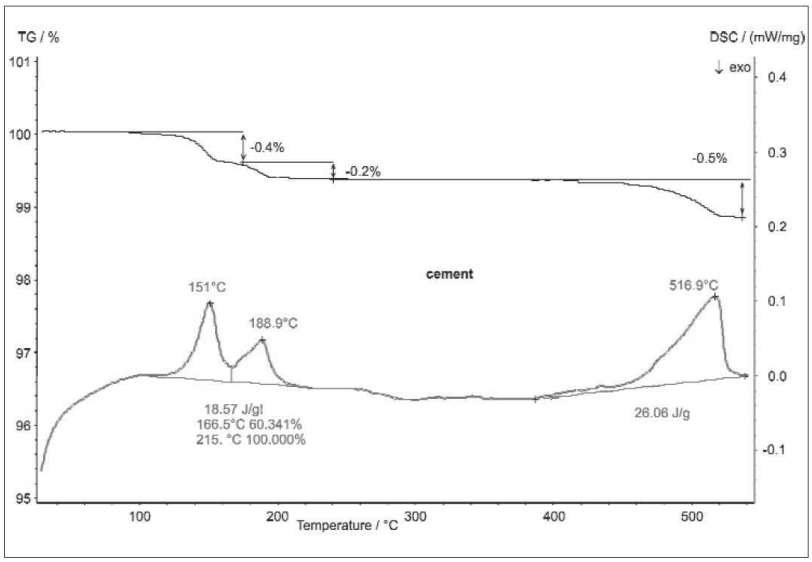

Fig 8. Curves from TGA and DSCA of a cement sample, heating rate: 10 K/min, atmosphere: Air purged at 50 ml/min, sample mass: 39.5 mg (from Schindler [16]).

Comparing the DTGA curve in Fig 7 with the DSCA curve in Fig 8, the former curve gives more detailed but less quantitative information about the superficial microstructure

of cement. The quantification of di- and hemihydrate of $CaSO_4$ in cement could be affected by prehydration of aluminate appearing as a peak at approximately 115 ˚C partly overlapping the peak at 151 ˚C [46]. Instead of the amounts of the hydrates and carbonates, the thermograms from DTGA were included in the examinations of the influences of the superficial microstructure on the properties. A qualitative/quantitative interpretation of the thermograms is, however, an important part of the examination to explain the influence mechanistically.

2.4.4 Determination of the particle size and the fineness of cement

Methods applied in the process industry to determine particle size distribution of powder (PSD) are as follows: sieving, sedimentation, electrozone sensing, microscopy and laser diffraction. For characterization of the surface area of cement the Blaine air permeability apparatus is much used. Particle size distribution could be presented in a cumulative form or a differentiate form. The specific fineness, SF, can be calculated from the particle size distribution:

$$SF = \frac{6\sum_{i=1}^{m}\frac{V_i}{d_i}}{\sum_{i=1}^{m} V_i \ \rho} \qquad (1)$$

where V_i is the volume fraction in size class no i, d_i is the average diameter of the particles in the same size class and ρ is the specific weight of the cement [II].

The method used in this work is laser diffraction analysis. The method depends upon analysis of the "halo" of diffracted light produced when a laser beam passes through a dispersion of particles in air or in a liquid. The angle of diffraction increases with decreasing particle size. Due to the hydroscopic properties of cement, ethanol is a more appropriate liquid for dispersion of cement than water.

In the quality control of grinding clinker to cement to achieve wanted values of compressive strength and setting time the specific fineness measured by Blaine's method has been much focused. Tailoring the cement quality to meet more special requirement, more attention should be paid to the whole particle size distribution. An example of variation in the particle size distribution giving no variation in specific fineness [is shown in Fig 9 [II].

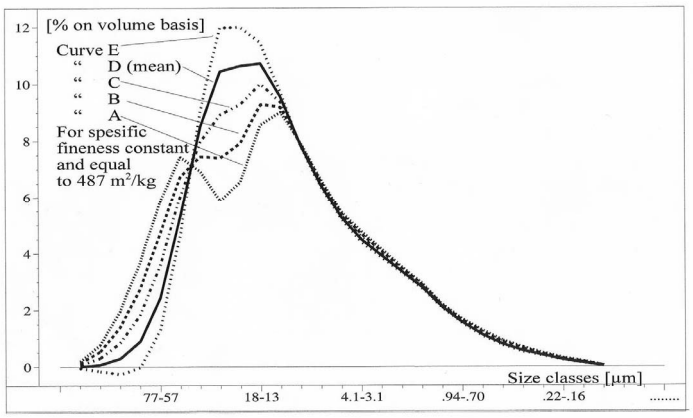

Fig 9. Variation in the particle size distribution by varying a latent variable giving no variation in the specific fineness [II]

Intergrinding clinker with limestone or other replacement constituents, it could be interesting to study the particle size distribution or the fineness of each of the materials as they exist in the finished product. One possible method could be separating the material chemically or physically prior to the particle size analysis or application of another method for at least indicating differences in the fineness. From examinations of cement produced at Brevik Plant, Norway [15], Fig 10 shows a pronounced variation in the position of the DTG trough which is designated the decarbonation of the limestone filler. The reason for this variation could be changes in the fineness of the limestone filler. Due to pregrinding the limestone before feeding it into the mill, the limestone filler as it exists in the cement is presumed to be finer than the clinker part of the cement. Considering the decarbonisation reaction during TGA to be a heterogeneous and diffusion-controlled reaction, the temperature at maximum rate of the reaction will probably increase with a decrease in the fineness of the filler part of the cement [44]. The variation in the fineness of limestone filler as it exists in cement could be due to the variation in the feed of grinding aid. The fineness is probably decreasing with increasing feed of grinding aid.

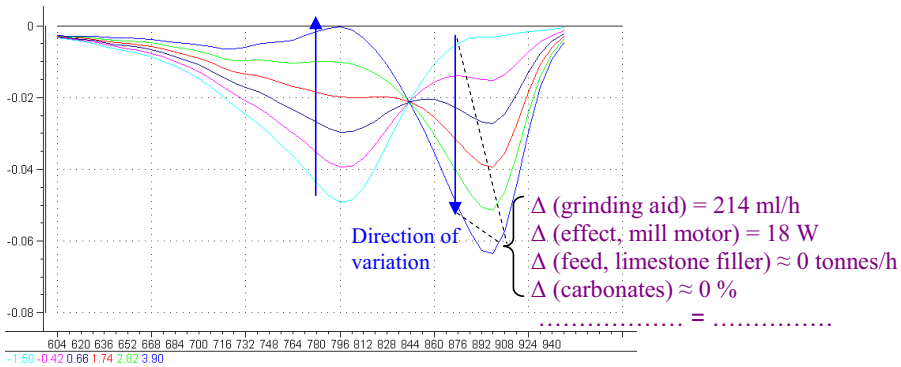

Fig 10. Variation in the superficial microstructure described by mass losses [% of the total sample weight] per 8 ˚C from TGA (ordinate) in the range 604 – 946 ˚C (abscissa), from varying a latent variable giving no variation in the feed of limestone and in the amount of carbonate analyzed (from Svinning and Datu [15])

2.5 Testing the properties of cement

In table 1 in chapter 2.2 mechanical properties are related to the different reaction stages. Properties related to the first hours are setting and workability. Then changes from plastic to rigid consistence (initial and final set) and early strength development follow. In the post-accelerating stage the strength develops continuously.

The setting time (ST) is determined by observing the penetration of a needle into cement paste of standard consistence until it reaches a specified value. Cement of standard consistence has a specified resistance to penetration by a standard plunger. The amount of water required to achieve standard consistency (SC) is determined by trial penetration of pastes with different water content. Testing the setting time is performed according to the European standard EN 196-3 [47].

The specimens to be tested are cast from a batch of plastic mortar containing one part by mass of cement and three parts by mass of standard sand with a water/cement ratio of 0.50. The mortar is prepared by mechanical mixing and is compacted in a mould using standard jolting apparatus. The specimens in the mould are stored in a moist atmosphere for 24 h and then the demoulded specimens are stored under water until strength testing. At the required age, the specimens are taken from their wet storage and tested for strength in compression. The European standard EN 196-1 [48] describes the method to determine compressive strength.

2.6 Statistical analysis

2.6.1 Introduction

Generally, any investigation could be carried out in four steps: experimental design, experiments and sampling, multivariate data analysis and sensitivity analysis. The experimental design could be in the form of various types of factorial design. In the investigation on the influence of production conditions in a cement mill on the cement properties [5] the experiments were carried out in two stages. In the first stage experiments with 2^3 factorial designs, *i.e.* designs with variation of three variables and from a low to a high level, were performed. The respective variables chosen were Blaine, amount of limestone, temperature of cement leaving the mill, amount of gypsum, amount of water sprayed into the mill at the inlet and amount of grinding aid. The purpose of performing this type of experiment in Ref. [5] was, however, to achieve a better span of the observation **X**-space. The calculations of effects after each factorial designed experiment were dropped in favour of PLS at the end, including all the relevant variables and available observations included.

Statistical analysis applied in this work is mainly statistical modelling and sensitivity analysis. The complexity of the processes of the manufacture of cement and the great number of variables of characterization make it difficult to evaluate a mechanistic model for predicting the properties of cement. The mechanistic models should reflect physical laws, chemical thermodynamics and/or kinetics expressed by mathematical models containing transforms of the original variables like square, square root or others and nonlinear combinations of variables to achieve the best fit to the observations. A mechanistic model could be evaluated by regression analysis. Lacking knowledge of any dominant mechanism to explain the relation between the properties, **y**, and the production or the characteristic variables, **x**, the initial model should be a linear model of the form $y = b_0 + \sum_{k=1}^{K} b_k x_k$. Plotting predicted versus measured y showing a lack of fit appearing as systematic tendencies, could indicate deviation from linearity [11]. The model could be improved by introducing another transform of *y* or one or several *x*. As mentioned in chapter 1.1, in the case of intercorrelation within the observation matrices **X** and **Y**, the correlation analysis should be carried out by applying multivariate rather than multivariable data analysis [8]. Partial least square regression (PLS) was used in the work presented in the thesis.

There are two approaches to sensitivity analysis, one is considering the influence of samples, the other is theinfluence of variables [49]. In this work the latter consideration was focused. The purpose of sensitivity analysis is the interpretation of a complex statistical model like PLS with respect to how much, in what direction and how significantly an *x*- variable influences y. The sensitivity of an x-variable could be defined as the predicted effect of the *x*-variable on the response *y*-variable relative to a defined confidence range of the predicted *y*. An alternative to the sensitivity analysis described above, might be performing uncertainty testing on the regression coefficients. Martens and Martens [50] have developed an improved method for uncertainty testing based on

cross-validation, Jack knifing, and stability plot. In addition to studying the influence of the separate x-variable on y, the influence of latent variables should be paid attention to. In Refs. [3, 4] the influence of an *x*-variable or of the relevant latent variable on y, are compared with respect to significance. The term relevant is related to how much the x-variable will vary by varying the latent variable.

The influence of the different parts of the characteristics and the production conditions on the properties were examined by simulation, optimisation and prediction [V, VIII, IX]. The different parts of the microstructure could be related to the different steps of the production of cement.

The influence of the characteristics or the microstructure of Portland cement on compressive strength up to 28 days was investigated statistically by application of partial least square (PLS) analysis by Svinning et al. [6]. The main groups of characteristics were mineralogy and superficial microstructure represented by curves from X-ray diffraction analysis (XRDA) and differential thermogravimetric analysis (DTGA), as well as particle size distributions. Prediction of potential compressive strength of clinker from the mineralogy [6, V] was based on a PLS model evaluated for prediction of compressive strength from the whole microstructure of the cement [IV]. The observation **X**-matrix was partitioned into the sub-matrices: $\mathbf{X}_{\text{mineralogy}}$, $\mathbf{X}_{\text{part distr}}$, $\mathbf{X}_{\text{superficial micr LT}}$ and $\mathbf{X}_{\text{superficial micr HT}}$ (LT and HT refer to the low and high temperature range of differential thermogravimetric analysis (DTGA)) .The potential compressive strength was predicted from an artificial observation matrix where only $\mathbf{x}_{\text{mineralogy}}$ was varied. As an alternative to the examinations above, multi-block methods were applied [VII]. The philosophy of multi-block methods is to emphasize the role of each data block with respect to the influence on the response variable.

2.6.2 Evaluation of PLS prediction model

Partial least square regression (PLS) is used to find the fundamental relations between two matrices, **X** and **Y**, i.e. a latent variable approach to modeling the covariance structure in these two spaces. A PLS model will try to find the multidimensional direction in the **X** space that explains the maximum multidimensional variance direction in the **Y** space. PLS-regression is particularly suited when the matrix of predictors has more variables than observations, and when there is multi-collinearity among **X** values. Similar to eigenvectors of a matrix, the latent variables or the PLS-components are orthogonal. That means that a latent variable may vary independently of the others. Optimization of a response variable *y* constrained by principal directions of variation in the observation **X**-matrix or the latent variables is demonstrated by Svinning et al [I].A more complete and detailed presentation of PLS are given by Martens and Næs [8] and Høskuldsson [49] among others.

The data are compressed by expressing the original x-variables by fewer latent variables or factors. The models which relate the PLS-model terms are then given by the two expressions in the equations below:

$$\mathbf{X} = \mathbf{T}\mathbf{P}^T + \mathbf{E} \tag{2}$$

$$\mathbf{Y} = \mathbf{U}\mathbf{Q}^T + \mathbf{F} \tag{3}$$

T and **U** are factor scores, **P** and **Q** are x and y variables loadings and **E** and **F** are the residuals in **X** and **Y**, respectively. Alternatively, Eq. 1 could be expressed in the form:

$$\mathbf{X} = \mathbf{t}_1\mathbf{p}_1^T + \mathbf{t}_2\mathbf{p}_2^T + .. + \mathbf{t}_k\mathbf{p}_k^T + .. + \mathbf{t}_l\mathbf{p}_l^T + \mathbf{E} \tag{4}$$

l is equal to maximum number of latent variables for maximum explanation of variance in **Y**. If there is only one y-variable to be modelled Eq. 2 could be replaced by the following equation:

$$\mathbf{y} = \mathbf{T}\mathbf{q}^T + \mathbf{f} \tag{5}$$

PLS with one or several y-variables is denoted PLS1 or PLS2, respectively. In case of PLS1 the regression coefficients to be used in the predictor $\hat{\mathbf{y}} = \mathbf{1}b_0 + \mathbf{X}\hat{\mathbf{b}}$ are computed as follows:

$$\hat{\mathbf{b}} = \hat{\mathbf{W}}(\hat{\mathbf{P}}^T\,\mathbf{W})^{-1}\,\hat{\mathbf{q}} \tag{6}$$

and $$b_0 = \bar{y} - \bar{\mathbf{x}}^T\hat{\mathbf{b}} \tag{7}$$

where **W** are loading weights used in PLS1

Similarly, for PLS2:

$$\hat{\mathbf{B}} = \hat{\mathbf{W}}(\hat{\mathbf{P}}^T\,\hat{\mathbf{W}})^{-1}\hat{\mathbf{Q}}^T \tag{8}$$

and $$\mathbf{b}_0^T = \bar{\mathbf{y}}^T - \bar{\mathbf{x}}^T\hat{\mathbf{B}}$$

By scaling the variables, unreasonable domination of variables with dominating standard deviations, s(x), on the model can be avoided. The weighting of $x_{i,k}$ by centring and scaling is performed according to the following formula:

$$x_{ik,w} = \frac{x_{ik} - \bar{x}_k}{s(x_k)} \tag{9}$$

PLS does calculation and optimization of a number of factors for maximum explanation of variance in the y-variables. In addition, model parameters are calculated for prediction of y for new values of the x-variables.

Validation means determining the number of PLS-components or latent variables that give the best prediction of *y* from **X** in future objects that lack the value of the *y*-variable. The most common validation methods are leverage correction, validation on a separate test set and cross-validation. The latter method was applied in this work. In Refs. [11, 24], the calibration set was split into ten segments, and the validation was repeated ten times, each time treating one tenth of the calibration set as prediction objects. The cross-validated residual variance in *y* after inclusion of *n* latent variables is as follows:

$$\mathrm{Var}(y)_{\mathrm{val},n} = \frac{1}{I_{pr}} \sum_{i=1}^{I_{pr}} (\hat{y}_i - y_i)^2 \tag{10}$$

where I_{pr} is equal to the number of validation objects, which is equal to the number of the calibration objects. $\hat{y}_i$ is the predicted value and y_i the respective observed value. The explained variance of the total variance in *y*, $\mathrm{Var}(y)_0$, is calculated in this way:

$$Expl.Var.[\%] = \frac{\mathrm{Var}(y)_0 - \mathrm{Var}(y)_{\mathrm{val},n}}{\mathrm{Var}(y)_0} \tag{11}$$

Other quality criteria, which describe the validity of the prediction, are the root mean square error of prediction (RMSEP), the bias and the standard error of prediction. The parameters are calculated by the following formulas:

$$RMSEP = \sqrt{\mathrm{Var}(y)_{\mathrm{val},n}} \tag{12}$$

$$Bias = \frac{1}{I_{pr}} \sum_{i=1}^{I_{pr}} (\hat{y}_i - y_i) \tag{13}$$

$$SEP^2 \approx RMSEP^2 - Bias^2 \tag{14}$$

The iterative algorithms for calibration, validation and prediction are described in detail by Martens and Næs [8].

2.6.3. Methods for sensitivity analysis

Having a model from PLS on centred and scaled data, the influence of x-variables on the y-variable(s) may be evaluated in different ways:

- Comparison of the regression coefficients of the various variables from PLS with centred and scaled data. Significance testing on the coefficients by application of jack-knifing estimation [50] with a confidence interval of 0.95. Examples are shown in figure 1. The estimated uncertainty variance of B is estimated by jack-knifing

$$\mathbf{s}_{\mathbf{b}}^2 = \sum_{m=1}^{M} ((\mathbf{b} - \mathbf{b}_m) g)^2 \tag{15}$$

$$\mathbf{S}_{\mathbf{B}}^2 = \sum_{m=1}^{M} ((\mathbf{B} - \mathbf{B}_m) g)^2 \tag{16}$$

where

$\mathbf{B}(K \times J)$ is the regression coefficient at the cross-validated A using all the N objects,
$\mathbf{B}_m \left(K \times J\right)$ is the regression coefficient at the rank A using all objects except the objects left out in the cross-validated segment m,
g is the scaling coefficient (in the Unscrambler software: $g = 1$)

When the variance for B has been estimated, it can be utilized to find significant parameters. As a rough significance test, a t-test is performed for each element in B relative to the square root of its estimated uncertainty variance $\mathbf{S}_{\mathbf{B}}^2$, giving the significance level for each parameter.

- Prediction of variation in y including confidence intervals equal to $\hat{y} \pm s(y)$, from variation of one x-variable in one direction and in equal steps while the others are kept constant and equal to their respective mean values. The range of variation in this work is set to $\bar{x}_k \pm 1.5 s(x_k)$.
- Prediction of variation in y or $\mathbf{y}$ as from variation of a latent variable at a time from one 'observed' extreme to the other. By varying the k'th latent variable $\Delta t\ \mathbf{p}_k$ the variation in Δx_k in its original form, i.e. not scaled, can be calculated in the following way:

$$\Delta x_k = (\Delta t\ p_{ka})\ s(x_k) \tag{17}$$

Similar to the previous type of sensitivity analysis with variation of only one x-variable the score, t, is varied in one direction and in equal steps, Δt. Calculation of x_j, neither centred nor scaled, will then be as follows:

$$x_k = (t\ p_{ka}) s(x_k) + \bar{x}_k \tag{18}$$

In the two latter ways of sensitivity analysis presented above variation in X was simulated prior to the prediction by constructing an artificial observation X-matrix. In some cases sensitivity analysis in the form of prediction from simulated variation of a selection or a group of variables could be appropriate.

An influence of one or several *x*-variables on a *y*-variable is defined in this work as being significant if there is no overlap of confidence intervals of $\hat{y} \pm 1 std.$ of predicted maximum and minimum y, respectively. Evaluating the significance of the influence of a variable x_k from Jack knifing estimation, the influence could be defined as being significant if the uncertainty level is less than $2|b_{wk}|$.

*2.6.4 Examination of the influences of different parts of **X** on y*

The examination of the influence of different parts of **X** on *y* can be carried out in the following way [II]:

Having an overall model

$$y = \mathbf{b}^{\mathrm{T}}\,\mathbf{x} + b_0 = \mathbf{b}^{\mathrm{T}}\left(\mathbf{x}_1 \mid \mathbf{x}_2 \mid \ldots \mid \mathbf{x}_j \mid \ldots \mid \mathbf{x}_n\right) + b_0 \qquad (19)$$

where $\mathbf{x}_1, \ldots, \mathbf{x}_n$ could represent the different parts of the microstructure or production , the examination of the influence of $\mathbf{x}_j$ on *y* is carried out by the following procedure:

1. Prediction of $\hat{\mathbf{y}}$ from $\left(\begin{array}{c|c|c|c|c|c} (\bar{\mathbf{x}}_1)_1 & & (\bar{\mathbf{x}}_{j-1})_1 & & (\bar{\mathbf{x}}_{j+1})_1 & \\ \vdots & \cdots & \vdots & \mathbf{X}_j & \vdots & \ldots \\ (\mathbf{x}_1)_m & & (\bar{\mathbf{x}}_{j-1})_m & & (\bar{\mathbf{x}}_{j+1})_m & \end{array}\right.$ where m is the number of rows in the observation **X**-matrix
2. To reveal the latent structure of $\mathbf{x}_j$ evaluate a new model $y = \hat{y} = \mathbf{b}^{\mathrm{T}}\left(\mathbf{x}_j \mid \mathbf{x}_{n+1}\right) + b_0$ by PLS. $\mathbf{x}_{n+1}$ may contain a few supplementary variables relevant for interpretation of variation in $\mathbf{x}_j$.
3. Simulation of variation in $\mathbf{x}_j$ by varying one or several latent variables and establishing an artificial observation matrix $\mathbf{X}_{j\,\mathrm{art}}$ with *m*, art rows where $m, \mathrm{art} < \mathrm{m}$ and $m - 1, \mathrm{art}$ is the number of changes in equal steps of $\mathbf{x}_j$
4. Prediction of $\hat{\mathbf{y}}$ from
$$\left(\begin{array}{c|c|c|c|c|c} (\bar{\mathbf{x}}_1)_1 & & (\bar{\mathbf{x}}_{j-1})_1 & & (\bar{\mathbf{x}}_{j+1})_1 & \\ \vdots & \cdots & \vdots & \mathbf{X}_{j,\mathrm{art}} & \vdots & \ldots \\ (\mathbf{x}_1)_{m,\mathrm{art}} & & (\bar{\mathbf{x}}_{j-1})_{m,\mathrm{art}} & & (\bar{\mathbf{x}}_{j+1})_{m,\mathrm{art}} & \end{array}\right.$$

In the examples shown in Paper [II], $\mathbf{x}_{n+1}$ contains only one variable which is the specific fineness of the cement.

2.6.5 Model-based optimization.

The optimization based on a PLS-model could have the form of a linear program, where the constraints describing the influence of one variable on the others are given by one original PLS component or one equal a combination of several [I, III]. Having a model $y = b_0 + \sum_{k=1}^{K} b_k x_k$ from PLS on mean-centered and scaled data, using weights based on the standard deviation and selecting the latent variable No. k to constrain the variation in **X** then mathematically, the linear programming problem could be presented as follows:

Minimise or maximise

$$y = \sum_{k=1}^{K} b_k x_k \quad \text{or} \quad y = \mathbf{x}^{\mathrm{T}}\,\mathbf{b} \tag{20}$$

subject to

$$\mathbf{A}_1\,\mathbf{x} = \mathbf{c}_1,\ \mathbf{A}_2\,\mathbf{x} \le \mathbf{c}_2,\ \mathbf{A}_2\,\mathbf{x} \ge \mathbf{c}_3 \text{ and } \mathbf{x} \ge \mathbf{0}$$

where

$$\mathbf{A}_1 = \begin{pmatrix} -p_{k\,a}\,s(x_k) & \cdots & 0 & p_{1\,a}\,s(x_1) & 0 & \dots & 0 \\ \vdots & \ddots & \vdots & \vdots & \vdots & \ddots & \vdots \\ 0 & \dots & -p_{k\,a}\,s(x_k) & p_{k-1\,a}\,s(x_{k-1}) & 0 & \dots & 0 \\ 0 & \dots & 0 & p_{k+1\,a}\,s(x_{k+1}) & -p_{k\,a}\,s(x_k) & \dots & 0 \\ \vdots & \ddots & \vdots & \vdots & \vdots & \ddots & \vdots \\ 0 & \cdots & 0 & p_{K\,a}\,s(x_K) & 0 & \dots & -p_{k\,a}\,s(x_k) \end{pmatrix}$$

$$\mathbf{A}_2 = \begin{pmatrix} 1 & \cdots & 0 \\ \vdots & \ddots & \vdots \\ 0 & \cdots & 1 \end{pmatrix}$$

$$\mathbf{c}_1 = \begin{pmatrix} \bar{x}_k\, p_{1\ a}\, s(x_1) - \bar{x}_1\, p_{k\ a}\, s(x_k) \\ \vdots \\ \bar{x}_k\, p_{k-1\ a}\, s(x_{k-1}) - \bar{x}_{k-1}\, p_{k\ a}\, s(x_k) \\ \bar{x}_k\, p_{k+1\ a}\, s(x_{k+1}) - \bar{x}_{k+1}\, p_{k\ a}\, s(x_k) \\ \vdots \\ \bar{x}_k\, p_{K\ a}\, s(x_K) - \bar{x}_K\, p_{k\ a}\, s(x_k) \end{pmatrix} \qquad \mathbf{c}_2 = \begin{pmatrix} x_{1\ upper\ \lim it} \\ \vdots \\ x_{K\ upper\ \lim it} \end{pmatrix} \quad \mathbf{c}_3 = \begin{pmatrix} x_{1\ lower\ \lim it} \\ \vdots \\ x_{K\ lower\ \lim it} \end{pmatrix}$$

$\bar{x}_k$, $s(x_k)$ and $p_{k\ a}$ are the mean value, standard deviation and the loading of x_k, respectively. The constant b_0 is not included in the optimization but is added afterwards. x_k is selected to influence the other x-variables in the constraints if $\left| p_{k\ a}\, s(x_k) \right|$ is of max value for $k = 1, 2, \cdots, K$.

In order to achieve the most optimal solution, several PLS-components could be involved in the optimization. The "loadings" in the new constraints are linear combinations of the original ones and could be expressed as follows:

$$\mathbf{p}_{\text{combination of several PLS-components}} = \sum_{a=1}^{A} n_a \mathbf{p}_a \tag{21}$$

where $\sum_{a=1}^{A} n_a = 1$ and $0 < n_a < 1$

The latter constraint prevents absolute values of the scores, |t|, of optimal $\mathbf{x} = (x_1\ x_2 \cdots x_K)$ to be unreasonably high.

The stepwise optimisation could be carried out in this case by stepwise changes of some or all $n_1, \cdots, n_A$ before the next optimisation, until maximum value of y is obtained, on the conditions that the constraints are consistent.

A useful method for optimizing a combination of several latent variables is the simplex method [51]. This is not to be confused with the simplex methods of linear programming.

2.6.6 Multi-block methods

A short review of multi-block methods is presented here. Further details are found in Papers [VI, VIII].

The four data blocks ($\mathbf{X}_1$, $\mathbf{X}_2$, $\mathbf{X}_3$, $\mathbf{X}_4$) and the vectors that are involved in the optimisation task are illustrated in Figure 5. A weight vector $\mathbf{w}_i$ is found for the $\mathbf{X}_i$ data block for i = 1,

2, 3, 4. The Y-loadings are computed as $\mathbf{q}_i=\mathbf{Y}^T\mathbf{t}_i=\mathbf{Y}^T\mathbf{X}_i\mathbf{w}_i$. The task is thus to find the weight vectors $\mathbf{w}_1$, $\mathbf{w}_2$, $\mathbf{w}_3$ and $\mathbf{w}_4$ in such a way that the total of the resulting Y-loading vectors has the largest possible size,

$$\text{maximise } |\mathbf{q}_1+\mathbf{q}_2+\mathbf{q}_3+\mathbf{q}_4|^2, \qquad \text{subject to } |\mathbf{w}_1| =|\mathbf{w}_2|=|\mathbf{w}_3|=|\mathbf{w}_4|=1. \tag{22}$$

This is solved by iterating the set of equations,

$$\begin{array}{lllll}
\mathbf{X}_1^T\mathbf{Y}\mathbf{Y}^T\mathbf{X}_1\mathbf{w}_1 & +\mathbf{X}_1^T\mathbf{Y}\mathbf{Y}^T\mathbf{X}_2\mathbf{w}_2 & +\mathbf{X}_1^T\mathbf{Y}\mathbf{Y}^T\mathbf{X}_3\mathbf{w}_3 & +\mathbf{X}_1^T\mathbf{Y}\mathbf{Y}^T\mathbf{X}_4\mathbf{w}_4 & = \lambda_1\,\mathbf{w}_1 \\
\mathbf{X}_2^T\mathbf{Y}\mathbf{Y}^T\mathbf{X}_1\mathbf{w}_1 & +\mathbf{X}_2^T\mathbf{Y}\mathbf{Y}^T\mathbf{X}_2\mathbf{w}_2 & +\mathbf{X}_2^T\mathbf{Y}\mathbf{Y}^T\mathbf{X}_3\mathbf{w}_3 & +\mathbf{X}_2^T\mathbf{Y}\mathbf{Y}^T\mathbf{X}_4\mathbf{w}_4 & = \lambda_2\,\mathbf{w}_2 \\
\mathbf{X}_3^T\mathbf{Y}\mathbf{Y}^T\mathbf{X}_1\mathbf{w}_1 & +\mathbf{X}_3^T\mathbf{Y}\mathbf{Y}^T\mathbf{X}_2\mathbf{w}_2 & +\mathbf{X}_3^T\mathbf{Y}\mathbf{Y}^T\mathbf{X}_3\mathbf{w}_3 & +\mathbf{X}_3^T\mathbf{Y}\mathbf{Y}^T\mathbf{X}_4\mathbf{w}_4 & = \lambda_3\,\mathbf{w}_3 \\
\mathbf{X}_4^T\mathbf{Y}\mathbf{Y}^T\mathbf{X}_1\mathbf{w}_1 & +\mathbf{X}_4^T\mathbf{Y}\mathbf{Y}^T\mathbf{X}_2\mathbf{w}_2 & +\mathbf{X}_4^T\mathbf{Y}\mathbf{Y}^T\mathbf{X}_3\mathbf{w}_3 & +\mathbf{X}_4^T\mathbf{Y}\mathbf{Y}^T\mathbf{X}_4\mathbf{w}_4 & = \lambda_4\,\mathbf{w}_4
\end{array}$$

Initial values of $\mathbf{w}_i$ are computed from $\mathbf{X}_i^T\mathbf{Y}\mathbf{Y}^T\mathbf{X}_i\mathbf{w}_1= \lambda_i\,\mathbf{w}_i$, i=1,2,3,4.

Four score vectors are the results of each step. Supposing that the vectors are collected in a matrix $\mathbf{T}$, $\mathbf{T}=(\mathbf{t}_1,\mathbf{t}_2,\mathbf{t}_3,\mathbf{t}_4)$, the task is a stepwise regression of selection of variables. The variables (score vectors) are ranked according to how well they explain the variation in $\mathbf{Y}$. For each score vector the value of the explained variation, $|\mathbf{Y}^T\mathbf{t}_i|^2/(\mathbf{t}_i^T\mathbf{t}_i)$, is computed. Suppose, for example, that $\mathbf{t}_2$ has the largest explained variation. Then $\mathbf{Y}$ and $\mathbf{T}$ are adjusted for $\mathbf{t}_2$, $\mathbf{Y}\leftarrow\mathbf{Y}-\mathbf{t}_2\mathbf{q}_2^T/(\mathbf{t}_2^T\mathbf{t}_2)$ and $\mathbf{T}\leftarrow\mathbf{T}-\mathbf{t}_2\mathbf{s}_2^T/(\mathbf{t}_2^T\mathbf{t}_2)$, where $\mathbf{q}_2=\mathbf{Y}^T\mathbf{t}_2$ and $\mathbf{s}_2=\mathbf{T}^T\mathbf{t}_2$. For this reduced $\mathbf{Y}$ the explained variation is computed for the reduced vectors $\mathbf{t}_1$, $\mathbf{t}_3$ and $\mathbf{t}_4$. $\mathbf{Y}$ and $\mathbf{T}$ are again reduced for the score vector among these three that gives the largest explained variation. This is continued until all score vectors have been used or until there is a (reduced) score vector that does not give a significant explained variation. This and later score vectors are hence not used in the analysis. The criterion for not using a score vector in the multi-block analysis is given in Paper [VI]. This is a rather weak criterion. At a step a score vector is dropped only, if it is certain that it does not contribute to the modelling task. As in the case study below, the estimation procedure will give some overfitting. Therefore, some post-processing may be needed, like e.g. cross-validation of the results. There are many ways to carry out the cross-validation, e.g. for all blocks, for only one block at a time or to include cross-validation in the stepwise regression.

The score vectors between blocks can be highly correlated. This can be the case, for instance, if $\mathbf{X}_i$ is redundant in describing the $\mathbf{Y}$'s, when some other $\mathbf{X}_j$'s are used. This does not give any numerical problem in the estimation procedure. The score vectors that are found at each step are only used if they contribute to the regression equations. If the diagonal elements of $\mathbf{T}^T\mathbf{T}$ become too small due to high correlations, the corresponding variable (score vector) is not used. It might be that a score vector, say $\mathbf{t}_2$ of block 1, is highly correlated to some score vectors in the other blocks. This does not give us numerical problems, because $\mathbf{t}_2$ is only evaluated relative to block 1. The importance of multi-block methods is to emphasize the role of each data block in the modelling task by getting score vectors from the data blocks. For redundant data blocks we may get score vectors for some blocks that score vectors of other blocks may be able to account for, if we asked that question.

In summary, at each step four score vectors are found that are derived from the solution of the optimization task above. The score vectors are ranked according to their significance, and only significant ones are included in the analysis. If no score vector is found significant, the computations of finding score vectors stop.

2.7 Previous investigation on influence of cement characteristics and production conditions on cement properties

2.7.1 Methods of investigating the influence

In the many investigations of the influence of the cement characteristics on the cement properties multiple linear regression (MLR) or multivariable regression analysis is applied [27, 52, 53, 54]. The *x*-variables are usually well defined in a physical or a chemical meaning and could represent the amounts of the different minerals (from XRDA) and component composition (from XRFA) and fineness from measurements by Blaine's method or calculated from the particle size distribution. Any correlations between the *x*-variables could cause instability in MLR analysis [55]. In the cases of difficulties with determining the value of the defined variables by for instance interpretation of spectral variables, the spectral data should be included directly as *x*-variables instead. However, by including spectral data, the risk of correlation within **X** will increase. Instead of specific fineness, a particle size distribution will in some cases give more relevant information for explaining variation in the properties from the variations in the particle size [5]. From the more or less symmetrical shape of the curve and the describing the differential size distribution and the continuity of the curve, presence of correlation within **X** can be presumed. Examining the influence of the latent variables was then more relevant. For this purpose partial least square regression analysis (PLS) is an appropriate statistical method.

Besides ordinary multivariable regression, fuzzy logic [56], stepwise regression [57], genetic algorithms – artificial neural networks (GAs-ANNs) [58], gene expression programming (GEP) and neural networks (NNs) [59] and PLS [6, 24, 33, 60, II] have been applied in the evaluation of the model for prediction of cement strength. GAs-ANNs and PLS represent different types of multivariate calibration or modelling with hidden layers or latent variables. In Paper [II], the latent variables were taken into consideration in the sensitivity analysis while in [58] the hidden layers were not. In Paper [II], examples of sensitivity analysis in the form of a simulated variation of a latent variable from which cement properties are predicted are shown. In the Refs [56-59], only variables presenting chemical component composition, and not the mineralogy of clinker, were included in the modelling.

The sensitivity analysis can be applied in exploration as well as in optimisation. Exploration can be performed as a two-step operation: simulation of variation in the x-variables and prediction of variation in y [56, 58]. Akkurt *et al.* [56] defined the sensitivity analysis as feeding of input parameters (values of *x*-variables) at varying levels

into the developed model and producing prediction outputs of *y*. Significance or uncertainty is not taken into consideration. The sensitivity analysis has more a character of visualising the effects of the various *x*-variables on *y*. The term sensitivity analysis may be replaced in this case by the term verification of the model. However, a complex process with many process variables or use of many variables in characterisation of the product makes it necessary to visualise the variation in $\mathbf{x}$ and $\hat{\mathbf{y}}$ to enable people not skilled in PLS to understand and implement the results.

2.7.2 Influence on cement properties at early ages

The properties: Setting time and compressive strength, together with fineness and soundness, form the basis of all specifications for the cement. Therefore, a large number of investigations on the correlation between cement characteristics and the two properties have been published. According to Lea [5], fineness, amount of di- and hemihydrate of $CaSO_4$ and aeration of cement have major impacts on setting time. A pronounced influence of free lime on setting time as reported earlier in Refs. [5, 15], made it appropriate to include the amount of free lime as a variable in the investigation of the influence on cement characteristics.

The determination of setting time is affected to a marked degree by the quantity of water used in gauging. The amount of water required is that necessary to bring the cement paste to a defined consistency. The variable: Water content required to achieve standard consistency (SC) is defined to be a response variable in this work, but at the same time it can be regarded as an input *x*-variable in the investigation of the *y*-variable setting time. SC indicates the flow behaviour of cement pastes. Wallevik has studied the rheological properties of fresh paste, mortar and concrete [61, 62]. Considering that the cement paste behaves like a Bingham's plastic-viscous liquid, SC could for lower water cement ratio be related to the yield stress at which cement begin to deform plastically [63].

According to Mork [30], the more hemihydrate present, the better the flow properties over time, except initially, when the highest gypsum content gives the best flow properties. Vikan [64] has studied rheology and reactivity of cementitious binders with plasticizers. Correlations between "flow resistance" and variables expressing combination effects of Blaine's fineness, C_3A and C_3S, were evaluated. "Flow resistance" was measured as the area below the flow curve for a selected range of shear rate. The mineralogy of the cement was determined by multi-component analysis of an X-ray diffractogram.

Ellerbrock et al [27] have studied the influence of the grinding process on the particle size distribution and the properties of cement. They found the particle size distribution to be dependant on the type and mode of operation of the grinding system and on the grindability of the cement constituents. All the factors have an important influence on the amount of water required to achieve standard consistency (SC), setting behaviour and strength development of the cement. The major part of the mixing water required to achieve standard consistency is used for wetting the particles and filling the voids. A

smaller part is bound chemically by the hydration products. This part increases with increasing part of fine particle in the cement. Further, Ellerbrock et al [27] studied how interground but not reactive additives such as limestone filler reduce SC under conditions where the additive has a broad particle size distribution. Intergrinding an additive of narrow particle size distribution will also increase SC.

2.7.3 Influence on compressive strength

Knöfel [52] established a formula for predicting compressive strength at 28 days as a function of clinker phases. The strength increased most with increasing portions of alite and less by the increasing portions of belite and aluminate. The strength decreased with an increase in the portion of ferrite. Lawrence [65] has established a formula for predicting compressive strength at 1 day. The predicted strength increased with the amount of C_3S and decreased with decreasing amounts of C_3A and C_4AF. According to Aldridge [53], the influence of C_3S decreases with increasing age of curing whereas the influence of C_2S increases. Odler and Wonnemann [54] [66] have studied the effect of alkalis on Portland cement hydration. In Ref. [54] the effect of alkali oxides incorporated into the crystalline lattice of clinker minerals was studied and in Ref. [66] the effect of alkali sulphates.

Richartz [67] have studied the effect of the K_2O and the degree if sulphatization on the setting and hardening of cement. It was found that in the course of hydration, between 6 hours and 1 day, the reactivity of C_3S at first increase with increasing K_2O content of clinker but the further reaction is inhibited by the K_2O. For this reason, the early strength of the cement increases with increasing K_2O content, but the strengths at 7 and 28 days decrease.

Ono developed methods to interpret kiln conditions and formulae to predict 28-day mortar-cube strength (F28d). Ono latest equation (from Campbell [8]) is:

$$\begin{aligned} F(28d)[MPa] &= 0.513 \cdot (alite\,size[\mu m]) + 2.027 \cdot (alite\,birefringence) \\ &+ 0.344 \cdot (belite\,size[\mu m]) + 2.1798 \cdot belite\,color + 25.309 \end{aligned} \tag{23}$$

The alite size indicates the heating rate, alite birefringence the maximum temperature, belite size the retention time at maximum temperature and the belite colour the degree of cooling. The equation should be modified if the magnesia content is higher than 1.8 % or lower than 1.2 %. According to Ono [40] the alite birefringence will vary with lattice constants of alite, which in turn will vary with the amount of SO_3 and magnesia as well as with the burning temperature and hydraulic activity. From this he concluded that the X-ray powder diffraction analysis may be an alternative method to microscopy with respect to characterizing and controlling the quality of clinker. Tricalcium silicate exhibits seven polymorphs depending on the impurities and the temperature: T_1, T_2, T_3 for the three triclinic forms, M_1, M_2, M_3 for the three monoclinic forms and R for the rhombohedral one [68]. The most common modifications are M_1 and M_3.

The formation temperature for M_3 is higher than for M_1. Maki et al [69] have shown that the M_1 and M_3 can be distinguished by means of birefringence measurements. Stanek and Sulovský [70] have monitored the influence of the alite polymorphism on the strength of cement. They found that the strength of cements with the M_1 modification was 10 % higher than the strength of cement with the M_3 modification at ages up to 28 days. According to [70], the M_3 form has two times higher birefringence than M_1 does. The conclusion in Ref. [69] will therefore contradict Eq 1 which gives an increase in the compressive strength at 28 days with an increase in the alite birefringence.

Portions of XRD powder pattern of the different modifications of C_3S were presented by Maki and Kato [41]. The 2 θ ranges of the patterns being examined were 32-33 º and 51-52 º. The peak at approximately 32.6 º could explain the change in compressing strength from the change in the birefringence of alite. The profile of the peak rather than its position is changing by changing the modification from M_3 to M_1. The peak position seems, however, to move slightly to a lower 2 θ angle with an increase in M3 and a decrease in M1. In an XRD powder pattern of cement the C_3S peak at 32.6 º will overlap a peak of belite, which will make interpretation of the XRD pattern even more complicated.

Theisen and Johansen [71] examined the influence of prehydration of Portland cement on its strength development. The effect of an increase in prehydration was a decrease in the early compressive strength. The decrease correlated linearly with the corrected loss on ignition, w_k, determined from TGA. Depending on the clinker properties, the compressive strengths at 3 and 7 days were decreased to a smaller extent than the strength at 1 day. The 28 days strength was unaffected or only slightly increased.

Tsivilis et al [72] studied the contribution of the fineness of the cement on its strength. The measurement showed that most important variables were uniformity factor and the content of particle size fraction 3-32 μm. The uniformity factor, n, was determined from the slope of a curve describing modified Rosin-Rammler distribution

$$\log(\log(100/R) = n\log(d)) + b \qquad (24)$$

where R is residue at sieve with openings d. The influence of the 3-32 μm fraction and of the uniformity factor is higher in cements with higher specific surface (< 400 kg/m^2). The optimal granulometric distribution of cement is a continuous and steep (high uniformity factor) distribution with a high content of 3-32 μm fraction and low content of very fine particles.

Tsivilis and Parissakis [57] developed a mathematical model for predicting cement compressive strength after 2, 7 and 28 days. The model is based on stepwise regression. The strengths at early ages are affected mainly by the fineness variables. At higher ages the chemical-mineralogical synthesis of cement influences the growth of strength. The 28 days strength is strongly affected by the distribution of the cement particles in the size fractions < 3 µm, 3-16 µm, 16-24 µm and 24-32 µm.

Garcías-Casillas et al [73] have developed a mathematical model for predicting compressive strength at 3, 7 and 28 days. A linear model was chosen to explain the relationship between cement performances and cement characteristics. The number of variables in the model was reduced by stepwise regression. The conclusion coincides closely with the conclusion in Ref [57].

3 CONTRIBUTIONS

3.1 Developing method for model-based optimization

From the experiences and conclusions in Ref. [15], an idea of how to optimize a response variable constrained by principal directions of variation in the observation **X**-matrix [I]. This type of optimization is later called model based-model based optimization (MBO). MBO had the form of a linear program, where the constraints describing the influence of one variable on the others were given by one PLS component or latent variable or a combination of several. Linear programs are much used for solving economic problems. The function to be minimized (or maximized) is then expressing a function of cost. In MBO the cost function is replaced by a function from the regression analysis. The feasibility region is reduced to a straight line of infinitesimal thickness. The length of the line is bound by the min and max limits of variation of at least one x. Optimal y was achieved by combining the original loadings and including these new loadings in a new optimization. A manual search for the linear combination giving the optimal point was performed. MBO was demonstrated on a PLS model for predicting compressive strength of cement from the particle size distribution.

At the 9th Scandinavian Symposium on Chemometrics two papers on the manufacture and design of cement – application of sensitivity analysis in exploration and optimization, were presented [II, III]. In the first paper, which emphasises exploration, a review of earlier works on multivariate data analysis is presented and also the calculation of confidence intervals of the regression coefficients [50] and the predicted response variables [74]. Referring to the examinations in Refs [72, 73], the variations of compressive strength up to 28 days were predicted from simulated variations of particle size distribution. One of the simulations gave no variation in specific fineness (Fig 9, Chapter 2.4.4). The predictions and the simulations are presented in Paper [II]. The use of confidence intervals in the sensitivity analysis is presented and comparisons of confidence intervals of $\hat{y}$ predicted from a single x and a latent variable, respectively, were made. It was concluded that the influence of a latent variable was much more significant than that of a single x-variable. Simulation of variation of **X** constrained by PLS-components or latent variables will therefore be a better basis for the design of the cement and will improve quality control during production. Implicitly, the optimization of production conditions and product characteristics to achieve optimal product properties should be based on simulated variations of latent variables.

In Paper [II] the principles of block partitioning (Eq 19, chapter 2.6.4) is presented and their use in establishing an artificial observation matrix where only a part of the x-

variables is varied. One of the demonstration cases was prediction of compressive strength from particle size distribution (PSD) whose variation was simulated in such a way that the overall specific fineness was kept constant and equal to its mean variable (Fig 9, chapter 2.4.4). Another case of demonstration was predictions in two steps from the production conditions in a cement mill via characterized superficial microstructure of the cement (Fig 11). A combination of PLS-components was chosen which gave no variation in the feed of gypsum, to reveal better the influence of the water spray into the mill on the properties at early ages. The DTGA-curves in the temperature range 85 – 217 ˚C indicate the degree of dehydration of gypsum described by the reaction $CaSO_4 \cdot 2H_2O = CaSO_4 \cdot ½ H_2O + 1½H_2O$.

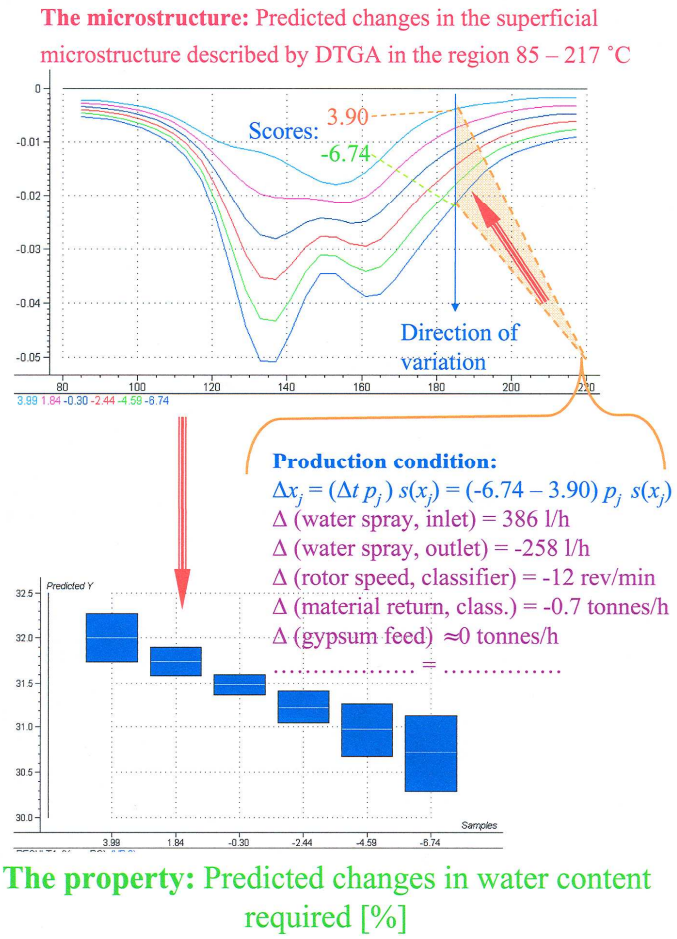

Figure 11. Prediction of variation in the water content required to achieve standard consistency in two steps from the production conditions in the cement mill via the superficial microstructure of cement.

Paper [III] deals with further development of the model-based optimisation presented in Paper I. The manual search for the linear combination giving the optimal point was replaced by an automatic search using simplex method for function minimisation developed by Nelder and Mead [51]. The principle of the optimization is presented in chapter 2.6.5. The program OptPilot consists of three subprograms. The first one, MainPilot, does minimising or maximising constrained by one original PLS-component or one equal to a combination of several, the second one, Optimal, performs searching for the optimal combination of PLS-components to achieve max and min *y*, and the third one, Modelparms, updates the PLS-model by regression on updated *y* and **X**-matrices. Schematic presentation of the principles of OptPilot is presented in Fig 12 and a flow diagram of the structure of OptPilot in Fig 13. The demonstration of a PLS model for predicting compressive strength of cement from the particle size distribution in Paper [I] is continued in Paper [III].

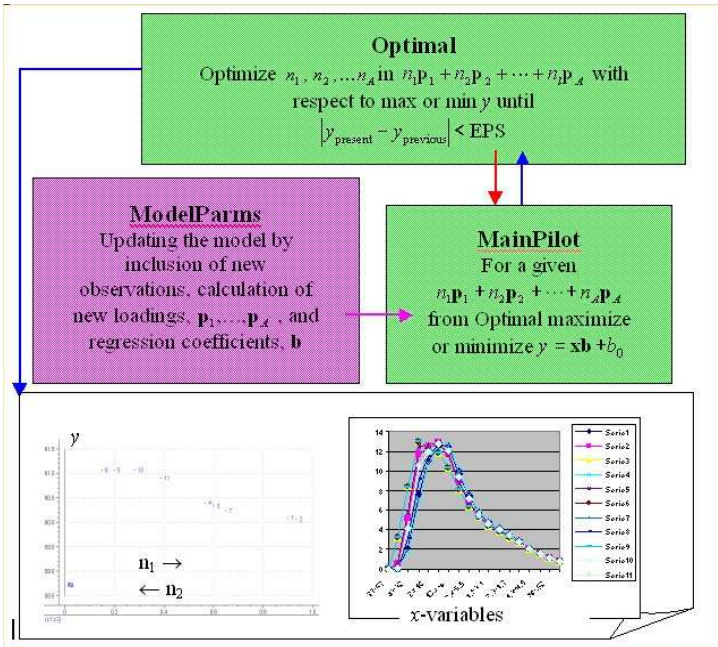

Fig 12. Schematic presentation of the principles of Optpilot

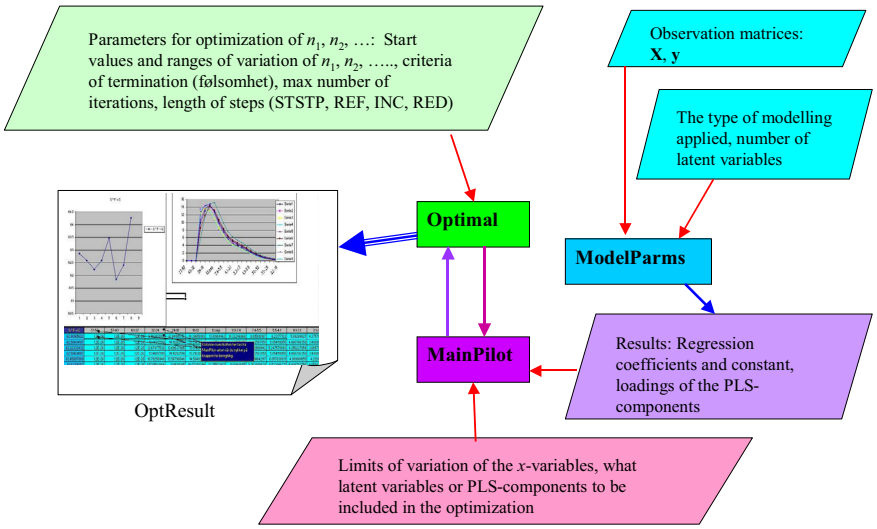

Figure 13. The structure of Optpilot given as a flow diagram

The original contribution of Papers [I, III] is the development of the program for model-based optimization of cement properties like compressive strength constrained by the latent structure of the observation matrices representing variation in for example PSD. Paper [II] presents a review of the previous work of the author, and also gives original presentations of sensitivity analyses in the form of simulation and prediction of compressive strength, amount of water required to achieve standard consistency. Prediction of compressive strength from a complete particle size distribution of cement has not been presented before.

3.2 Modelling compressive strength of cement on the characteristics of cement, prediction and optimization of potential compressive strength of clinker from its mineralogy

To establish a basis for later prediction and sensitivity analysis in Papers [V, IX], a PLS-model of compressive strength as a function of the characteristics of cement was evaluated in Paper [IV]. The observation **X**-matrix was made up of the four sub-matrices: $\mathbf{X}_{\text{mineralogy}}$, $\mathbf{X}_{\text{particle size distr}}$, $\mathbf{X}_{\text{superficial micr LT}}$ and $\mathbf{X}_{\text{superficial micr HT}}$ (LT and HT refer to the low and high temperature range of the differential thermogravimetric analysis (DTGA)) . The different parts of the characteristics are presented in Figs 14-17. The two selected XRD regions or ranges presented in Fig 14, cover the responses for all the important cement

minerals. The major differences between the PSD-curves are those belonging to different types of cement, but there are also pronounced differences within each type.

The objective of the work was to establish a statistical model for the prediction of cement properties for all types of neat cement as well as cement containing small amounts (~5%) of limestone filler. To attain this objective, variables which presented a complete characterization of the microstructure of the cement, and observations which represented a great variety of types of cement, were included in the PLS. The distribution of observation in a space of t-score was shown and the evenness and the span of the distribution were discussed. The influence of the characteristics variables was evaluated and discussed from loading plot and regression coefficients of the *x*-variables. The indication of high influence of $x_{superficial\ micr\ HT}$ by high value of weighted regression coefficients $\mathbf{b}_w$ of the variables were contradicted by the uncertainty limits of the regression coefficients determined from Jack knifing estimation [50]. Most of the variance in the compressive strength up to 28 days can be explained from the variances of the variables describing the mineralogy and the particle size distribution. The variables describing the superficial microstructure influenced the compressive strength at 28 days less than the compressive strength at 1 day.

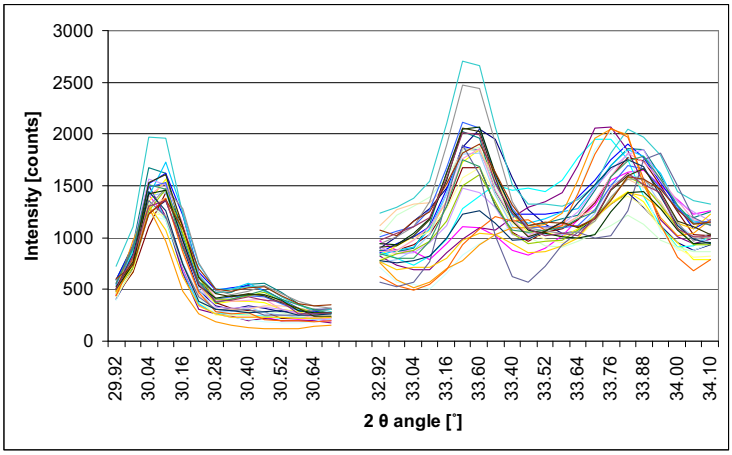

Fig 14. Mineralogy. The mineralogy of clinker part of the cement described by the XRD-profiles in the 2θ - ranges 29.88 – 30.70º and 32.90 – 34.10º, of every fifth observation of totally 146 observations.

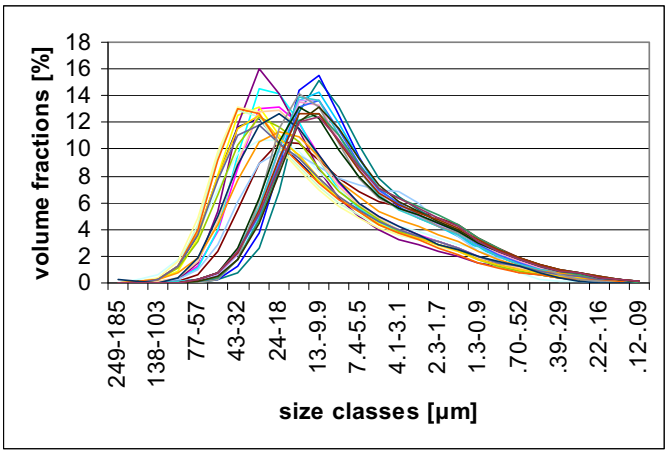

Fig 15. Particle size. The particle size distributions (PSD), of every fifth observation of totally 146 observations

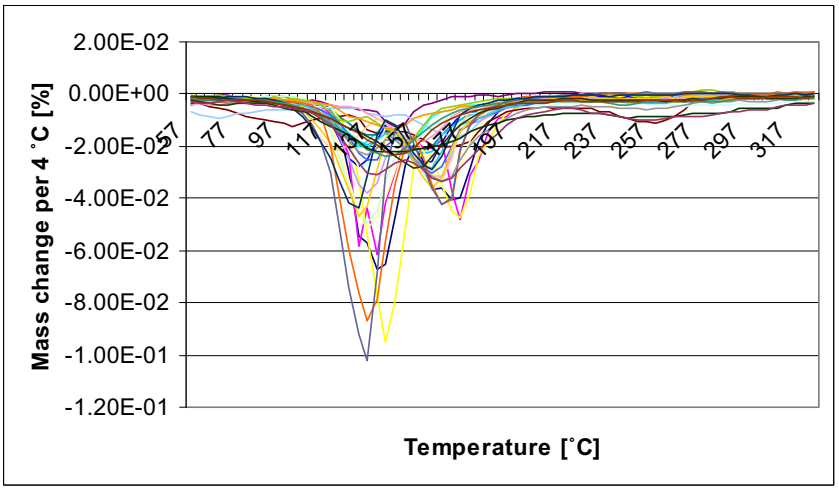

Fig 16. Microstructure, low temperature. The superficial microstructure from DTGA, describing the degree of dehydration of gypsum and prehydration of the clinker minerals of every fifth observation of totally 146 observations. The variables express the mass change [%] per 4 ºC

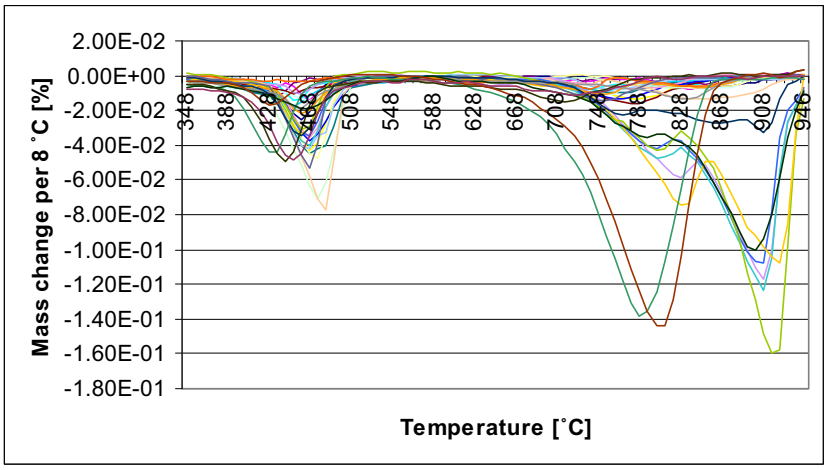

Figure 17. Microstructure, high temperature. The superficial microstructure from DTGA, describing the degree of prehydration of free lime, carbonation of $Ca(OH)_2$ and the amount of limestone filler of every fifth observation of totally 146 observations. The variables express the mass change [%] per 8 ºC

Prediction of potential compressive strength of Portland clinker from its mineralogy is presented in Paper [V]. Making a semi artificial observation matrix out the observation matrix in Paper IV, potential compressive strength of Portland clinker was predicted from $\left(\mathbf{X}_{\text{mineralogy}}\,(M \times K_{\text{mineralogy}}) \;\middle|\; \begin{matrix} (\bar{\mathbf{x}}_{\text{part distr}})_1 \\ \vdots \\ (\bar{\mathbf{x}}_{\text{part distr}})_M \end{matrix} \;\middle|\; \begin{matrix} (\bar{\mathbf{x}}_{\text{superficial micr LT}})_1 \\ \vdots \\ (\bar{\mathbf{x}}_{\text{superficial micr LT}})_M \end{matrix} \;\middle|\; \begin{matrix} (\bar{\mathbf{x}}_{\text{superficial micr HT}})_1 \\ \vdots \\ (\bar{\mathbf{x}}_{\text{superficial micr HT}})_M \end{matrix} \right)$ where M is the number of rows in the original observation **X**-matrix. All the submatrices except that one that describes the variation in the mineralogy were kept constant and equal to their mean values. The influence of the mineralogy on the potential compressive strength was examined by simulation, optimization and prediction. The latent structure of XRD intensities is found by evaluating a new PLS model for predicting potential strength from the XRD intensities only. Variation in the intensities was simulated by model-based optimizations of $\mathbf{x}_{\text{mineralogy}}$ to achieve compressive min and max strength at either 1 or 28 days. An example examination of influence of the mineralogy on the compressive strength development up to 28 days emphasized the potential compressive strength at 1 day is shown in Figs 18 a and b. Potential compressive strength at one day was minimized and maximized by varying the mineralogy of clinker. The potential compressive strengths at 2, 7 and 28 days where predicted from the optimal values of the mineralogy to achieve min and max compressive strength at 1 day. In minimising and maximising the potential compressive strength at one day, the variables describing the amounts of C_3S and aphthitalite were found to be the most influential. Change in the

structure of C_3S indicated by a shift in its XRD-peak in the selected 2θ - ranges influenced the potential compressive strength at 28 days significantly.

The original contribution in Paper [IV] is the inclusion of the complete characteristics like mineralogy, PSD and superficial microstructure of cement in the modelling of the compressive strength development and the use of the spectral data in these characterisations. The use of block partitioning to evaluate the model for predicting the potential compressive strength up to 28 days of clinker and minimizing and maximizing the potential strength from the mineralogy described by XRD-curves, are original contributions [V].

a)

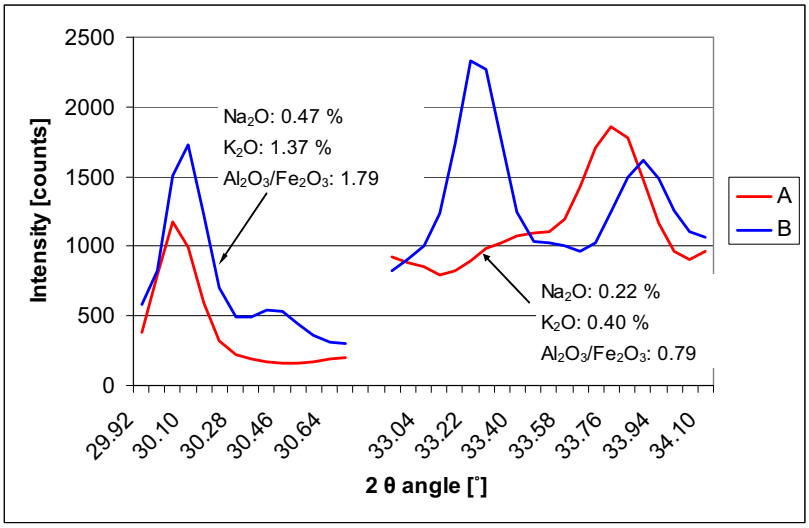

b)

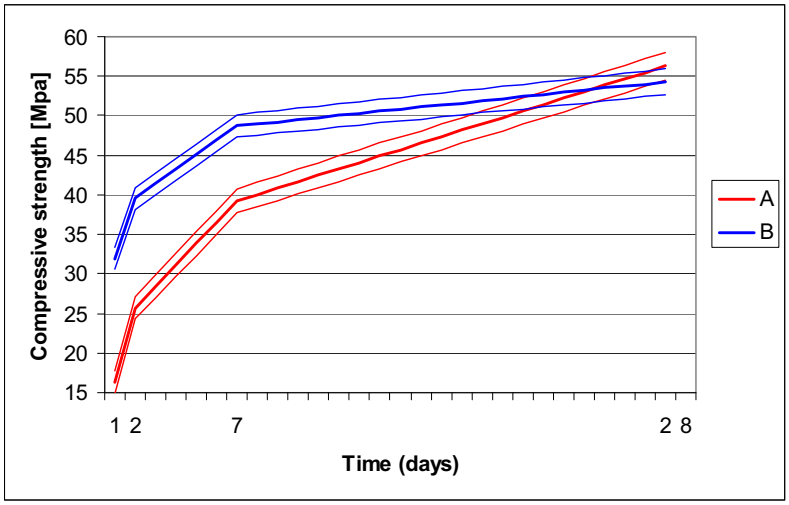

Fig 18. Minimizing and maximizing potential compressive strength of clinker at 1 day (PCS1)

a) Optimization of mineralogy of clinker described by the XRD-profiles in the 2θ - ranges 29.88 – 30.70º and 32.90 – 34.10º with respect to achieving min (A) and max PCS1 (B). $(n_1, n_2, n_3, n_4, n_5) = (0.717, 0.054, 0.090, 0, 0.138)$
b) PCS at 1, 2, 7 and 28 days predicted from the XRD-profiles in Fig 11 a). The confidence intervals of $\hat{\mathbf{y}}_i$ is $\hat{\mathbf{y}}_i \pm 1s(\hat{\mathbf{y}}_i)$.

3.3 Application of multi-block methods in cement production

The principles of the multi-block methods presented in Papers [VI, VII] are more briefly explained in chapter 2.6.6. Paper [VI] presents a unified approach to modelling multi-block regression data. The starting point is a partition of the data **X** into L data blocks, $\mathbf{X}=(\mathbf{X}_1, \mathbf{X}_2, \ldots, \mathbf{X}_L)$ and the data **Y** into M data blocks, $\mathbf{Y}=(\mathbf{Y}_1, \mathbf{Y}_2, \ldots, \mathbf{Y}_M)$. The methods of linear regression, $\mathbf{X} \Rightarrow \mathbf{Y}$, are extended to the case of a linear relationship between each $\mathbf{X}_i$ and $\mathbf{Y}_j$, $\mathbf{X}_i \Rightarrow \mathbf{Y}_j$. A modelling strategy is used to decide if the residual $\mathbf{X}_i$ should take part in the modelling of one or more $\mathbf{Y}_j$'s. The methods were illustrated by simulated data and data from cement production. The data in the production case were from grinding cement and are the same as included in the investigation presented in Papers [II, VIII]. The observation **X** and **Y** matrices contained 163 and 3 variables, respectively, and 50 observations. **X** and **Y** were partitioned into the following sub-blocks:

$\mathbf{X}_1$:	Chemical composition
$\mathbf{X}_2$:	Superficial microstructures
$\mathbf{X}_3$:	Variables describing particle size distribution
$\mathbf{X}_4$:	Process variables
$\mathbf{y}_1$:	Setting time
$\mathbf{y}_2$:	Water content required to achieve standard consistency

$\mathbf{y}_3$: Compressive strength at one day

The data structure of the modelling was, however, different than the one in Papers [II, VIII] in that the properties at early age were predicted from the observation **X** containing all sub **X**'s above. In Paper [II] the properties were predicted either from $\mathbf{X}_1$ and $\mathbf{X}_4$ directly or in two steps from $\mathbf{X}_4$ via $\mathbf{X}_2$ and $\mathbf{X}_3$. The results of the work in Paper [IV] showed that $\mathbf{X}_2$, $\mathbf{X}_3$ and $\mathbf{X}_4$ influenced $\mathbf{y}_1$ equally while $\mathbf{X}_1$ had only a minor influence, $\mathbf{X}_2$ had a major influence on $\mathbf{y}_2$, and $\mathbf{X}_3$ influenced $\mathbf{y}_3$ the most.

The objective with this work is optimize the model with respect to predictability whereas in Papers [I, III, V, VIII, IX] optimizing **X** based on an existing PLS model to achieve min and max **y** with max confidence in $\hat{\mathbf{y}}$, is emphasized.

The data used in the application of multi-block methods in cement production [VII] is from the observations in Paper [IV]. Compressive strength at 1 day of Portland cement as a function of microstructure or characteristics of cement was statistically modelled by the multi-block regression method. Applications of these methods are carried out for the characterisation of the microstructure with respect to explaining the variation of the cement properties. The four blocks of the observation **X** matrix, whose role or influence on the compressive strength to be identified are the same as in Papers [V, VI]; $\mathbf{X}_{\text{mineralogy}}$, $\mathbf{X}_{\text{particle size distr}}$, $\mathbf{X}_{\text{superficial micr LT}}$ and $\mathbf{X}_{\text{superficial micr HT}}$. The score vector of each block was analyzed together with score vectors of other blocks. Stepwise regression was used to find a minimum number of variables of each block to achieve max explanation of the variance in compressive strength.

The multi-block method proved to be useful in evaluating an optimal model respect to max explanation of the variance in the response variable with a minimum number of x-variables. The multi-block method proved also to be useful in finding what part of the data which has the highest influence on the compressive strength. The block representing the mineralogy, $\mathbf{X}_{\text{mineralogy}}$, had the dominant influence on the compressive strength, then $\mathbf{X}_{\text{particle size distr}}$ followed. The results were compared with standard PLS regressions. They coincide with the results in Paper [IV]. The results also confirm the usefulness of partitioning the observation **X** matrix in making an artificial observation **X** matrix for predicting potential compressive strength of clinker from its mineralogy.

The original contribution given in Papers [VI, VII] is the use of multi-block methods in examining the influence of the different parts of the characteristics of cement like mineralogy, PSD and superficial microstructure on the compressive strength of cement.

3.4 Optimizing production conditions to achieve optimal cement properties

Two cases of optimization of productions conditions in a cement mill and in a cement kiln, respectively, are presented in Papers [VIII, IX]. Setting time (ST) and the amount of water required to achieve standard consistency (SC) were predicted from the production

or process conditions in the cement mill and compressive strength and potential compressive strength of clinker (PCS) up to 28 days were predicted from the production conditions in the cement kiln. In both cases the observation **X** matrices were partitioned into two submatrices, one containing the information of the variation in the component composition of the cement, $\mathbf{X}_{\text{material}}$ [VIII] and $\mathbf{X}_{\text{component}}$ [IX], the other the variation in the process conditions. Models for predicting potential properties of the processes were evaluated. Sensitivity analysis based on simulation, optimization and prediction made it possible to study the influences of the processes on the cement properties.

The contribution of each *x*-variable to the optimization of a property was studied by comparing the calculated scaled difference in the *x*-variables giving max difference in the property. The *x*-variables were ranked by the absolute values of their weighted differences indicating the degree of influence on the property being optimized. The weighted differences were calculated by the formula:

$$\text{w.diff}\,(x_k). = \left| \frac{x_k\,(\text{B}) - x_k\,(\text{A})}{\text{s}\,(x_k)} \right| \qquad (23)$$

Where: A and B denote the optima of **x** giving minimum and maximum *y*, respectively.

The characteristics of the cement; superficial microstructure and mineralogy of clinker were predicted from optimal production conditions giving min and max SC and ST and min and max PCS, respectively. This was done to explain more mechanistically or chemically the variation in the properties. An example of optimization of PCS1 is in Fig 19 and Table 4 and prediction of mineralogy from optimal production conditions in the cement kiln in Fig 20.

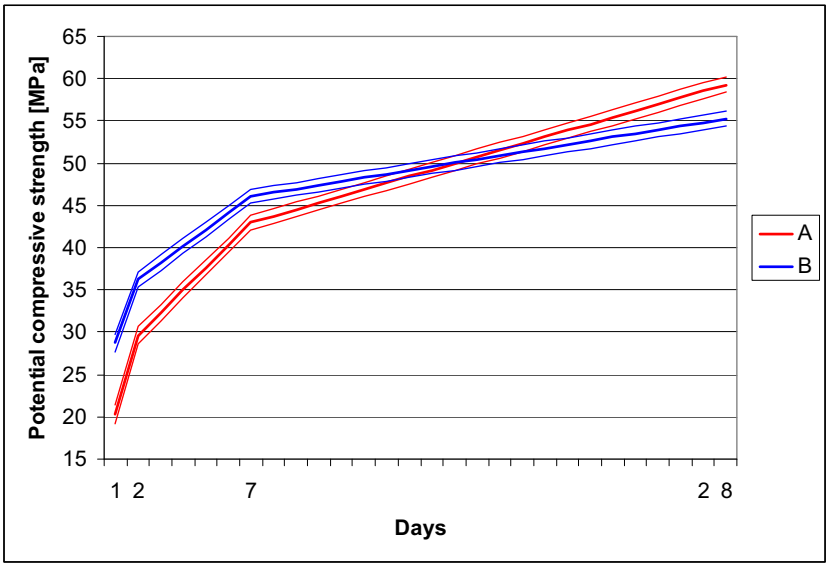

Fig19. The results from minimizing and maximizing PCS1, potential compressive strength at 2, 7 and 28 days are predicted from the optima of **x** (some of them are presented in table 4). The confidence intervals of $\hat{\mathbf{y}}_i$ is $\hat{\mathbf{y}}_i \pm s(\hat{\mathbf{y}}_i)$. The optimal combination of latent variables $(n_1 \quad n_2 \quad n_3) = (1 \quad 0 \quad 0)$ for achieving min and max PCS1.

Table 4: The results from minimizing and maximizing PCS1, changes in some of the *x*-variables to achieve min and max PCS1. The numbering of the variables refers to the ranking position of the variables.

Variables	Optima of **x** giving minimum (A) and maximum (B) of ST		Weighted difference, abs. value
	A	B	
x-variables, ranking based on the absolute value of weighted difference:			
1. Velocity of the grates in first part of the clinker cooler [recip/min]	7.97	11.64	2.40
2. Feed of tyres [tonnes/h]	0	0.7926	2.38
3. Velocity of the grates in the second part of the clinker cooler [recip/min]	22.37	17.50	2.21
4. Pressure, kiln hood [Pa, gauge]	-52	-45	2.05
5. Current or effect needed for maintaining constant speed of rotation of the kiln [A]	377	312	1.97
6. Concentration of CO at ESP [%]	0	0.095	1.95
7. Specific fineness, raw meal [m^3/kg]	315	353	1.65
8. Secondary air temperature [ºC]	1164	1069	1.56
9. Pressure, conditioning tower no 1 [kPa, gauge]	-6.72	-6.40	1.55
10. Temperature, in the lowest cyclone in the preheater [°C]	907	890	1.16
11. Feed of raw meal [tonnes/h]	235	223	0.92
12. Secondary feed of coal [tonnes/h]	8.58	7.54	0.77
13. NO_x emissions [mg/Nm^3]	951	776	0.67
14. Total volumetric flow of air into the clinker cooler [m^3/h]	63.2	64.1	0.61
15. Primary feed of solid hazardous waste [tonnes/h]	0.481	1.000	0.52
16. Pressure, conditioning tower no 2 [kPa, gauge]	-6.51	-6.40	0.44
17. Opening of valve tertiary air channel [%]	63.7	65.5	0.39
18. Primary feed of oil [m^3/h]	0	0.35	0.39
19. Rotational speed, kiln [rev/h]	80.5	80.1	0.11
20. Primary feed of coal [tonnes/h]	6.75	6.66	0.07

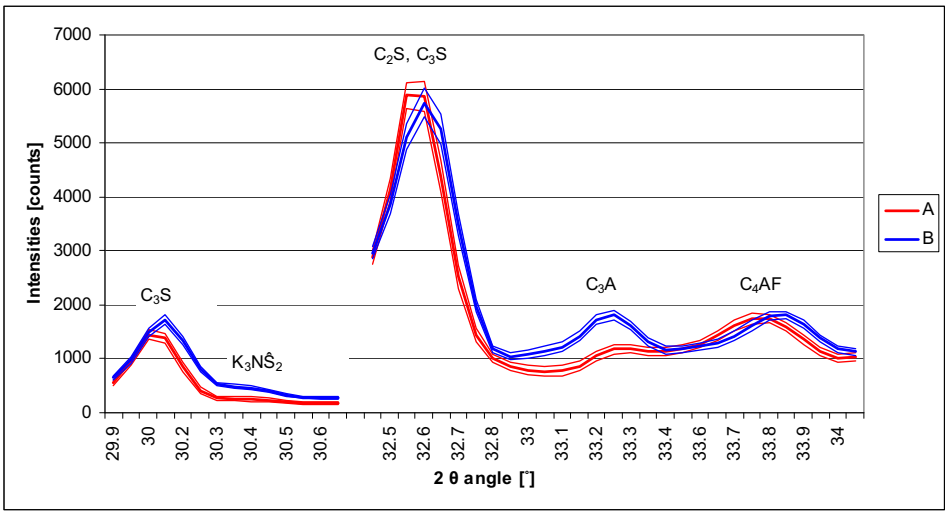

Fig 20. Optimal mineralogy of clinker described by the XRD-profiles in the 2θ-ranges 29.92 – 30.70º and 32.42 – 34.10º predicted from the production variables giving min (A) and max PCS1 (B). The confidence intervals of $\hat{\mathbf{y}}_i$ are $\hat{\mathbf{y}}_i \pm s(\hat{\mathbf{y}}_i)$.

The process variables of the cement mill: *the pressure of the air passing the dust filter*, and *the speed of the rotor in the classifier,* were found to be the most influential variables in minimizing and maximizing the water amount required to achieve standard consistency (SC). The amount of water sprayed into the first chamber of the cement mill influenced SC positively. The x-variable influenced negatively the degree of dehydration of gypsum, which explained positive influence of the variable on SC. The results from DTGA indicated a dispersive effect of the water spray on the cement in the grinding process. The process variables: *the amount of grinding aid* and *the total electric consumption* were found to be the most influential variables in minimizing and maximizing the setting time (ST).

Significant min and max PCS at 1 and 28 days, respectively, was achieved by optimizing the production conditions in the kiln. The influence of production conditions alone on the strength at 28 days was higher than on the strength at 1 day. XRD patterns predicted from the optima of the production conditions indicated a great influence of the ratio between the amounts of the polymorphs, M_1 and M_3, of C_3S on the compressive strength. The M_3 form can be related to clinker burnt at a higher temperature. The latter type of clinker is used in the production of high strength cement.

The original contributions of Papers [VIII, IX] are the optimizations of potential compressive strength from production conditions in the cement kiln and optimizations of amount of water required to achieve standard consistency and setting time from the production conditions in the cement mill.

4 CHALLENGES

Partitioning the observation X-matrix and relate each submatrix to a specific part of the production, challenges the fact that one type of material characteristics caused by one part or step of the production may influence the conditions of the next step of the production and the characteristics caused by this step. As mentioned in chapter 2.3.3 the influence of the clinker minerals (component composition and crystal size distribution) on the grindability of clinker has been studied [29]. The strong correlation between the grindability and the Bogue calculated belite and the crystal size of alite indicates influences of the mineralogy on the particle size distribution of the produced cement as well. The particle size distribution could be related to production conditions in the kiln but not as much as to the production conditions in the cement mill.

In the simulation part of the sensitivity analyses the different parts of the characteristics as mineralogy, particle size distribution and superficial microstructure have been varied separately independently of the other parts. In a cement of higher fineness, more of the surface is likely to be exposed to moisture and more of the cement will be prehydrated. The finer the cement that is ground together with the limestone filler, the lower the temperature of decarbonation of limestone filler will be (Fig 9, chapter 2.4.4). From a characterisation or measurement point of view, there may be a relation between particle size distribution and the superficial microstructure measured by TGA.

The multi-block method can handle the problem of correlating variables from different blocks, to a certain degree by analyzing the score vector of each block together with score vectors of other blocks [VI, VII]. The problem connected to sensitivity analysis based on simulated variation on one single block only, could be solved by redefining the block with respect to the content of variables or by making a new block out of two or several previous blocks.

The characteristics of the cement; superficial microstructure of cement from DTGA and mineralogy of clinker from XRDA, were predicted from optimal production conditions with respect to cement properties [VIII, IX]. This was done to explain more mechanistically or chemically the variation in the properties. Another way to explain the strength development mechanistically is presented by Kjellsen [21]. The strength development is compared with the change in the microstructure in the cement paste during hydration. The experimental investigation included cement paste, mortar and concrete. The influence of the characteristics mentioned above of cement on the change in the microstructure during hydration and further correlation of the results with the strength development is still not known to a sufficient degree.

Difficulties in predicting cement properties from fly ash cement EN 197-1-CEM II/A-V 42.5 R have been discussed. The high amount of amorphous material in fly ash cement makes it difficult to characterise the mineralogy by XRDA. Characterizing fly ash cement by TGA/DTGA gives a DTGA-curve distinctly different from that of neat cement. The

curves indicate the presence of materials that are easily oxidised and calcium carbonates. The DTGA-curves will, however, be difficult to interpret quantitatively, and accordingly, defining variables to present the interpretation, will be impossible. In any case, the curves might contain valuable information to give a good model for prediction of compressive strength. The ability and the potential of PLS models to predict cement properties from spectral data like the DTGA curves have been documented in this work. The proportion of fly ash cement is increasing in the Norwegian market. More attention should therefore be paid to investigations on the interaction between the microstructure of fly ash cement and its properties.

5 CONCLUSION

The characterizations of the mineralogy by XRDA, the superficial microstructure by TGA and particle size distribution of the cement seemed to give sufficient information for predicting cement properties like compressive strength from the characteristics of cement. The correlation within observation matrices made it necessary to apply methods of multivariate data analysis like partial least square regression (PLS) in the analysis of correlation between the cement characteristics, the production conditions and the cement properties.

Based on a sensitivity analysis that focuses the influence of input variables on a response variable, a program for model-based optimization was developed. Constraining the optimization by the latent structure of the observation matrix containing variation in the input variables, an optimal value of high confidence of the response variable was achieved. The applicability of the model-based optimization and reliability of the results were confirmed by examination on how the cement characteristics and production conditions in the cement mill and kiln influence the cement properties.

The results from model-based optimization examining the different parts of the cement characteristics coincided with the results from the multi-block regression analysis. Without any use of sensitivity analysis, the application multi-block methods showed directly which parts had the greatest influence on compressive strength of cement. The mineralogy had the most dominant influence on the strength, followed by the particle size distribution. The results of multi-block methods confirmed the usefulness of partitioning the observation **X** matrix in making an artificial observation **X** matrix for predicting potential compressive strength of clinker from its mineralogy.

The application of multivariate data analysis, sensitivity analysis and model-based optimization is very useful in the design and manufacture of cement. The methods enabled tailoring of cement aiming at target values of properties like compressive strength, setting time and initial flow properties. The tailoring can be based on the variables representing the characteristics of cement as well as the variables representing the production conditions in the cement kiln and the cement mill. The max values of the compressive strengths at 1 and 28 days were achieved by optimizing the production conditions in the kiln giving the optimal mineralogy. Optimal values of cement properties

at early ages were achieved by optimizing the production conditions in the cement mill giving the optimal superficial microstructure.

The methodologies demonstrated in this work are not limited to strength, amount of water required to achieve standard consistency and setting time, but it is also applicable to other parameters difficult and expensive to obtain like the microstructure of the paste. The parameters may be optimized via prediction from cement characteristics before actually documenting the most promising final products.

6 REFERENCES

[1] Bye, G. C., Portland cement, Composition, production and properties, 2nd Ed., *Thomas Telford Publishing*, London 1999, 1-5

[2] Tokheim, L.-A., The impact of staged combustion on the operation of a precalciner cement kiln, *Doctoral thesis at Norwegian University of Science and Technology*, Porsgrunn 1999

[3] Thomassen, T. R., Document PR0074: Prosessbeskrivelse for produktutvikling, *Management System Norcem AS*, 2007

[4] Wallevik O. H., Den ferske betongens reologi og anvendelse på betong med og uten tilsetning av silikastøv, Doktor ingeniøravhandling 1990:45, *ved Universitetet i Trondheim, Norges tekniske Høgskole,* Trondheim 1990

[5] K. Svinning, K. A. Datu, Prediction of microstructure and properties of Portland Cement from production conditions in cement mill. Part I: Evaluation of prediction models, *Proceedings of 11th international congress on the chemistry of cement*, Durban 2003

[6] Svinning K, Justnes H, Viggh E, Bremseth S K, Johansson S-E, 'Examination of clinkers from four Scandinavian plants with respect to microstructure and cement properties', *Proceedings of the 22nd International Conference on Cement Microscopy, Montreal* 2000, 137-153

[7] Martens, H., Næs, T., Multivariate calibration, 2nd edition, *Chichester: Wiley* 1989

[8] Campbell, D. H., "Microscopical examination and interpretation of Portland cement and clinker", 2nd ed., *Portland Cement Assoc*. Skokie 1999

[9] Schneider, R., Pyrostep® - the 3rd grate cooler generation, *KHD Symposium '92*, Köln 1993

[10] Müller-Pfeiffer, M., Modern grinding techniques – overview and new results, *Modern Grinding Techniques, ecra*, Bygdoszcz 2005

[11] Svinning K., Tokheim L.-A., Bjerketvedt D., Statistical analysis of the correlation between NOx emissions and production conditions in a cement kiln applying staged combustion, *World Cement* 29(1998)68-75

[12] Viggh, E., Edholm, A., The effect of burner configuration when using plastic derived fuels on clinker microstructure, *Proceedings of the 18th International Conference on cement microscopy*, Houston 1996, 125-133

[13] Caveny, B., Waste tires fuel oilfield cement manufacture, *Proceedings of the 20th International Conference on cement microscopy*, Guadalajara 1996

[14] Fredvik, T. I., Initial strength development of fly ash and limestone blended cement at various temperatures predicted by ultrasonic pulse velocity, *Doctoral thesis at Norwegian University of Science and Technology*, Trondheim 2005

[15] K. Svinning, K. A. Datu, "Prediction of microstructure and properties of Portland Cement from production conditions in cement mill, Part II: Prediction and sensitivity analysis", *11th international congress on the chemistry of cement*, Durban 2003
[16] Schindler A., Application Sheet AS-043-2006, *Netzsch Gerätebau*, Selb 2006

[17] Rietveld, H. M., A profile refinement method for nuclear and magnetic structures, *Journal of Applied Crystallography* **2**(1969)65-71

[18] ASTM C150-07: Standard specification for Portland Cement

[19] NS-EN 197-1: 2000+A1: Cement, Part 1: Composition, specification and conformity criteria for common cements

[20] Jawed, I., Skalny, J., Young, J. F., Hydration of Portland cement, in Structure and performance of cement (Barnes, P. ed.), *Applied Science Publishers*, London and New York, 1983, pp. 237-317

[21] Kjellsen, K. O., Physical and mathematical modeling of hydration and hardening of Portland cement concrete as a function of time and curing temperature, *Dr.ing. thesis, The Norwegian Institute of Technology*, Trondheim 1990

[22] Roy, D. M., Portland cement: Constitution and Processing, Part 1: Cement manufacture (Instructional modules in cement science, ed. Roy, D. M.), *Journal of Materials Education*, Pennsylvania 1985, 73-89

[23] H. F. W. Taylor, Cement chemistry, 1st edition, London: *Academic Press Ltd*. 1990, 24

[24] Svinning K, Bremseth S K, Justnes H. X-ray diffraction studies on variations in microstructure in Portland clinker correlated to variations in production in the kiln,

Proceedings of the 18th International Conference on cement microscopy, Houston 1996, 382-403 , reprinted in *World Cement*, 10(1999)80-86

[25] Kerton, C. P., Murray, C. P., Portland cement production, (Barnes, P. ed., Structure and performance of cement), *Applied Science Publishers*, London and New York, 1983, pp. 205-236

[26] Summer, M. S., Cement mill process technology & the application of cement additives, in *Cement Milling Technology Course*, (Taylor, N., ed), Cementa and Intec Service P/L, Slite 2002

[27] Ellerbrock, H.-G., Sprung, S., Kuhlmann, Korngrösserverteilung und Eigensshaften von Zement. Tel III: Einflüsse des Mahlpozesses (in German), *Zement-Kalk-Gips* 43 (1990) 13-19

[28] Sprung, S., Influence of process technology on cement properties (English translation), *Zement-Kalk-Gips* 37(1985)309-316

[29] Theisen, K., Estimation of cement clinker grindability, *Proceedings of the 15th International Conference on cement microscopy*, Dallas 1996

[30] Mork, J. H., Effekt av sementens forhold mellom gips og hemihydrat på den ferske betongens reologi, *Doktor ingeniøravhandling 1994:4, NTH, Institutt for bygningsmateriallære*, Trondheim 1994

[31] Svinning, K., Bremseth, S. K., The influence of microstructure in clinker and cement on setting time and strength development until 28 days, *Proceedings of the 18th International Conference on cement microscopy*, Houston 1996, 514-533

[32] Goldstein, J, I., Newbury, D. E., Echlin, P., Joy, D. C., Fiori, C., Lifshin, E., Scanning electron microscopy and X-ray microanalysis, *Plenum Press*, New York 1981

[33] Svinning, K., Bremseth, S. K., The influence of material and process parameters on crystal size distribution of alite in Portland clinker, *Proceedings of the 15th International Conference on cement microscopy*, Dallas 1996, 233-249

[34] Regourd, M., Crystal Chemistry of Portland cement phases, in Structure and performance of cement (Barnes, P. ed.), *Applied Science Publishers*, London and New York, 1983, pp. 128-135

[35] Stutzman, P., Leigh, S., Phase composition Analysis of the NIST reference clinkers by optical microscopy and X-ray powder diffraction, *NIST Technical Note 1441*, Washington 2002

[36] Goetz-Neunhoeffer, F., Neubauer, J., Crystal structure refinement of Na-substituted C_3A by Rietveld analysis and Quantification in OPC, *Proceedings of the 10th International Congress on the Chemistry of Cement*, Gothenburg 1997 li056 8pp

[37] Neubauer, J., Kuzel, H.-J., Siber, R., Rietveld quantitative XRD analysis of Portland cement: Part II. Quantification of Synthetic and Technical Portland cement clinkers, *Proceedings of the 18th International Conference on cement microscopy*, Houston 1996, 100-111

[38] Neubauer, J., Pöllmann, H., Meyer, H. W., Quantitative X-ray analysis of OPC clinker by Rietveld refinement, *Proceedings of the 10th International Congress on the Chemistry of Cement*, Gothenburg 1997 3v007 12pp

[39] Kuzel, H.-J., Rietveld quantitative XRD analysis of Portland cement: Part I. Theory and application to the hydration of C_3A in presence of gypsum, *Proceedings of the 18th International Conference on cement microscopy*, Houston 1996, 87-99

[40] Ono, Y., Lattice Constants of alite in plant clinker, Review of the 38th General Meeting, Technical Session, *The Cement Association of Japan*, Tokyo 1984 pp 28-31.

[41] Maki, I., Kato, K., Phase identification of alit in Portland cement clinker, *Cement and Concrete Research* 12 (1982) 93-100

[42] Dubina E., Plank, J., Black, L., Wadsö, L., König, H., nanocem, Core project 7, Fundamental Mechanisms of cement prehydration, First progress report, April – September 2009, *Technische Universität München,Germany*, München 2009

[43] Dubina E., Sieber, R., Plank, J., Black, L., Effects of pre-hydration on hydraulic properties on Portland cement and synthetic clinker phases, In: Fentiman, C. H., Mangabai, R, J., (eds.) *28th Cement and Concrete Science: Proceedings, 15-16 September 2008, Manchester, England*

[44] Wenlandt, W., WM., Thermal analysis, 3rd ed., John Wiley & Sons, New York 1986

[45] http://en.wikipedia.org/wiki/Differential_scanning_calorimetry 2010

[46]Ramachandran, V. S., Applications of differential thermal analysis in cement chemistry, *Chemical Publishing Company, Inc.*, New York 1969

[47] NS-EN 196-3, Methods of testing cement, Part 3: Determination of setting time and soundness

[48] NS-EN 196-1, Methods of testing cement, Part 1: Determination of strength

[49] A. Høskuldsson, Prediction Methods in Science and Technology, Vol. 1, *Thor Publishing*, Copenhagen 1996, p. 266

[50] H. Martens, M. Martens, Modified Jack-knife estimation of parameter uncertainty in bilinear modeling by partial least squares regression (PLSR), *Food quality and Preference*, 11(2000)5-16

[51] J. A. Nelder, R. Mead, *Comput. J.*, 7(1965) 308-313

[52] Knöfel D., Interrelation between proportion of clinker phases and compressive strength of Portland cements, Proceedings of the 11th International conference on cement microscopy, New Orleans, pp 246-262.

[53] Aldridge, L. P., Estimating strength from cement composition. In: *Proceedings of the 7th International Congress on the Chemistry of Cement*, Paris, 1980; Communication: vol. III, VI-83-6

[54] Odler, I., Wonnemann, R., Effects of alkalis on Portland cement hydration. I. Alkali oxides incorporated into the crystalline lattice of clinker minerals, *Cement and Concrete Research*, 13 (1983) 477-482

[55] Box, G. E. P., Hunter, W. G., Hunter, J. S., An introduction to design, data analysis, and model building, *Wiley*, New York 1978

[56] Akkurt S., Tayfur G., Sever C., Fuzzy logic model for the prediction of cement compressive strength, *Cement and Concrete Research* 34 (2004) 1429-1433

[57] Tsivillis, S., Parissakis, G., A mathematical model for prediction of cement strength, *Cement and concrete research* 28 (1988) 9-14

[58] Akkurt, S., Ozdemir, S., Tayfur, G., Akyol, B., The use of GA-ANN in the modelling of compressive strength of cement mortar, *Cement and Concrete Research*, 33 (2003) 973-980

[59] Baykasoglu, A., Türkay, D., Serkan, T., Prediction of cement strength using soft computing techniques, *Cement and Concrete Research* 34(2004)2083-2090

[60] Svinning, K. and Justnes, H., Application of partial least square regression analysis in examination of correlations between production conditions, microstructure of clinker and cement and cement properties, *Proceedings of the 10th international congress on the chemistry of cement*, Gothenburg 1997, li038, 8 pp

[61] Wallevik, J. E., Rheological properties of cement paste: Thixotropic behaviour and structural breakdown, *Cement and Concrete Research*, 39 (2009) 14-29

[62] Wallevik, J.E., Relationship between the Bingham parameters and slump. Cement and Concrete Research, 36 (2006) 1214-1221.

[63] Wallevik, J. E., telephone conversation 2010-03-01

[64] Vikan , H., Rheology and reactivity of cementitious binders with plasticizer, *Doctoral thesis for the degree of Philosophiae Doctor at the Norwegian University of Science and Technology*, Trondheim 2005

[65]Lawrence, C. D., A study of the microstructure of hardened cement paste by nitrogen and butane sorbtion, *PhD thesis, Brunel University*, 1981

[66] Odler, I., Wonnemann, R., Effects of alkalis on Portland cement hydration. II. Alkalis present in forms of sulphates, *Cement and Concrete Research*, 13 (1983) 771-777

[67] Richartz, W., Effect of the K_2O content and degree of sulphatization on the setting and hardening of Cement (in German), *ZKG* 39 (1986) 678-687

[68]Dunstetter, F., de Noirfontaine, M.-N., Courtial, M., "Polymorphism of tricalcium silicate, the major compound of Portland cement clinker, 1. Structural data: review and unified analysis", *Cement and Concrete Research* 36(2006) 39-53

[69] Maki, I., Chromy, S., Characterization of the alite phase in Portland cement clinker by microscopy, *Il Cemento* 3(1978)301-308

[70] Stanek, T.,Sulovsky, P., "The influence of the alite polymorphism on the strength of the Portland cement", *Cement and Concrete Research* 32(2002) 1169-1175

[71] Theisen, K., Johansen, V., Prehydration and strength development of Portland cement, *The American Ceramic Society Bulletin*, 54(1975)9

[72]Tsivilis, S., Tsimas, S., Benetatou, A., Haniotakis, E., Study on the contribution of the fineness on cement strength, *ZKG* 43(1990)1 26-29

[73] García-Casillas, P. E., Martinez, C. A., Camacho Montes, H., García-Luna, A., Prediction of Portland cement strength using statistical methods, *Materials and Manufacturing Processes*, 22 (2007) 333-336

[74] S. De Vries, C. J. F. Ter Braak, *Chemometrics and Intelligent Laboratory Systems* 30(1995)239-245

Appendix I: Papers I-IX

Paper I

Is not included due to copyright

Paper II

Available online at www.sciencedirect.com
ScienceDirect
Chemometrics and Intelligent Laboratory Systems 84 (2006) 177–187
Chemometrics and intelligent laboratory systems
www.elsevier.com/locate/chemolab

Design and manufacture of Portland cement—application of sensitivity analysis in exploration and optimisation Part I: Exploration

Ketil Svinning *

Norcem, R&D Department, N-3950 Brevik, Norway

Received 4 January 2006; received in revised form 3 April 2006; accepted 20 April 2006
Available online 17 August 2006

Abstract

Examples of application of different types of sensitivity analysis in explorations to be used in design and manufacture of Portland cement have been shown. The sensitivity analysis was based on results from partial least square regression. The sensitivity of an *x*-variable was defined as the predicted effect on *y* or **y** relative to confidence intervals of $\hat{\mathbf{y}}$. Exploration was performed as a two-step operation: simulation of variation in **X** and prediction of variation in **y**. For comparison, uncertainty testing on regression coefficients was performed. The goodness of the different methods of sensitivity was evaluated from the significance of the predicted values.

The influence of a latent variable on *y* was as expected much more significant than that of a single *x*-variable. Application of simulated variation of **X** constrained by PLS-components will therefore be a better basis for the design of cement and will improve the quality control during production. Sensitivity analysis by jackknifing on the regression coefficients will not be of any use in the implementation in the design and manufacture in the cases where the latent structure in **X** has to be taken into consideration.

Keywords: Portland cement; PLS; Sensitivity analysis; Exploration

1. Introduction

For more than 10 years multivariate analysis has been applied at Brevik Plant, Norcem, Norway, in quality control of cement during production and design of the product. The statistical method that was frequently used was *p*artial *l*east *r*egression (PLS). An important part of this work has been implementation of the results in the development of new products, the understanding of the reactions and formation of the minerals in the cement; how they influence the cement properties after hydration and optimising the process to achieve an acceptable quality and performance. The implementation has been based on sensitivity analysis considering the influence of variables.

Sensitivity analysis is concerned with how the results of estimation depend on the present data. There are two approaches to sensitivity analysis, one is to consider the influence of the samples and the other is the influence of the variables [1]. In this work the latter consideration will be focused. The manuscript will contain two parts: Part I: Exploration, Part II: Optimisation. In Part I different types of sensitivity analysis are focused with respect to significance of the influence of **x** on **y**. The intention of using sensitivity analysis was to interpret a complex statistical model like for example *p*artial *l*east *s*quare regression (PLS) with respect to how much, in what direction, and how significantly an *x*-variable influences *y*. The sensitivity of an *x*-variable could be defined as the predicted effect of the *x*-variable on the response *y*-variable relative to a defined confidence range of the predicted *y*. Alternatively to the sensitivity analysis described above, uncertainty testing on the regression coefficients could be performed. Martens and Martens [2]

* Tel.: +47 35572314; fax: +47 35570400.
E-mail address: ketil.svinning@norcem.no.

0169-7439/$ - see front matter © 2006 Elsevier B.V. All rights reserved.
doi:10.1016/j.chemolab.2006.04.011

have developed an improved method for uncertainty testing based on cross-validation, jackknifing, and stability plot. In addition to studying the influence of the separate *x*-variable on *y*, attention should be paid to the influence of latent variables. In Refs. [3,4] the influence of an *x*-variable and of the relevant latent variable, respectively, on *y* are compared with respect to significance. The term relevant is here related to how much the *x*-variable will vary by varying the latent variable.

As suggested by the title the sensitivity analysis can be applied in exploration as well as optimisation. Exploration can be performed as a two-step operation: simulation of variation in the *x*-variables and prediction of variation in *y* [3,4]. Akkurt et al. [5] defined sensitivity analysis as feeding input parameters (values of *x*-variables) at varying levels into the developed model and producing prediction outputs of *y*. Significance or uncertainty is not taken into consideration. The sensitivity analysis has more a character of visualising the effects of the various *x*-variables on *y*. The term sensitivity analysis may in this case be replaced by the term verification of the model. However, a complex process involving many process variables or use of many variables in the characterisation of the product makes it necessitates visualisation of the variation in **x** and **y** to enable people not skilled in PLS to understand the results.

The examples of application of sensitivity analysis in exploration are collected from earlier works on the influence of production conditions and microstructure or characteristics of Portland clinker and cement on the cement properties [6]. In Refs. [3,4] the influence of the production conditions in a cement mill on the microstructure and properties of Portland rapid cement has been statistically investigated by application of PLS.

2. Description and manufacture of Portland cement

Cement is a material that binds together solid bodies by hardening from a plastic state. The cement functions by forming a plastic paste when mixed with water, which develops rigidity (sets) and then steadily increases in compressive strength (hardens) by chemical reaction with the water (hydration). The major components of Portland cement are tri- and di-calcium silicates, tri-calcium aluminates and tetra-calcium aluminate ferrates [7].

In short, cement is made by heating a mixture of calcareous and argillaceous materials to a temperature of about 1450 °C. In the process, partial fusion occurs and nodules of so-called clinkers are formed. The cooled clinker is mixed with a few percent of gypsum, which act as a hydration modifier, and sometimes other additives, and ground to cement.

To enable design or tailoring of Portland cement aiming at target values of properties as compressive strength up to 28 days, setting time and initial flow properties of the paste, characteristics of the cement as chemical or mineral composition, particle size distribution, the degree of dehydration of gypsum and prehydration of the clinker minerals should be available.

With relevance to the application of sensitivity analysis presented in this work the last step of the manufacture of cement will be described in more detail. Fig. 1 shows a schematic figure of a two-chambered ball mill for grinding cement. In addition, the mill system consists of a classifier, dust filters, silos and a feeding system. The finished product leaves the separator at the top and is deposited in a set of four cyclones. During the production it is possible to intergrind iron(II)sulphate and limestone in addition to clinker and gypsum. Internal water sprays can be used at both the inlet and outlet ends of the mill to

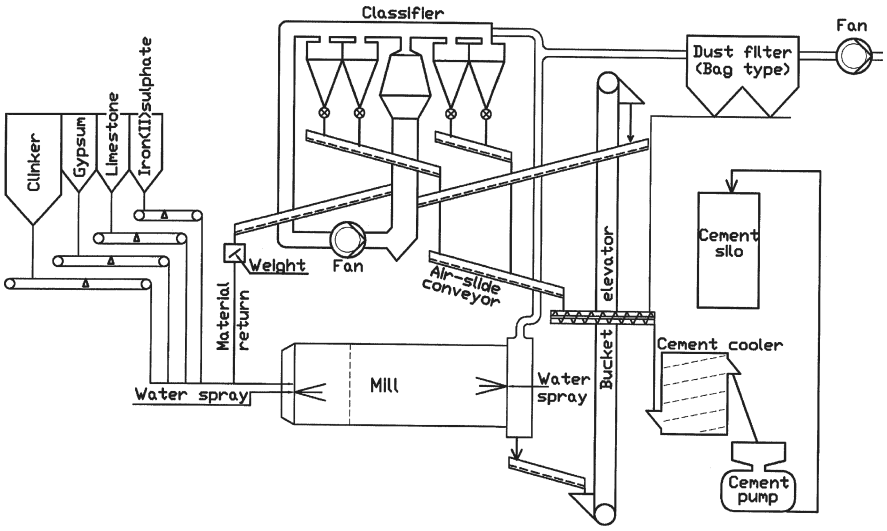

Fig. 1. A schematic figure of the cement mill. From Ref. [4], Copyright 2003 Cement and Concrete Institute. Reproduced with permission.

prevent dehydration of gypsum and to cool the cement before storing and delivery.

3. Methods of sensitivity analysis considering influences of variables

Having a model from PLS on centred and scaled data the influence of x-variables on the y-variable(s) may be evaluated in different ways:

- Comparison of the regression coefficients of the various variables from PLS with centred and scaled data. Significance testing on the coefficients was done by application of jackknifing estimation [2] with a confidence interval of 0.95. Examples are shown in Figs. 4 and 5. The estimated uncertainty variance of **B** is estimated by jackknifing

$$\mathbf{s}_{\mathrm{b}}^2 = \sum_{m=1}^{M} ((\mathbf{b} - \mathbf{b}_m)g)^2 \tag{1}$$

$$\mathbf{S}_{\mathrm{B}}^2 = \sum_{m=1}^{M} ((\mathbf{B} - \mathbf{B}_m)g)^2 \tag{2}$$

where $\mathbf{B}(K \times J)$ is the regression coefficient at the cross-validated A using all the N objects, $\mathbf{B}_m(K \times J)$ is the regression coefficient at the rank A using all objects except the objects left out in the cross-validated segment m, g is the scaling coefficient (in the Unscrambler software: $g=1$).
When the variance for **B** has been estimated, it can be utilized to find significant parameters. As a rough significance test, a t-test is performed for each element in **B** relative to the square root of its estimated uncertainty variance $\mathbf{S}_{\mathrm{B}}^2$, giving the significance level for each parameter.
- Prediction of variation in y including confidence intervals equal to $\hat{y} \pm s(y)$, from variation of one x-variable in one direction and in equal steps while the others are kept constant and equal to their respective mean values. The range of variation in this work is set to $\bar{x}_k \pm 1.5s(x_k)$.
- Prediction of variation in y or **y** as from variation of a latent variable at a time from one 'observed' extreme to the other. By varying the kth latent variable $\Delta t\mathbf{p}_k$ the variation in Δx_k in its original form, i.e. not scaled, can be calculated in the following way:

$$\Delta x_k = (\Delta t p_{ka}) s(x_k) \tag{3}$$

Similar to the previous type of sensitivity analysis with variation of only one x-variable the score, t, is varied in one direction and in equal steps, Δt. Calculation of x_j, neither centred nor scaled, will then be as follows:

$$x_k = (t p_{ka}) s(x_k) + \bar{x}_k \tag{4}$$

In the two latter ways of sensitivity analysis presented above variation in **X** was simulated prior to the prediction by constructing an artificial observation **X**-matrices. In some cases sensitivity analysis in the form of prediction from simulated variation of a selection or a group of variables could be appropriate. Schematic presentations of the two types of sensitivity analysis are shown in Figs. 2 and 3.

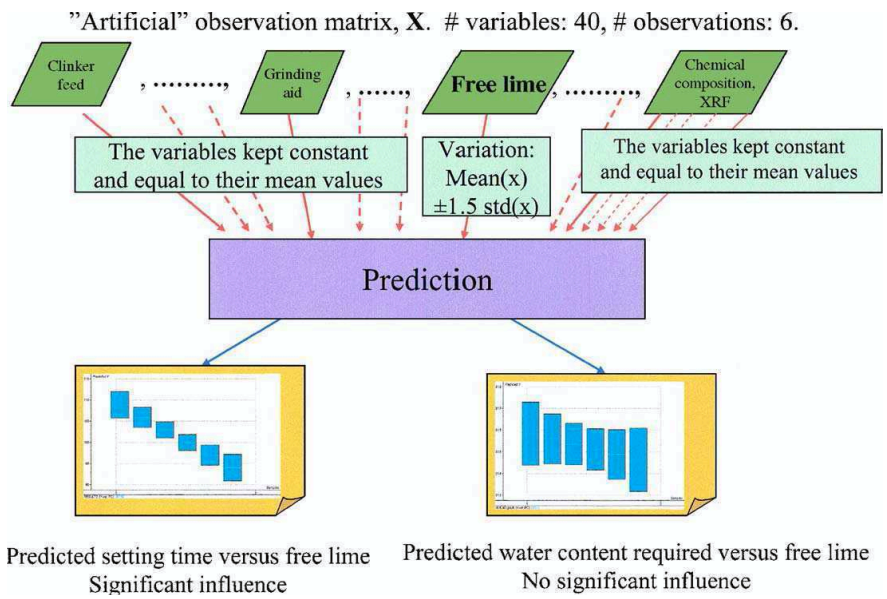

Fig. 2. Schematic presentation of sensitivity analysis in the form of prediction of variation in y from simulated variation of one x-variable.

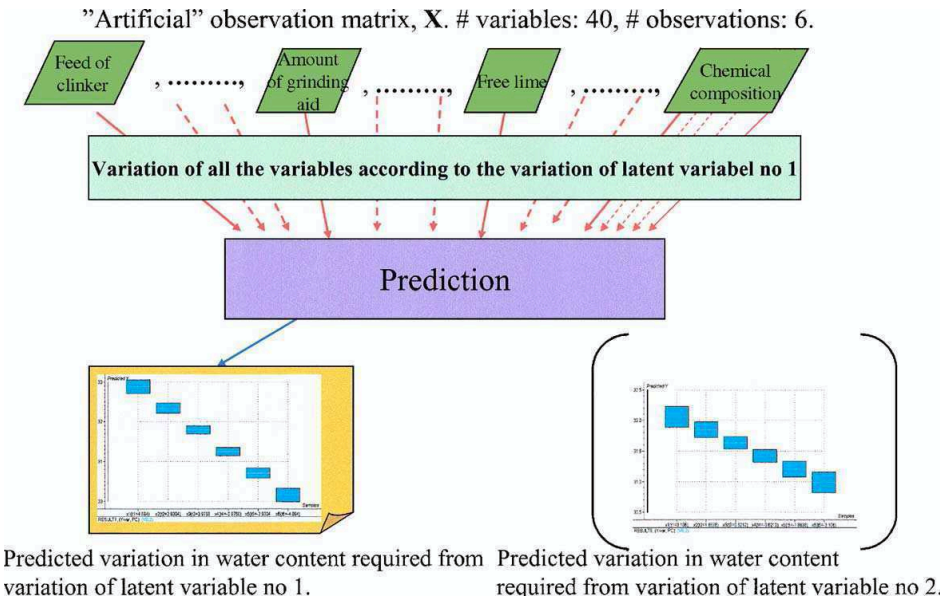

Fig. 3. Schematic presentation of sensitivity analysis in the form of prediction of variation in y from simulated variation of a latent variable.

An influence of one or several x-variables on a y-variable is defined in this work as being significant if there is no overlap of confidence intervals of $\hat{y}\pm 1$S.D. of predicted maximum and minimum y, respectively. For evaluation of the significance of the influence of a variable x_k from jackknifing estimation, the influence could be defined significant if the uncertainty level is less than $2|b_{wk}|$.

The estimate of the reliability of the predicted values $\hat{y}_i$(Dev (y_i)) is calculated as follows [8]

$$\mathrm{Dev}(y_i) = \sqrt{\mathrm{ResYVALVar}\left(\frac{\mathrm{ResXValSamp_{pred}}}{\mathrm{ResXValTot}} + H_i + \frac{1}{I_{\mathrm{cal}}}\right) 2\left(1 - \frac{A+1}{I_{\mathrm{cal}}}\right)} \tag{5}$$

where ResYValVar is the y-residual variation in the validation set, $\mathrm{ResXValSamp_{pred}}$ is the x-residual variance in the prediction objects, ResXValTot is the average x-residual variance in the validation objects, H_i is the leverage of the prediction object with respect to A PLS-components and I_{cal} is the number of calibration objects, n. The reliability of the prediction of y related to the object i is given by the two terms $\mathrm{ResXValSamp_{pred}}$ and H_i (Fig. 3),

$$\mathrm{ResXValSam_{pred}} = \frac{1}{K-A}\sum_{a=1}^{K}\left(x_{ik} - \bar{x}_k - \sum_{a=1}^{A}\hat{t}_{ia,pr}\hat{p}_{ak}\right)^2 \tag{6}$$

$$H_i = \sum_{a=1}^{A}\frac{\hat{t}_{ia,pr}}{t_a^T t_a} \tag{7}$$

4. Application of sensitivity analysis in exploration

4.1. Prediction of quality of cement from production conditions in a cement mill

To enable statistical investigations of the influence of production conditions in a cement mill on the microstructure and properties of Portland rapid cement, prediction models have been evaluated [3,4]. In more detail, partial least square regression (PLS) models for the prediction of the following y- or group of y-variables from the following x-variables was evaluated:

Cement properties:

- Water content required to achieve standard consistency
- Setting time
- Compressive strength

All the three properties predicted from:

- Production condition in the cement mill
- Microstructure of cement.

Microstructure of cement:

- Superficial microstructure from DTGA (85–946 °C), describing mainly the degree of dehydration of gypsum, prehydration of clinker minerals and free lime, carbonation of clinker and the amount of limestone used as filler
- Particle size distribution of cement

The two cement properties which will be focused in this part of the work are water content required to achieve standard

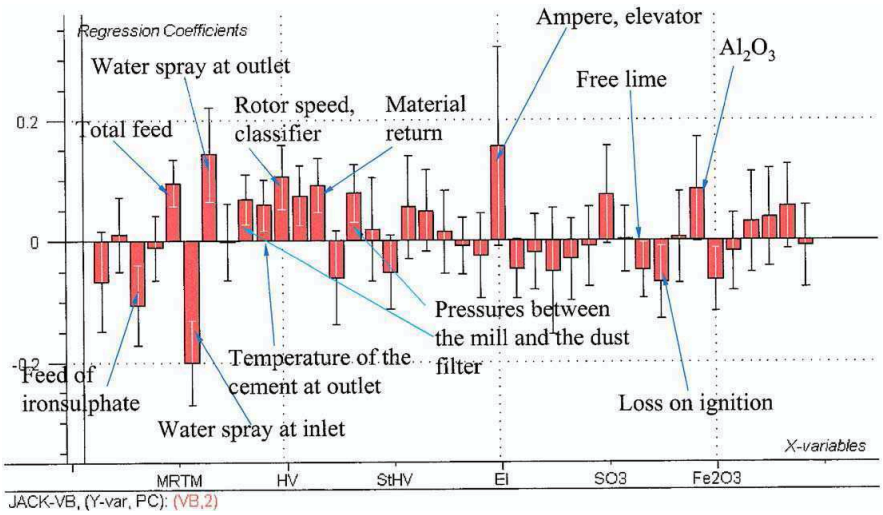

Fig. 4. Regression coefficients (vertical axis) for prediction of water content required to achieve *s*tandard *c*onsistency (SC) from variables (horizontal axis) describing production condition in the cement mill. From Ref. [4], Copyright 2003 Cement and Concrete Institute. Reproduced with permission.

*c*onsistency (SC) and *s*etting *t*ime (ST). The determination of setting time is among other factors affected to a marked degree by the quantity of water in gauging. The quantity of water used is that which is necessary to bring the cement paste to a defined consistency [9]. SC indicates the flow behaviour of cement pastes [4].

The observation **X**-matrix contained 50 observations and 40 variables. 30 of these variables described production process and the rest the chemical composition in the cement. PLS was performed on mean-centred and scaled data, using weights based on the standard deviation. The explained variances in SC and ST were 54% and 61%, respectively.

Figs. 4 and 5 shows the influences of x_i expressed by the size and uncertainties of the b_{iw} for prediction of SC and ST, respectively.

As shown in Fig. 4 free lime or the amount of CaO not converted to calcium silicates has a significant influence on ST but not on SC. The sensitivity analysis in the form of simulation and prediction as presented in Fig. 2 confirms what can be concluded from Fig. 4.

Fig. 5 shows that the amount of water sprayed into the mill at inlet significantly influences SC. From Figs. 6 and 7 it can be seen that the influence of the amount of water on SC is much less significant than that of the relevant latent variable. Fig. 7

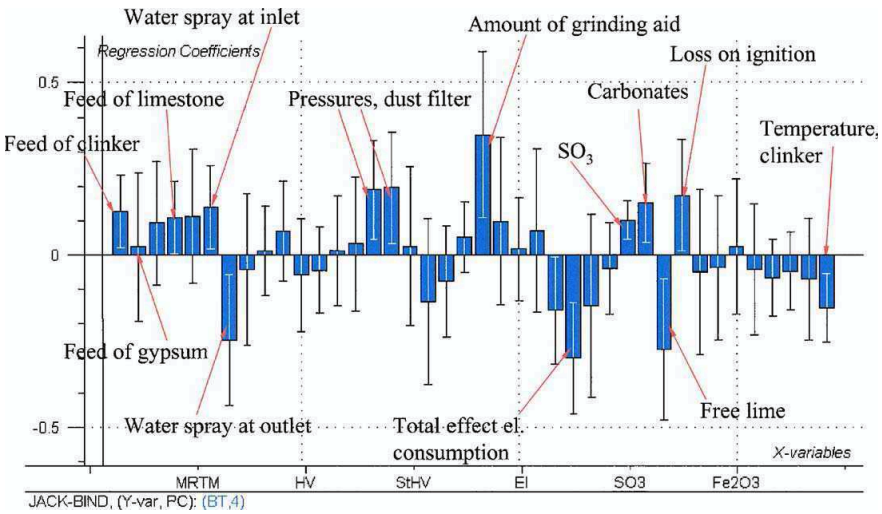

Fig. 5. Regression coefficients (vertical axis) for prediction of *s*etting *t*ime (ST) from variables (horizontal axis) describing production condition in the cement mill. From Ref. [4], Copyright 2003 Cement and Concrete Institute. Reproduced with permission.

Fig. 6. Predicted changes in water content required to achieve standard consistency [%] (vertical axis) from changes in the amount of water sprayed into the mill at the inlet [l/h]. From Ref. [4], Copyright 2003 Cement and Concrete Institute. Reproduced with permission.

shows that by varying the latent variable in such a way that SC will increase, the amount of water at the inlet will increase and the amount of water at the outlet will decrease simultaneously. The presence of autocorrelation between the two variables could be explained by how the process is controlled and the experiment designed. The autocorrelation is verified by the first PLS-component contributing to the explanation of the major part of the variance in y. In the experiments of varying the amount of water sprayed into the first chamber the set point of the temperature of cement leaving the mill was kept constant. This is according to the usual procedure of the process control at this plant.

The parabolic-like form of lines marking the limits of the confidence area of $\hat{y}$ predicted from a simulated case of variation of only one variable x_j, as shown in Figs. 2 and 6, can be explained from the sample leverage, H_i (Eq. (7)). Performing

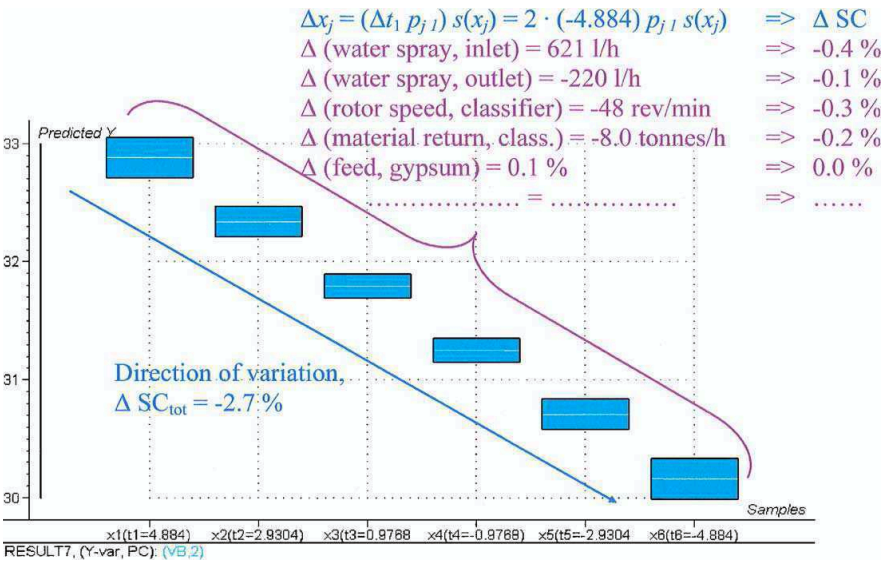

Fig. 7. Predicted changes in water content required to achieve standard consistency (SC) [%] (vertical axis) from changes in latent variable (PLS-comp. no. 1) (scores, $4.884 > t > -4.884$, on the horizontal axis). Contributions of some of the x-variables are calculated. From Ref. [4], Copyright 2003 Cement and Concrete Institute. Reproduced with permission.

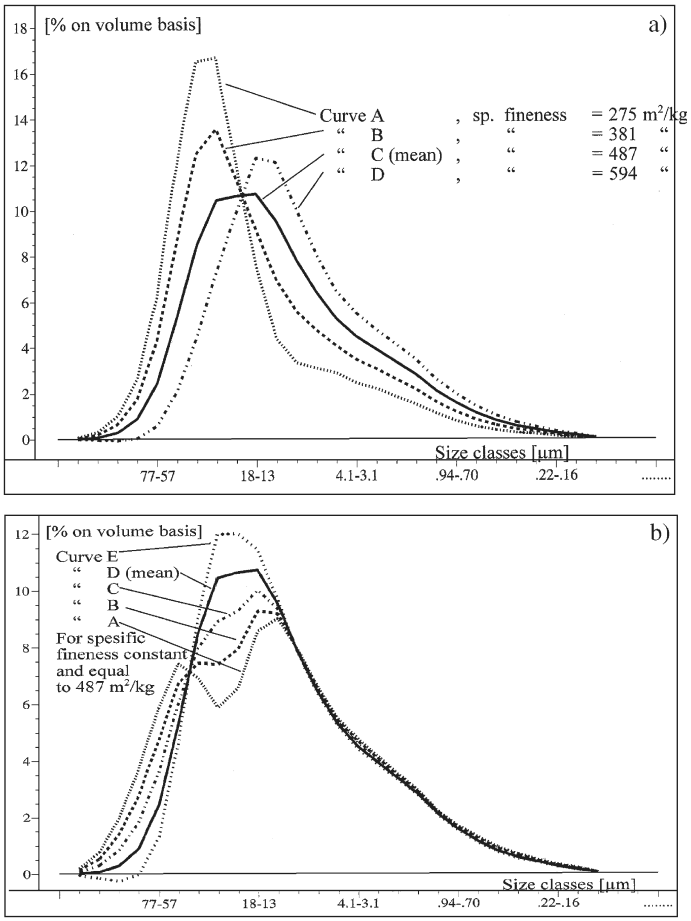

Fig. 8. Variation in the particle size distribution by variation of a latent variable giving: a) variation in the specific fineness, b) no variation in the specific fineness.

PLS on mean-centred data, $\hat{t}_{ia,pr}$ is equal to 0 for $\mathbf{x}=\overline{\mathbf{x}}$ but will increase with the increase in $x_{ij}-\overline{x}_j$.

The decrease in the confidence intervals from the case of predicting variation in y from variation of only one x-variable to the case of predicting from variation in a latent variable could be explained from two principles. The first principle is based on the fact that the usability of PLS is connected to the existence of principal directions of variations in the observation **X**-matrix. The variation of a latent variable is within the space R^n where for this model $n=2$. The limits of variation of a single x-variable, x_j, of $\overline{x}_j \pm 1.5s(x_j)$ are most likely outside R^2. The simulated variation should therefore be considered as being less realistic. The second principle is based on the following statistical consideration.

In the prediction of $y=\hat{y}$ from a simulated variation of a latent variable j, Eq. (7) can be reduced to

$$H_i = \frac{\hat{t}_{ia,pr}}{t_a^T t_a} \tag{8}$$

In the same manner Eq. (6) can be reduced to

$$\mathrm{ResXValSam}_{\mathrm{pred}} = \frac{1}{K-A}\sum_{k=1}^{K}\left(x_{ik} - \overline{x}_k - \hat{t}_{ia,pr}p_{ak}\right)^2 \tag{9}$$

H_i and $\mathrm{ResXValSam}_{\mathrm{pred}}$ will be smaller than in the case of varying only one variable. The confidence intervals of $\hat{y}$ will consequently be smaller.

The selection of the m elements applied in the cross-validation and jackknifing is random.

In the estimation of the uncertainty variance of the PLS regression coefficients by jackknifing (Eqs. (1) and (2)) the latent structure of the observation **X**-matrix is not taken into consideration. It is therefore more relevant to compare the results from sensitivity analysis with application of cross-validation and jackknifing with those from the sensitivity analysis with variation of only one x-variable.

4.2. Exploration of the influence of microstructure of cement on the cement properties

In connection with examination of clinkers from Scandinavian plants with respect to microstructure and cement properties a PLS-model for prediction of cement properties from the complete microstructure of the cement was evaluated [6]. The complete microstructure was defined as mineral composition and structure described by profiles or curves from *X-r*ay *d*iffraction *a*nalysis (XRDA), superficial microstructure recorded from *t*hermogravimetric *a*nalysis (TGA) and particle size distribution. In this work, exploration of the influence of the particle size distribution on compressive strength up to 28 days is demonstrated.

The particle size distribution is given here as volume fractions of the cement particles in the size classes between 249 and 0.16 μm. In the more current quality control of cement during grinding adjustment of the specific fineness is considered to be effective to maintain stable quality regarding the cement properties. The specific fineness given as weight-specific surface area is usually determined by an air permeability method developed by Blaine. However, the method reveals no information of the particle size distribution, which is determined in these examples by laser diffractometry. The

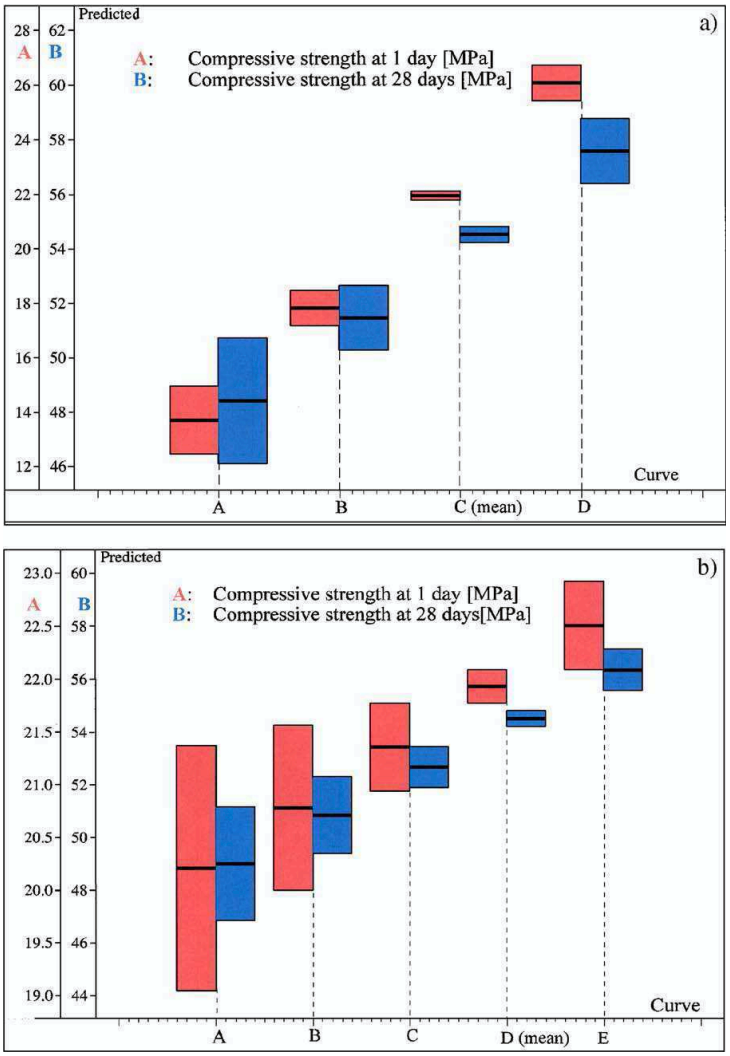

Fig. 9. Prediction of compressive strength at 1 and 28 days, including confidence intervals of ±1S.D., from variation of the latent variables presented in Fig. 8a) and b), respectively.

specific fineness, SF, can be calculated from the particle size distribution:

$$\mathrm{SF} = \frac{6\sum_{i=1}^{m} \frac{V_i}{d_i}}{\sum_{i=1}^{m} V_i \rho} \tag{10}$$

where V_i is the volume fraction in size class i, d_i is the average diameter of the particles in the same size class and ρ is specific weight of the cement.

The simulation of the variation of the particle size distribution and general specific fineness was based on variation of two latent variables of the particle size distribution, one at a time.

The examination of the influence was carried out in the following way.

Having an overall model

$$y = \mathbf{b}^T\mathbf{x} + b_0 = \mathbf{b}^T\left(\mathbf{x}_1|\mathbf{x}_2|\ldots|\mathbf{x}_j|\ldots|\mathbf{x}_n\right) + b_0 \tag{11}$$

where $\mathbf{x}_1,\ldots,\ \mathbf{x}_n$ represent the different parts of the microstructure, the examination of the influence of $\mathbf{x}_j$ on y is carried out by the following procedure:

1. Prediction of $\acute{\mathbf{y}}$ from

$$\left(\begin{array}{c|c|c|c|c|c|c} (\bar{\mathbf{x}}_1)_1 & & (\bar{\mathbf{x}}_{j-1})_1 & & (\bar{\mathbf{x}}_{j+1})_1 & & (\bar{\mathbf{x}}_n)_1 \\ \vdots & \ldots & \vdots & \mathbf{X}_j & \vdots & \ldots & \vdots \\ (\mathbf{x}_1)_m & & (\bar{\mathbf{x}}_{j-1})_m & & (\bar{\mathbf{x}}_{j+1})_m & & (\bar{\mathbf{x}}_n)_m \end{array}\right)$$

where m is the number of rows in the observation **X**-matrix.

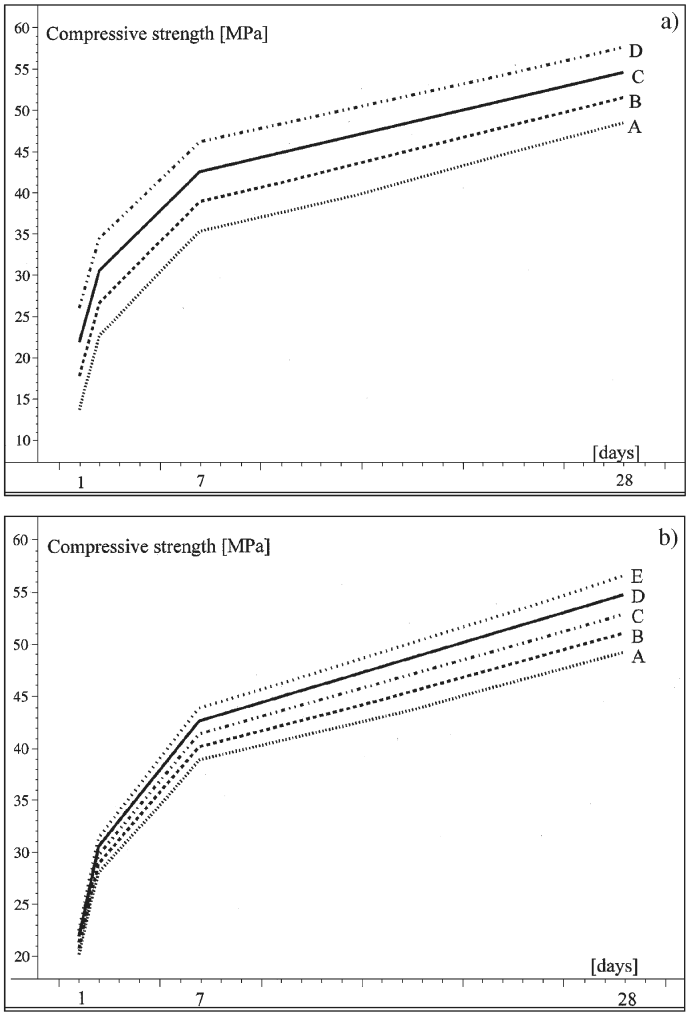

Fig. 10. Prediction of compressive strength up to 28 days from variation of the latent variables presented in Fig. 8a) and b), respectively.

2. To reveal the latent structure of $\mathbf{x}_j$ evaluate a new model $y=\acute{y}=\mathbf{b}^{\mathrm{T}}(\mathbf{x}_j|\mathbf{x}_{n+1})+b_0$ by PLS. $\mathbf{x}_{n+1}$ may contain a few supplementary variables relevant for interpretation of variation in $\mathbf{x}_j$.
3. Simulation of variation in $\mathbf{x}_j$ by varying one or several latent variables and establishing an artificial observation matrix $\mathbf{X}_{j,\mathrm{art}}$ with m, art rows where m, art$<m$ and $m-1$, art is the number of changes in equal steps of $\mathbf{x}_j$.
4. Prediction of $\acute{\mathbf{y}}$ from

$$\left(\begin{array}{c|c|c|c|c|c|c} (\overline{\mathbf{x}}_1)_1 & & (\overline{\mathbf{x}}_{j-1})_1 & & (\overline{\mathbf{x}}_{j+1})_1 & & (\overline{\mathbf{x}}_n)_1 \\ \vdots & \ldots & \vdots & \mathbf{X}_{j,\mathrm{art}} & \vdots & \ldots & \vdots \\ (\mathbf{x}_1)_{m,\mathrm{art}} & & (\overline{\mathbf{x}}_{j-1})_{m,\mathrm{art}} & & (\overline{\mathbf{x}}_{j+1})_{m,\mathrm{art}} & & (\overline{\mathbf{x}}_n)_{m,\mathrm{art}} \end{array}\right)$$

In the examples shown here $\mathbf{x}_{n+1}$ contains only one variable which is the specific fineness of the cement.

In Fig. 8a) the simulated variation in the size distribution gives a change in the specific fineness, while in Fig. 8b) the variation is simulated in such a way that the specific fineness is kept constant. Fig. 9a) and b) show the degree of significance with which the latent variables influence the compressive strength at 1 and 28 days. Fig. 10a) and b) show prediction of compressive strength up to 28 days predicted from latent variables in Fig. 8a) and b), respectively.

4.3. Exploration of the influence of production conditions in the cement mill on the cement properties explained by the microstructure of the cement

Ref. [4] shows two examples of prediction in two steps of cement properties from production condition in a cement mill via characterised superficial microstructure of the cement. In the examples presented here, superficial microstructure of the

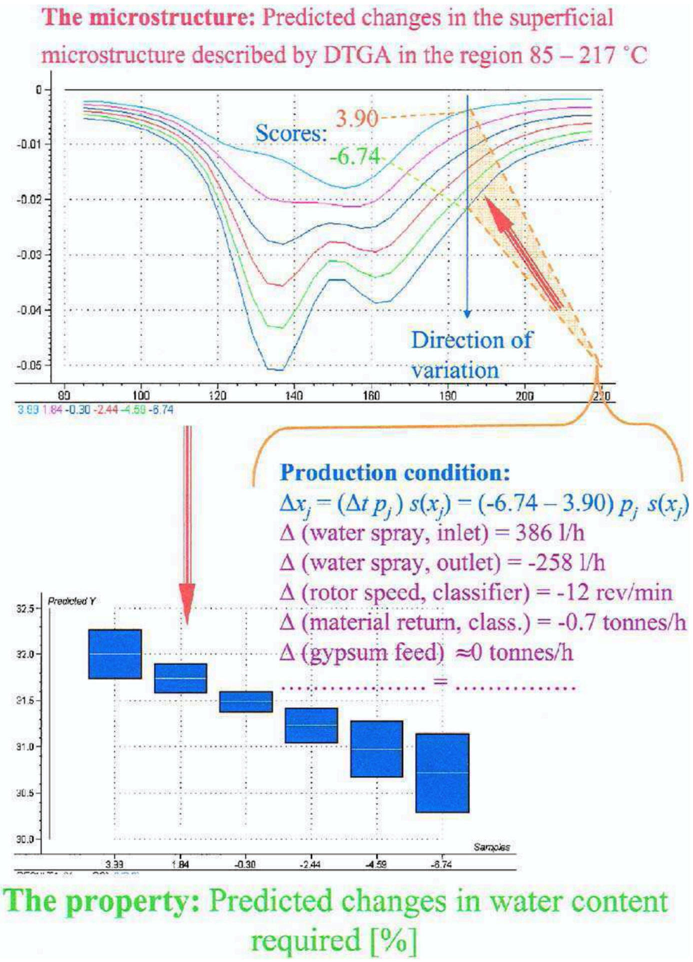

Fig. 11. Prediction of variation in the water content required to achieve standard consistency in two steps from production condition in the cement mill via superficial microstructure of the cement.

gypsum part of the cement was predicted from production conditions. In the second step SC was predicted from the microstructure. The superficial microstructure was described by a thermogram from *d*ifferential *t*hermo*g*ravimetric *a*nalysis (DTGA) in the temperature range 85–217 °C. When gypsum, $CaSO_4 \cdot 2H_2O$, is heated it undergoes dehydration in two consecutive steps to hemihydrate, $CaSO_4 \cdot 1/2H_2O$, and anhydrite, $CaSO_4$, respectively. The process of the two-step prediction is schematically presented in Fig. 1. The simulated variation in the process variables is given by latent variables 1 and 2 combined in such a way that gives $\Delta(\text{gypsum feed}) \approx 0$. The latent variable being varied was a combination of latent variables 1 and 2: $t\mathbf{p} = t(0.61\mathbf{p}_1 + 0.38\mathbf{p}_2)$.

Decreasing the amount of water sprayed into the mill at inlet, the gypsum, represented by a DTGA curve with two "peaks", dehydrates to hemihydrate represented by a curve with one "peak". SC increases significantly with the degree of dehydration, which increase significantly with an increase in water spray at inlet. The conclusion is in agreement with what can be concluded from Fig. 7. However, the confidence intervals in Fig. 11 are larger than in Fig. 4. The difference is due to the fact that the local latent variable DTGA-data is not an original latent variable with respect to prediction of SC and ST. Only a part of the whole microstructure is included in the modelling.

5. Conclusion

The influence of a latent variable on y was as expected much more significant than that of a single x-variable. Application of simulated variation of the observation **X**-matrix constrained by PLS-components will therefore be a better basis for the design of cement and will improve the quality control during production. Sensitivity analysis by jackknifing on the regression coefficients will not be of any use in the implementation in the design and manufacture in the cases where the latent structure of the observation **X**-matrix has to be taken into consideration.

References

[1] A. Høskuldsson, Prediction Methods in Science and Technology, vol. 1, Thor Publishing, Copenhagen, 1996, p. 266.
[2] H. Martens, M. Martens, Food Quality and Preference 11 (2000) 5–16.
[3] K. Svinning, K.A. Datu, Prediction of microstructure and properties of Portland Cement from production condition in cement mill: Part I. Evaluation of prediction models, 11th International Congress on the Chemistry of Cement, Durban, 2003.
[4] K. Svinning, K.A. Datu, Prediction of microstructure and properties of Portland Cement from production condition in cement mill: Part II: Prediction and sensitivity analysis, 11th international congress on the chemistry of cement, Durban, 2003.
[5] S. Akkurt, S. Ozdemir, G. Tayfur, B. Akyol, Cement and Concrete Research 33 (2003) 973–980.
[6] K. Svinning, H. Justnes, E. Viggh, S.K. Bremseth, S.-E. Johansson, Examination of clinkers from four Scandinavian Plants with respect to microstructure and cement properties, 22nd International Conference on Cement Microscopy, Montreal, 2000, pp. 137–153.
[7] G.C. Bye, Portland Cement, 2nd edition, Thomas Telford Publishing, London, 1999, p. 1.
[8] S. De Vries, C.J.F. Ter Braak, Chemometrics and Intelligent Laboratory Systems 30 (1995) 239–245.
[9] F.M. Lea, The Chemistry of Cement and Concrete, 3rd edition, Edward Arnold Ltd., London, 1970, p. 363.

Paper III

Available online at www.sciencedirect.com
ScienceDirect
Chemometrics and Intelligent Laboratory Systems 84 (2006) 188 – 194
Chemometrics and intelligent laboratory systems
www.elsevier.com/locate/chemolab

Design and manufacture of Portland cement—application of sensitivity analysis in exploration and optimisation Part II. Optimisation

Ketil Svinning [a,*], Agnar Høskuldsson [b]

[a] Norcem, R&D Department, N-3950 Brevik, Norway
[b] Danish Technical University, Luntofte, Denmark

Received 4 January 2006; received in revised form 3 April 2006; accepted 20 April 2006
Available online 17 August 2006

Abstract

A program for a model-based optimisation has been developed. The program contains two subprograms. The first one does minimising or maximising constrained by one original PLS-component or one equal to a combination of several. The second one does searching for the optimal combination of PLS-components, which gives max or min *y*. The program has proved to be applicable for achieving realistic results for implementation in the design of Portland cement with respect to performance and in the quality control during production.

Keywords: PLS; Sensitivity analysis; Latent variables; Optimisation

1. Introduction

In Part I of this work, application of sensitivity analysis in the design and manufacture of Portland cement was presented [1]. As mentioned in Høskuldsson [2], there are two approaches to sensitivity analysis, one is to consider the influence of samples and the other is influence of variables. In this work, the latter consideration has been focused. The sensitivity analysis was defined by how much, in what direction and how significantly an *x*-variable or a latent variable influences *y*. The sensitivity of an *x*-variable was defined as the predicted effect on *y* or **y** relative to a defined confidence interval. Exploration was performed as a two-step operation: simulation of variation in the *x*-variables and prediction of variation in *y*. For comparison, uncertainty testing on regression coefficients based on cross validation, Jack knifing, and stability plot [3] were performed. It was concluded in Part I that the influence of a latent variable on *y* was much more significant than that of a single *x*-variable. Optimisation of *y* constrained by PLS-components will therefore give a more realistic and better solution for implementation in the design of cement and the quality control during production.

The utility of a model-based optimisation depends on the different approaches to experimental planning prior to the PLS-modelling. According to Martens and Martens [4] two main routes of approach could be outlined: (a) explorative design based on random and natural sampling and (b) controlled experiments with factorial design followed by new experiments added to the previous with optimisation design. Lack of design may be due to the preliminary nature of the project as having a high risk of obtaining a process out of balance or deteriorating the quality of the product as resulting from uncritical variation of a variable. In a design of a type of cement based on variation of the particle size of the cement, one particle size fraction cannot be varied independently of the others. However, in a process described by many variables, whose variation of many of them being dependant on the others, factorial design could be applied with additional variables describing the product quality more than the process [5]. An additional purpose of carrying out designed experiments could be to increase the span of the observation **X**-space

* Corresponding author. Tel.: +47 35572314; fax: +47 35570400.
E-mail address: ketil.svinning@norcem.no (K. Svinning).

0169-7439/$ - see front matter © 2006 Elsevier B.V. All rights reserved.
doi:10.1016/j.chemolab.2006.04.012

prior to PLS-modelling. An alternative to the application of optimisation design could be a model-based optimisation of the response variable constrained by PLS-components or latent variables and set limits of variation of each x-variable. This type of optimisation could have a form of a linear program, where the constraints describing the influence of one x-variable on the others are given by one PLS component or a combination of several [6]. In searching for an optimal combination of latent variables it would be beneficial to have at least two latent variables available for the optimisation. This can be achieved by increasing the span of the observation **X**-matrix.

The principles of model-based optimisation are presented in Ref. [6]. Further, optimisation of compressive strength of cement as a function of particle size distribution was demonstrated. A more complete method of optimisation developed after [6] was published, will be presented here.

2. Methods

2.1. Model-based optimisation. Basic principles

The optimisation based on a PLS-model could have the form of a linear program, where the constraints describing the influence of one variable on the others are given by one original PLS component or one equal a combination of several [6]. Having a model $y = b_0 + \sum_{k=1}^{K} b_k x_k$ from PLS on mean-centred and scaled data, using weights based on the standard deviation and selecting the latent variable no k to constrain the variation in **X** then mathematically, the linear programming problem could be presented as follows:

Minimise or maximise

$$y = \sum_{k=1}^{K} b_k x_k \text{ or } y = \mathbf{x}^{\mathrm{T}}\mathbf{b} \tag{1}$$

subject to

$$\mathbf{A}_1\mathbf{x} = \mathbf{c}_1,\ \mathbf{A}_2\mathbf{x} \le \mathbf{c}_2,\ \mathbf{A}_2\mathbf{x} \ge \mathbf{c}_3 \text{ and } \mathbf{x} \ge 0$$

where

$$\mathbf{A}_1 = \begin{pmatrix} -p_{ka}s(x_k) & \cdots & 0 & p_{1a}s(x_1) & 0 & \cdots & 0 \\ \vdots & \ddots & \vdots & \vdots & \vdots & \ddots & \vdots \\ 0 & \cdots & -p_{ka}s(x_k) & p_{k-1a}s(x_{k-1}) & 0 & \cdots & 0 \\ 0 & \cdots & 0 & p_{k+1a}s(x_{k+1}) & -p_{ka}s(x_k) & \cdots & 0 \\ \vdots & \ddots & \vdots & \vdots & \vdots & \ddots & \vdots \\ 0 & \cdots & 0 & p_{Ka}s(x_K) & 0 & \cdots & -p_{ka}s(x_k) \end{pmatrix}$$

$$\mathbf{A}_2 = \begin{pmatrix} 1 & \cdots & 0 \\ \vdots & \ddots & \vdots \\ 0 & \cdots & 1 \end{pmatrix}$$

$$\mathbf{c}_1 = \begin{pmatrix} \bar{x}_k p_{1a}s(x_1) - \bar{x}_1 p_{ka}s(x_k) \\ \vdots \\ \bar{x}_k p_{k-1a}s(x_{k-1}) - \bar{x}_{k-1} p_{ka}s(x_k) \\ \bar{x}_k p_{k+1a}s(x_{k+1}) - \bar{x}_{k+1} p_{ka}s(x_k) \\ \vdots \\ \bar{x}_k p_{Ka}(x_K) - \bar{x}_K p_{ka}s(x_k) \end{pmatrix} \quad \mathbf{c}_2 = \begin{pmatrix} x_{1\ \text{upper limit}} \\ \vdots \\ x_{K\ \text{upper limit}} \end{pmatrix} \quad \mathbf{c}_3 = \begin{pmatrix} x_{1\ \text{lower limit}} \\ \vdots \\ x_{K\ \text{lower limit}} \end{pmatrix}$$

$\bar{x}_k$, $s(x_k)$ and p_{ka} are the mean value, standard deviation and the loading of x_k, respectively. The constant b_0 is not included in the optimisation but is added afterwards. x_k is selected to

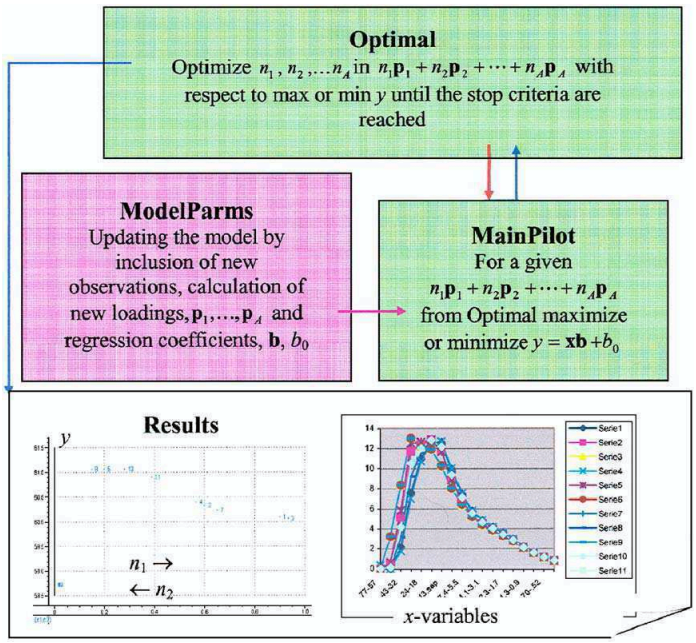

Fig. 1. Schematic presentation of the principles of Optpilot.

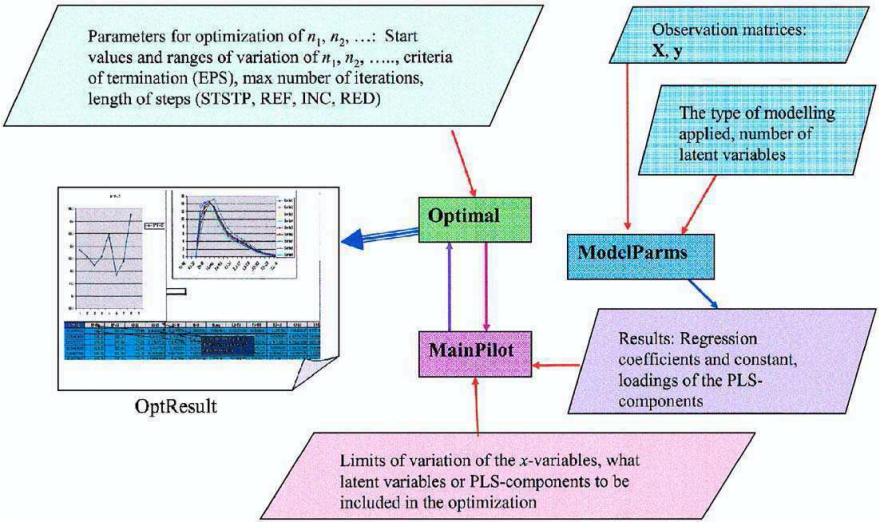

Fig. 2. The structure of Optpilot given as a flow diagram.

influence the other x-variables in the constraints if $|p_{ka}s(x_k)|$ is of max value for $k=1, 2, \cdots, K$.

In order to achieve the most optimal solution, several PLS-components could be involved in optimisation. The "loadings" in the new constraints are linear combinations of the original ones and could be expressed as follows:

$$p_{\text{combination of several PLS-components}} = \sum_{a=1}^{A} n_a p_a \tag{2}$$

where $\sum_{a=1}^{A} n_a = 1$ and $0<n_a<1$

The latter constraint prevents absolute values of the scores, $|t|$, of optimal $\mathbf{x}=(x_1, x_2, \cdots, x_K)$ to be unreasonably high.

The stepwise optimisation could in this case be carried out, by stepwise changes of some or all n_1, Λ, n_A before the next optimisation, until maximum value of y is obtained, on the condition that the constraints are consistent.

A useful method for optimising a combination of several latent variables is the simplex method [7]. This is not to be confused with the simplex methods of linear programming.

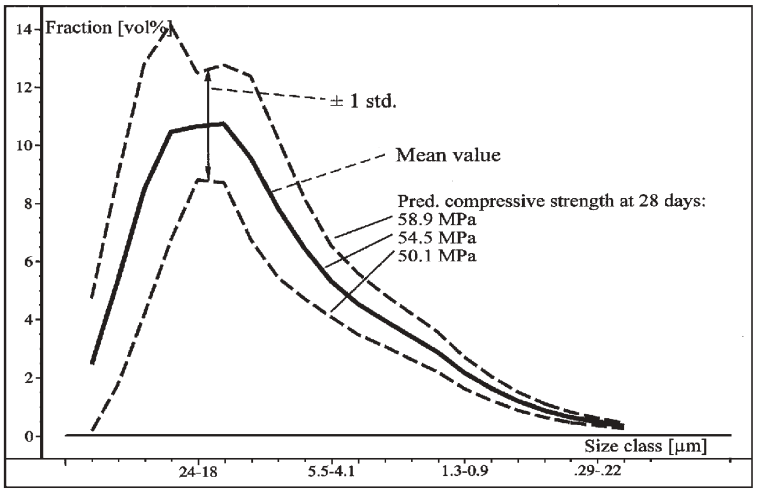

Fig. 3. Mean values and the confidence intervals of 1 standard deviation of the x-variables included in PLS. The x-variables describe the particle size distribution of cement. From [6], Copyright © 2000 John Wiley & Sons, Ltd. Reproduced with permission.

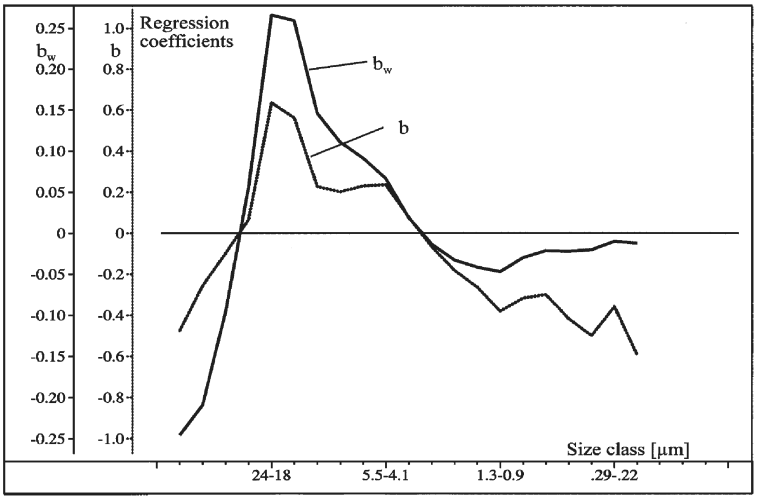

Fig. 4. The regression coefficients $\mathbf{b}_w$ and $\mathbf{b}$. b_0=41.8 MPa. From [6], Copyright © 2000 John Wiley & Sons, Ltd. Reproduced with permission.

2.2. Development of a program for optimisation

In the development of a program, Optpilot, for a more current control of process and quality a subprogram for updating the PLS-model by regression on updated **X**- and *y*-matrices was included (Fig. 1). The principles as applied in the program are schematic presented in Fig. 2. As shown in the figure, other subprograms in OptPilot are Optimal and MainPilot. MainPilot does minimising or maximising along a selected direction variation in **X** given by a PLS-component or a combination of several. Optimal is searching for the optimal combination of latent variables, which gives max or min *y*. The simplex method for function minimisation is developed by Nelder and Mead [7]. An additional option of OptPilot is the subprogram ModelParms for updating the PLS-model by inclusion of new observations.

3. Results and discussion

The examples of optimisation, presented here, compressive strength at 28 days as a function of particle size distribution are optimised. The prediction model which is applied here is the same as that applied by Svinning et al. [6]. Fig. 3 shows

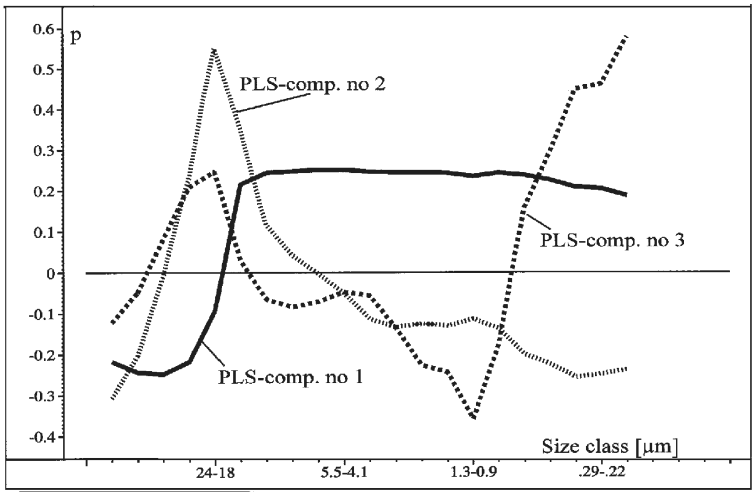

Fig. 5. Loading of the *x*-variables for the three PLS-components included. From [6], Copyright © 2000 John Wiley & Sons, Ltd. Reproduced with permission.

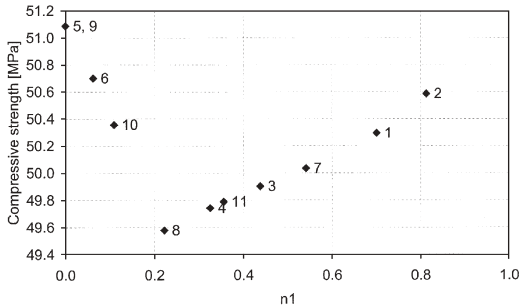

Fig. 6. Obtained min compressive strength at 28 days for various combinations of $\mathbf{p}_1$ and $\mathbf{p}_2$: $n_1\mathbf{p}_1+n_2\mathbf{p}_2=n_1\mathbf{p}_1+(1-n_1)\mathbf{p}_2$.

the mean values and the confidence intervals of ±1 S.D. of the x-variables giving the volume fraction of the cement powder in 21 size classes between 77 and 0.16 μm. Fig. 4 shows the regression coefficients, $\mathbf{b}_w$ and $\mathbf{b}$, from PLS of compressive strength at 28 days on the x-variables describing the particle size distribution and Fig. 5 shows the loadings. The latent variable nos. 1 and 2 explained more than 99% of the total variance in y. In the following examples of optimisation only these two latent variables will constrain the optimisation.

Figs. 6 and 7 show results from minimising compressive strength at 28 days when the x-variables are allowed to vary ±1 S.D. about their mean values. Fig. 6 shows minimum compressive strength for various combinations of latent variable nos. 1 and 2 (n_1, n_2). Fig. 7 shows the particle size distributions as results of combinations of the latent variables from which the compressive strengths in Fig. 6 are predicted. The minimum compressive strength at 28 days obtained is equal to 49.6 MPa for $n_1=0.22$, $n_2=0.78$. Fig. 8 shows particle size distribution for prediction of min and max compressive strength at 28 days for the same range of variation of $\mathbf{x}$. Min and max compressive strength obtain are 49.6 and 59.4 MPa for $n_1=0.22$, $n_2=0.78$, the same combination of latent variables as above.

In [6] problems in achieving optimal solutions due to lack of a bounded feasible region and inconsistent constraints are focused. A solution of model-based optimisation is more dependent on the presence of a bounded region giving a feasible solution than optimisation by application of response surface analysis using a quadratic model. The region of an optimisation constrained by one latent variable (a) is an unbounded straight line of infinitesimal thickness. In order to have a bounded region, variation of at least one x-variable should be limited. Constraints in the form of set limits on variation of two or several x-variables could conflict the wish to have a feasible region because of the risk of the constraints being inconsistent. The constraints are consistent and the linear programming has a solution if there are overlaps of all the ranges of the variation of the respective scores,

$$(t_{k+}, t_{k-1})_a = \left(x_{k,\text{upper limit}} - \bar{x}_k, x_{k,\text{lower limit}} - \bar{x}_k\right)/p_{ka}s(x_k) \quad \text{for } k = 1,\cdots,K \tag{3}$$

The x-variables are defined to vary according to latent variable a limited by the range of variation of x_k.

Allowing all the x-variables to vary $\pm c_k s(x_k)$ about their mean value the ranges of all the scores of the variables will overlap. As indicated above, the value of the constant c_k can be set individually for each x_k. In Fig. 8 all the constants are set equal to 1. In Fig. 9 an example optimisation of compressive

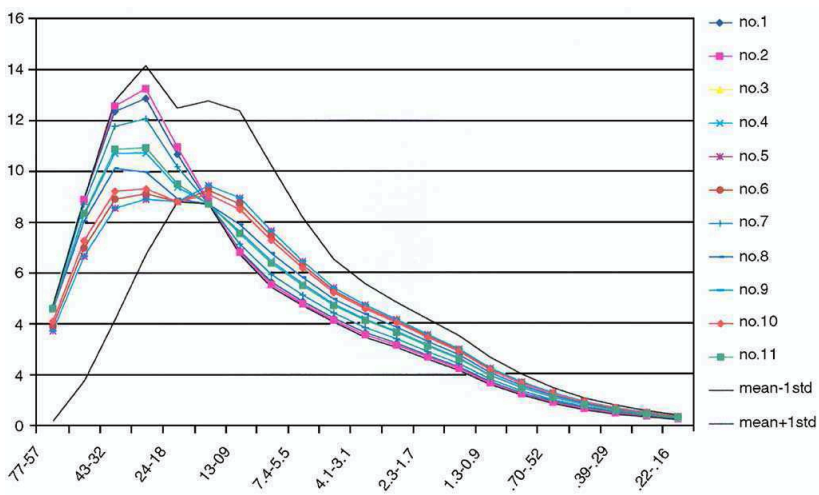

Fig. 7. Particle size distribution of cement calculated from combinations of the latent variable nos. 1 and 2: $t(n_1\mathbf{p}_1+n_2\mathbf{p}_2)$, where n_1 and n_1 are given in Fig. 6, and from which the compressive strength in Fig. 6 are predicted.

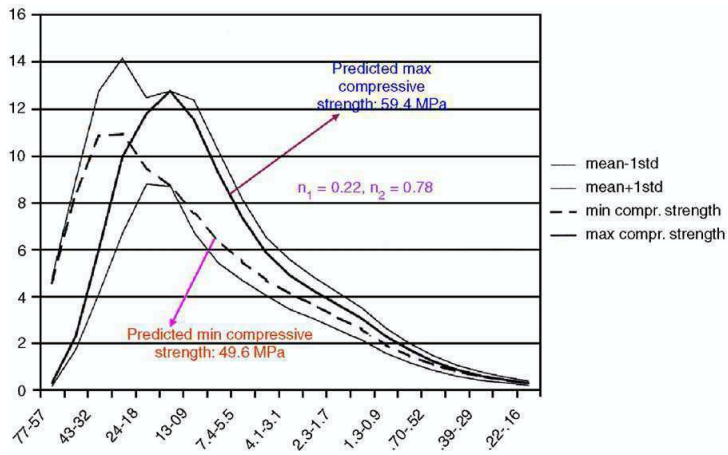

Fig. 8. Particle size distribution of cement from which min and max compressive strength at 28 days, allowing volume fractions of all the size classes to vary ±1 S.D. about their mean values.

strength similar to what is shown in Fig. 8 except that the value of c_5 is reduced from 1 to 0.27. Min and max compressive strength obtained are 50.07 and 58.9 MPa for $n_1=0.57$, $n_2=0.43$. In each of the two cases of optimisation as shown in Figs. 6 and 7 minimum and maximum obtained with same combination of latent variables given by n_1 and n_2. This could probably be due to that upper and lower limits of $\mathbf{x}$ are symmetrically placed about $\bar{\mathbf{x}}$. An example of optimisation with deviation from symmetry: $|x_{5,\text{upper limit}}-\bar{x}_5|=0.5$, $|x_{5,\text{upper limit}}-\bar{x}_5|=0.19$, gave max compressive strength equal to 49.6 MPa for $n_1=0.22$, $n_2=0.78$ and minimum equal to 58.9 MPa for $n_1=0.58$, $n_2=0.42$.

4. Conclusion

The method of model-based optimisation constraints by PLS-components or latent variables was very applicable for achieving realistic results for implementation in the design of Portland cement with respect to performance and quality control during production.

Acknowledgements

We wish to thank Professor Terje Hertzberg, NTNU, for his supply of software for optimisation by the simplex method and

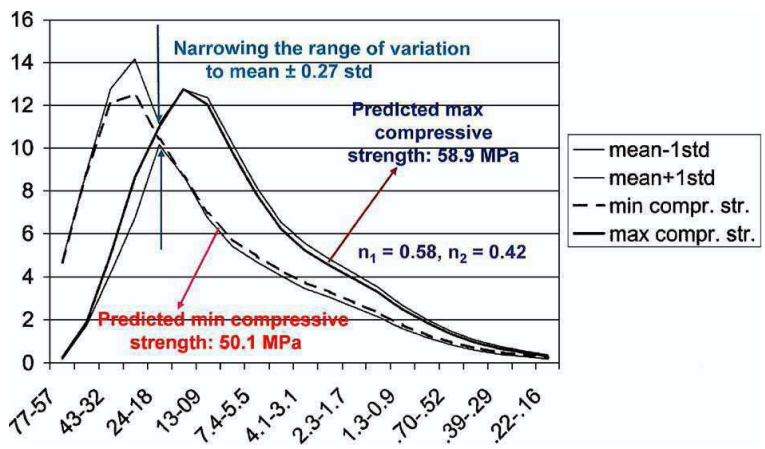

Fig. 9. Particle size distribution of cement from which min and max compressive strength at 28 days, allowing volume fractions of the size classes to vary ±1 S.D. about their mean values except for x_5 which was varied within $\bar{x}_5 \pm 0.27s(x_5)$.

the programmers Ø. Ingerøyen, Norcem and K. Dalsveen for their contribution.

References

[1] K. Svinning, Design and manufacture of Portland cement — application of sensitivity analysis in exploration and optimisation: Part I. Exploration. Proceedings of the 9th Scandinavian Symposium of Chemometrics, 21–24 August 2005, in press.
[2] A. Høskuldsson, Prediction Methods in Science and Technology, vol. 1, Thor Publishing, Copenhagen, 1996, p. 266.
[3] H. Martens, M. Martens, Food Qual. Prefer. 11 (2000) 5–16.
[4] H. Martens, M. Martens, Multivariate Analysis of Quality, An Introduction, vol. I, Wiley, Chichester, 2001, p. 209.
[5] K. Svinning, K.A. Datu, Prediction of microstructure and properties of Portland cement from production condition in cement mill: Part II. Prediction and sensitivity analysis, 11th International Congress on the Chemistry of Cement, Durban, 2003.
[6] K. Svinning, Ø. Ingerøyen, K. Dalsveen, J. Chemom. 14 (2000) 699–709.
[7] J.A. Nelder, R. Mead, Comput. J. 7 (1965) 308–313.

Paper IV

Available online at www.sciencedirect.com
ScienceDirect
Cement & Concrete Composites 30 (2008) 138–151
Cement & Concrete Composites
www.elsevier.com/locate/cemconcomp

Prediction of compressive strength up to 28 days from microstructure of Portland cement

K. Svinning [a,*], A. Høskuldsson [b], H. Justnes [c]

[a] NORCEM A/S, Process and Environmental Department, Brevik, Norway
[b] Danish Technical University, Luntofte, Denmark
[c] SINTEF Building and Infrastructure, Concrete, Trondheim, Norway

Received 10 January 2007; accepted 30 May 2007
Available online 29 June 2007

Abstract

The influence of the characteristics or the microstructure of Portland cement on compressive strength up to 28 days has been statistically investigated by application of partial least square (PLS) analysis. The main groups of characteristics were mineralogy and superficial microstructure represented by curves from X-ray diffraction analysis and differential thermogravimetric analysis, as well as particle size distributions.

PLS gave maximum explained variance in compressive strength at 1, 2, 7 and 28 days of 93%, 90%, 79% and 67%, respectively. The high explained variance makes the prediction of the compressive strength up to 28 days from the characteristics reliable.

The prediction ability makes it possible in this case to predict strength from cement characteristics and vice versa. Such a prediction can be utilized to design a cement to achieve target strength performance.

Keywords: Compressive strength; Cement characteristics; Multivariate data analysis; PLS

1. Introduction

Since 1991 a general investigation of microstructure of clinker and cement has been carried out as part of several succeeding projects at the cement producer Norcem A/S. More recently, the investigations have been organised in the three following subprojects:

1. Influences of the production conditions in the kiln and the cement mill on the microstructure of clinker and cement.
2. Influences of the microstructure of clinker and cement on the cement properties.
3. Establishment of models describing the influences of the production conditions in the kiln and the cement mill on the cement properties.

Results from the previous investigations are published by Svinning et al. [1,2], Svinning and Bremseth [3] and Svinning and Justnes [4].

Cement chemists use the short hand notation $C = CaO$, $S = SiO_2$, $A = Al_2O_3$, $F = Fe_2O_3$, $\overline{S} = SO_3$, $N = Na_2O$, $K = K_2O$, $H = H_2O$, etc. According to this notation the main mineral in cement, Ca_3SiO_5, should be written C_3S for simplicity. Cement microstructure can be described as composite grains from ground clinker consisting of domains of crystalline alite (C_3S) and belite (C_2S) partly embedded in frozen melt phase (interstitials) from where they are grown while in the kiln. The interstitials consist basically of C_3A and C_4AF. These minerals can attain several crystalline modifications. Alite is usually in the monocline form due to lattice contaminations like magnesium and aluminium and rapid cooling. Alkalis like potassium and sodium are present in the clinker in the order of 0.5–1.0% Na_2O-equivalents and will end up as contaminants stabilising different crystal modifications of other

* Corresponding author. Tel.: +47 35572314; fax: +47 35570400.
E-mail address: ketil.svinning@norcem.no (K. Svinning).

0958-9465/$ - see front matter © 2007 Published by Elsevier Ltd.
doi:10.1016/j.cemconcomp.2007.05.016

compounds (e.g. potassium in β-C_2S or sodium in C_3A) or as sulphates like aphthitalite, $K_3N\overline{S}_4$. Gypsum is ground together with clinker to form cement with controlled setting time. However, the temperature in the mill can be so high that gypsum ($C\overline{S}H_2$) may dehydrate to hemihydrate ($C\overline{S}H_{1/2}$). The distribution of main minerals in a neat Portland cement (i.e. without any other mineral additions than calcium sulphate) may typically be of the order 60% C_3S, 20% C_2S, 10% C_4AF, 5% C_3A and 5% $C\overline{S}H_2$.

Out of a great number of papers or articles regarding predictions and explanation of variation in compressive strength development based on examination of microstructure only a small selection is introduced. The compressive strength at three days was predicted by Goswani et al. [5] to increase with increasing ratio between the pulse counts for belite and alite, respectively. The pulse counts mentioned in [5] were actually XRD-(X-ray diffraction) peaks at $d_1 \approx 2.78$ Å (*p.h.* 1) and $d_2 \approx 2.74$ Å (*p.h.* 2). Brüggemann and Brentrup [6] evaluated a formula which used the amount of soluble alkali and the amount and the mean chord length of alite for predicting strength of cement. A formula generated by Knöfel [7] for prediction of compressive strength at 28 days used the amounts of alite, belite, aluminates and ferrite as variables. The amounts of minerals included in the prediction models in [6,7] were determined by microscopy.

The results presented in [5] encouraged Svinning and Bremseth [3] to continue research on the influence of the microstructure on the cement properties by statistical investigations. Compressive strength up to 28 days was predicted to increase with an increase in (*p.h.*1/*p.h.*2). The other variables included in the investigation in [3] were the chemical composition from XRF (X-ray fluorescence), the amount of di- and hemihydrate of $CaSO_4$ and various mass losses upon heating (i.e. thermogravimetry) describing the degree of prehydration and carbonation of the clinker minerals and specific fineness. In the work by Svinning et al. [2] on XRD studies on variations in the microstructure of Portland clinker correlated with the variation in the production conditions in the kiln, the whole profiles of selected XRD-peaks were included in the investigation. Statistically, this could be carried out by applying multivariate rather than multivariable modelling.

A further step in evaluating a model of prediction from the microstructure of the cement was to include more complete characteristics of the cement in the form of profiles from XRD and TG (thermogravimetry), and a complete particle size distribution (32 size classes). A prediction model evaluated from partial least square regression (PLS) on 200 variables and 120 observations was presented in Svinning et al. [1]. The presentation of the regression coefficients was limited to those needed for the prediction of potential compressive strength of the clinker from the XRD-profile of the clinker part of the cement. Prediction of compressive strength from another part of the microstructure: particle size distribution of cement is presented in Svinning [8]. In this work, more observations have been added to the observation **X**-matrix for inclusion in the PLS.

Beside ordinary multivariable regression, fuzzy logic [9], stepwise regression [10], genetics algorithms-artificial neural networks (GAs-ANNs) [11] and PLS [1–4,8] have been applied in the evaluation of the model for prediction of cement strength. GAs-ANNs and PLS represent different types of multivariate calibration or modelling with hidden layer or latent variables. In [8] the latent variables were taken into consideration in the sensitivity analysis, while in [11] the hidden layers were not. [8] shows examples of sensitivity analysis in the form of simulated variation of a latent variable from which cement properties are predicted.

The objective of this work was to establish a statistical model for the prediction of cement properties for all types of neat cement as well as cement containing small amounts (~5%) of limestone filler. To attain this objective, variables which presented a complete characterisation of the microstructure of the cement, and observations which represented a great variety of types of cement, were included in the PLS.

2. Methods

2.1. Characterisation of the microstructure of clinker

The XRD analysis was performed on ground clinker. The XRD-profiles consisted of intensities at every 0.02°. The scaling of the intensities and adjustment of the 2θ-position of the diffraction peaks were based on normalisation of the area and adjusting the 2θ-axis to match the diffraction peak at $d = 3.52$ Å for anatase (TiO_2), which was intermixed in an amount of 10 wt% of the total sample. Examples of diffractograms including the peak of the reference are shown in Fig. 1. To reduce the number of intensities (and the number of variables) and simultaneously increase the signal to noise ratio one variable was made out of three by averaging three adjacent variables in the diffraction profile before including the variables in PLS. The number of variables was further decreased by selecting two small regions (2θ) of diffractogram 29.88–30.70° and 32.90–34.10° (using CuKα-radiation) to be included in the modelling.

2.2. Characterisation of superficial microstructure

As mentioned above, the superficial microstructure is characterised by thermogravimetry (TG) analysis. The TG apparatus applied was a Netzsch STA – Apparatur 409 V/3/C®. A dynamic mode of thermogravimetry is used, in which the sample is heated in an environment whose temperature is changing in a predetermined manner, preferably at a linear rate. Weights of samples analysed were 4.2 g and the heating rate was 2 K/min. Fig. 2 shows two examples of thermograms from DTGA of neat cement and cement with limestone used as filler, respectively. The

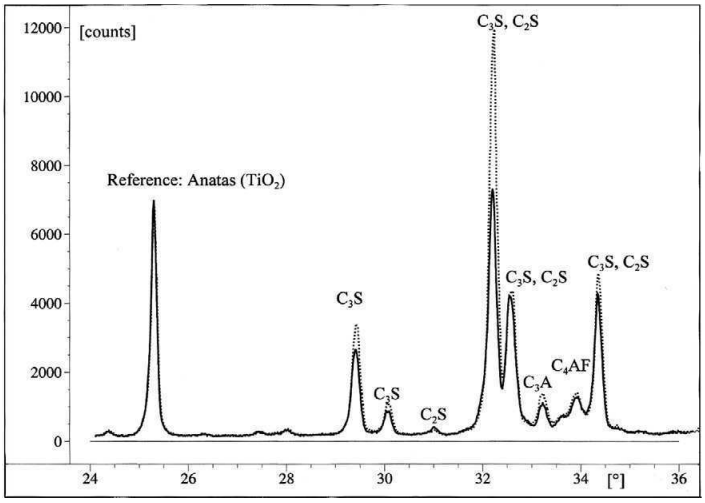

Fig. 1. Examples of two X-ray diffractograms of two neat cements in the 2θ range 24–36°.

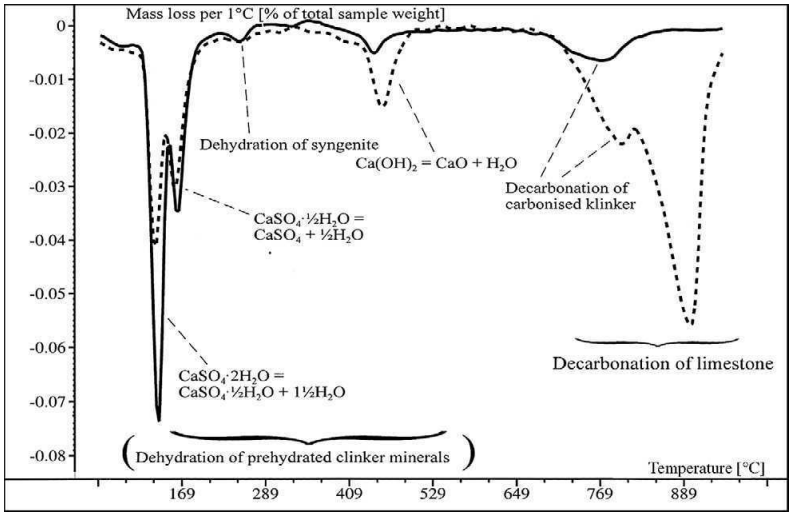

Fig. 2. Two examples of DTG (differentiated thermogravimetry) curves for neat cement and cement with limestone filler, respectively.

thermograms are interpreted with respect to the most common reactions occurring during the heating.

The information about superficial microstructure is included as x- or y-variables in PLS in the form of mass loss per 4 °C in the temperature range 20–330 °C and mass loss per 8 °C in the range 330–940 °C. No further interpretation of the results from DTGA prior to PLS was done.

2.3. Statistical modelling

In the case of a large number of variables relative to the number of observations or objects, data compression by expressing the original x-variables by fewer latent variables or factors could be necessary. Partial least square regression (PLS) does calculation and optimisation of a number of factors for maximum explanation of variance in the y-variables. In addition, model parameters are calculated for prediction of y for new values of the x-variables. In this work, PLS was performed on several y-variables combined expressed as a vector. The models which relate the PLS-model terms are then given by the two expressions in the equations below:

$$\mathbf{X} = \mathbf{T}\mathbf{P}^T + \mathbf{E} \tag{1}$$

$$\mathbf{Y} = \mathbf{U}\mathbf{Q}^T + \mathbf{F} \tag{2}$$

T and **U** are factor scores, **P** and **Q** are x and y-variables loadings and **E** and **F** are the residuals in **X** and **Y**, respectively. Alternatively, Eq. (1) could be expressed in the form:

$$\mathbf{X} = \mathbf{t}_1\mathbf{p}_1^T + \mathbf{t}_2\mathbf{p}_2^T + \cdots + t_k\mathbf{p}_k^T + \cdots + \mathbf{t}_l\mathbf{p}_l^T + \mathbf{E} \quad (3)$$

l is equal to maximum number of latent variables for maximum explanation of variance in **Y**. If there is only one y-variable to be modelled Eq. (2) could be replaced by the following equation:

$$\mathbf{y} = \mathbf{T}\mathbf{q}^T + \mathbf{f} \quad (4)$$

PLS with one or several y-variables is denoted PLS1 or PLS2, respectively. In case of PLS1 the regression coefficients to be used in the predictor $\hat{\mathbf{y}} = \mathbf{1}b_0 + \mathbf{X}\hat{\mathbf{b}}$ are computed as follows:

$$\hat{\mathbf{b}} = \widehat{\mathbf{W}}(\widehat{\mathbf{P}}^T\mathbf{W})^{-1}\hat{\mathbf{q}} \quad (5)$$

$$\text{and} \quad b_0 = \bar{y} - \bar{\mathbf{x}}^T\hat{\mathbf{b}} \quad (6)$$

where **W** are loading weights used in PLS1.

Similarly, for PLS2:

$$\widehat{\mathbf{B}} = \widehat{\mathbf{W}}(\widehat{\mathbf{P}}^T\widehat{\mathbf{W}})^{-1}\widehat{\mathbf{Q}}^T \quad (7)$$

and $\mathbf{b}_0^T = \bar{\mathbf{y}}^T - \bar{\mathbf{x}}^T\widehat{\mathbf{B}}$

By scaling the variables, unreasonable domination of variables with dominating standard deviations, $s(x)$, on the model can be avoided. The weighting of $x_{i,k}$ by centring and scaling is performed according to the following formula:

$$x_{ik,w} = \frac{x_{ik} - \bar{x}_k}{s(x_k)} \quad (8)$$

The type of validation applied in this work is cross validation. Validation means to determine the number of PLS-components or latent variables that give the prediction of y from **X** in future objects that lack the value of the y-variable. In this work, the calibration set was split into 10 segments, and the validation was repeated 10 times, each time treating one-tenth of the calibration set as prediction objects. The cross validated residual variance in y after inclusion of n latent variables is as follows:

$$\mathrm{Var}(y)_{\mathrm{val},n} = \frac{1}{I_{\mathrm{pr}}}\sum_{i=1}^{I_{\mathrm{pr}}}(\hat{y}_i - y_i)^2 \quad (9)$$

where I_{pr} is equal to the number of validation objects, which is equal to the number of the calibration objects. $\hat{y}_i$ is the predicted value and y_i the respective observed value. The explained variance of the total variance in y, $\mathrm{Var}(y)_0$, is calculated in this way

$$\mathrm{Expl.Var.}(\%) = \frac{\mathrm{Var}(y)_0 - \mathrm{Var}(y)_{\mathrm{val},n}}{\mathrm{Var}(y)_0} \quad (10)$$

Other quality criteria, which describe the validity of the prediction, are the root mean square error of prediction (RMSEP), the bias and the standard error of prediction. The parameters are calculated by the following formulas:

$$\mathrm{RMSEP} = \sqrt{\mathrm{Var}(y)_{\mathrm{val},n}} \quad (11)$$

$$\mathrm{Bias} = \frac{1}{I_{\mathrm{pr}}}\sum_{i=1}^{I_{\mathrm{pr}}}(\hat{y}_i - y_i) \quad (12)$$

$$\mathrm{SEP}^2 \approx \mathrm{RMSEP}^2 - \mathrm{Bias}^2 \quad (13)$$

The iterative algorithms for calibration, validation and prediction are described in detail in Martens and Næs [12]. The software applied for PLS was UNSCRAMBLER®, version 7.5.

3. Experimental

The types of cement included in the investigation, with reference to European (EN) and in addition, Norwegian Standards (NS) where they differ by national addendum, are as follows:

1. Low alkali, sulphate resistant cement, EN 197-1-CEM I 42.5 R, NS 3086-CEM I R-SR-LA.
2. Low alkali, high strength cement, EN 197-1-CEM I 52.5 N, NS 3086-CEM I 52.5 N-LA.
3. Standard Portland cement, EN 197-1-CEM I 42.5 R.
4. Rapid Portland cement, EN 197-1-CEM I 42.5 R, NS 3086-CEM I 42.5 RR.

Table 1 contains the typical mineral composition (calculated from the chemical composition by Bogue's formula) in the clinker used in the different types of cement presented above.

Some of the samples of Standard Portland cement, EN 197-1-CEM I 42.5 R, contained limestone filler.

Table 1

Mineral and chemical composition (%)	Sulphate resistant	High strength	Standard Portland	Rapid Portland
C_2S	16	12	13	12
C_3S	60	66	62	66
C_3A	0.5	6.1	7.7	6.1
C_4AF	15.8	11.0	10.0	11.0
Free lime	0.8	1.1	1.3	1.4
Na_2O-equiv.	0.53	0.55	1.05	1.15

Table 2
Results from PLS2 of compressive strengths up to 28 days as functions of the characteristics of the cement

Response variable, y	Maximum explained variance (%) with eight PLS-components included
Total	82
Compressive strength at one day	93
2 days	90
7 days	79
28 days	67

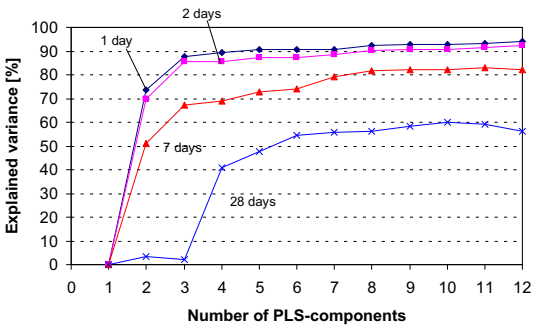

Fig. 3. Explained variances in compressive strength at 1, 2, 7 and 28 days versus the number PLS-component included in PLS2.

The *y*-variables: Compressive strengths at 1, 2, 7 and 28 days, were measured according to EN 196-10. The observation **X**-matrix consisted of 146 observations and 205 variables. The *x*-variable could be divided into the following groups or categories:

1. Mineralogy of the clinker part of the cement described by X-ray diffractogram sequences were taken as variables no. 1–14, 17–37.
2. Variables no. 38–106 and 137–213 were the superficial microstructure of the cement as described by thermograms from DTGA.
3. Particle size distribution of the cement were taken into account by variables no. 110–136.
4. Variables no. 15 and 16 consisted of the amount of SO_3 and free lime.

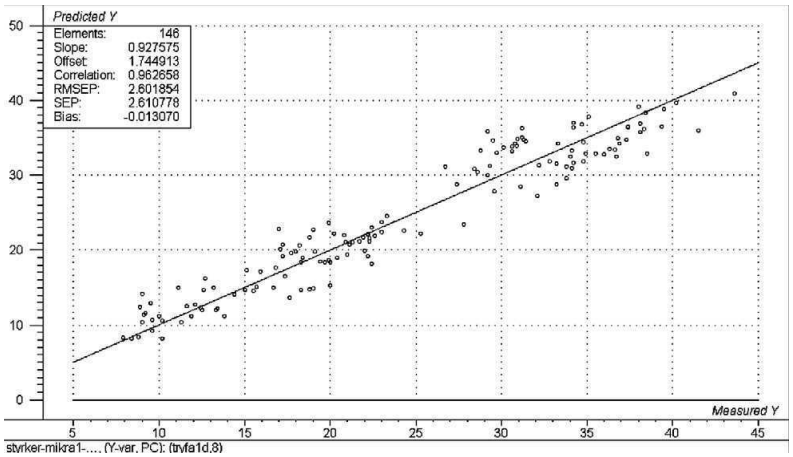

Fig. 4. Predicted versus measured compressive strength (MPa) at one day.

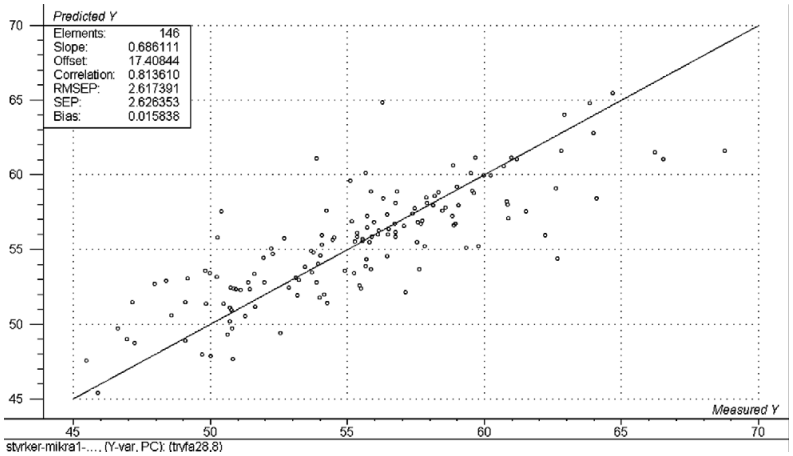

Fig. 5. Predicted versus measured compressive strength (MPa) at 28 days.

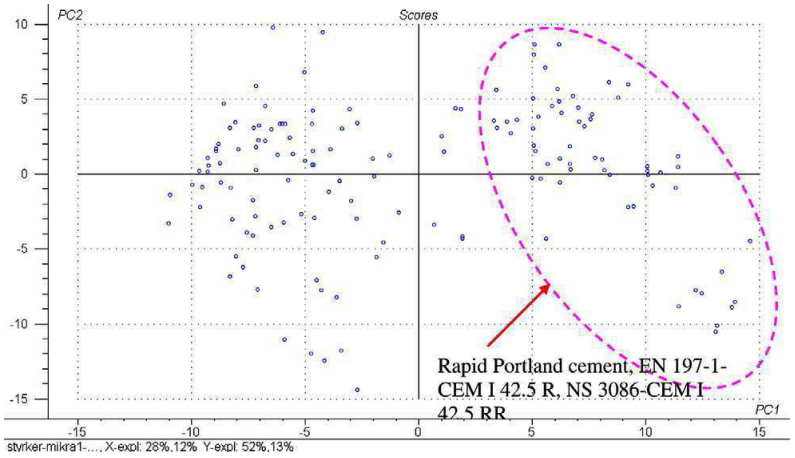

Fig. 6. 2-vector score plot for objects included in PLS. Levels of PLS-component no. 1 (PC1) and 2 (PC2) in each object.

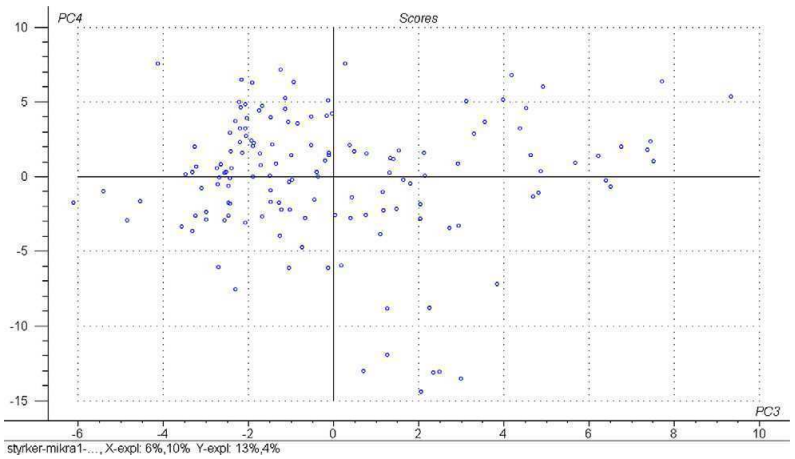

Fig. 7. 2-vector score plot for objects included in PLS. Levels of PLS-component no. 3 (PC3) and 4 (PC4) in each objects.

4. Results and discussion

The maximum explained variance from PLS of the respective *y*-variables and the number of PLS-components included for maximum explanation are presented in Table 2. Fig. 3 shows[1] the explained variance in compressive strength up to 28 days versus number of PLS-component or latent variables included. Predicted versus measured compressive strengths at 1 and 28 days are plotted in Figs. 4 and 5, respectively.

Fig. 4 demonstrates that the predicted versus measured compressive strength at 1 day fits the target line (predicted equal to measured) better than what is the case for compressive strength at 28 days in Fig. 5. This coincides with explained variances in the two properties from PLS. However, the points in Fig. 4 are not evenly distributed along the target line as in Fig. 5. This is confirmed by a group in the 2-vector score plot (PLS-component no. 1 and 2) shown in Fig. 6. The distinct group marked in Fig. 6 represents samples of cement of the type EN 197-1-CEM I 42.5 R, NS 3086-CEM I 42.5 RR. The relevant 2-vector score plot to find groups that have an influence on the prediction of compressive strength at 28 days is depicted in Fig. 7, which shows levels of PLS-component no. 3 and 4 in each objects. No distinct groups similar to the one in Fig. 6 can

[1] For interpretation of colors in Figs. 3, 6, 7 and 15–17, the reader is referred to the web version of this article.

be seen. Score plots could reveal if there are any outliers, i.e. observations that deviate statistically from the others, appearing as scores located relatively far away from the others. Working further with the data from [1] some of the outliers were removed before a new PLS.

According to the information in Fig. 3 the two first latent variables contribute very little to the explanation of variance in compressive strength at 28 days compared to compressive strength at an earlier age. From this observation, a separate PLS-model for prediction of strength at 28 days could be evaluated. 2-vector loading plots, examples of which are shown in Figs. 8 and 9, the figures not only show which of the variables are the most important for each PLS-component but also show correlation between the different variables. The figures contain correlation loadings, i.e. loadings marking 50% and 100% explained variance limits. Correlation loadings are helpful in revealing variable correlation. The loading plot in Fig. 8 confirms the low explained variance in compressive strength at 28 days including only PLS-component no. 1 and 2 while the explained variance in compressive strength up to 7 days is more than 50%. The loading plot shows also a positive correlation between the early strengths and one part of the variables describing the particle size distribution, located very close to each other. Simultaneously, the early strengths are negatively correlated to another part whose variables are lying along the diagonal through the *y*-variable and origin equidistantly on the other side of

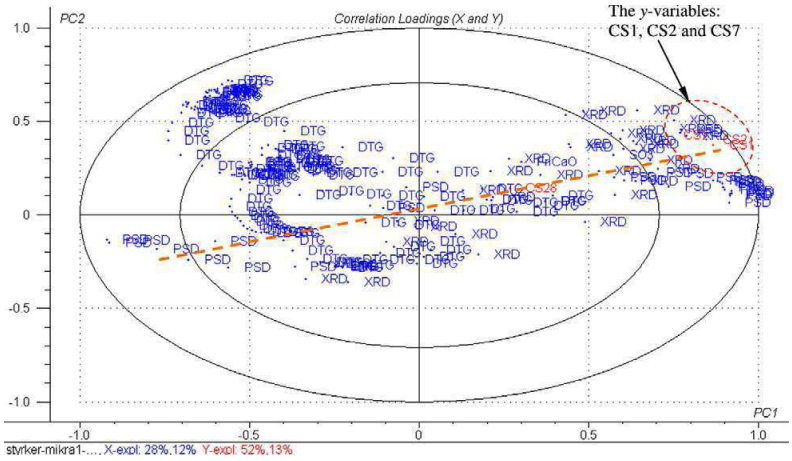

Fig. 8. 2-vector plot, *x*- and *y*-loadings for PLS-component no. 1 (PC1) and no. 2 (PC2). The variable legend refers to the analysis giving the value of variables: XRD = X-ray diffraction, DTG = differential thermogravimetry, PSD = particle size distribution and CS1, CS2, CS7 and CS28 = compressive strength at 1, 2, 7, and 28 days, respectively.

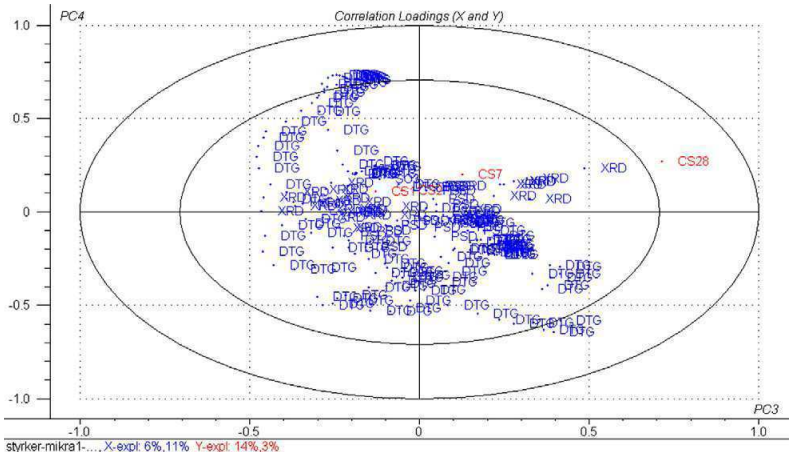

Fig. 9. 2-vector plot, *x*- and *y*-loadings for PLS-component no. 3 (PC3) and no. 4 (PC4). The variables presented here are the same as in Fig. 8.

origin. As expected, compressive strength at early ages correlates strongly with the fineness and the particle size distribution (PSD) of cement. The loading plot in Fig. 8 reveals that early strength also correlated with variables (labelled XRD) describing mineral composition and structure, while compressive strength according to Fig. 9 correlates more with the XRD- than the PSD-variables.

Figs. 10–14 show (a) the variation of and (b) the regression coefficient, $\mathbf{b}_w$, for prediction of compressive strengths up to 28 days from the variables presented in the experimental section. The regression coefficients $\mathbf{b}_w$: $b_{w1}, b_{w2}, \ldots, b_{wK}$ used in the prediction model $y_w = b_{0w} + b_{w1}x_{1,w} + b_{w2}x_{2,w} + \cdots + b_{wK}x_{K,w}$ for prediction of the four y-variables in centred and scaled form are presented in Figs. 10–14. The elements in $\mathbf{b}_w$, contrary to the respective elements in $\mathbf{b}$ used for prediction from the x-variables in their original forms, i.e. neither centred nor scaled, give the information about how much each x-variable influences the y-variables. Looking at 10b, $\mathbf{b}_w$ for predicting compressive strength at 28 days indicate that the compressive strength at 28 days will decrease with increasing amount of aphthitalite having a peak at $2\theta = 30.38°$ and increase with a shift of the C_3S-peak from $2\theta = 30.09°$ to $2\theta = 30.04°$.

However, $\mathbf{b}_w$ defined as an indicator of influence could be somewhat misleading, if the confidence intervals of $\mathbf{b}_w$ are not taken into consideration. Martens and Martens [13] have developed an improved method for uncertainty testing based on cross validation, Jack knifing, and stability plot. To obtain a better interpretation of $\mathbf{b}_w$, the standard deviations of the respective variables should be presented too. Alternatively, picking out every fifth observation of the variation, as illustrated in Figs. 10–14a, will give an idea about variance. However, $\mathbf{b}$ cannot then be calculated directly from $\mathbf{b}_w$.

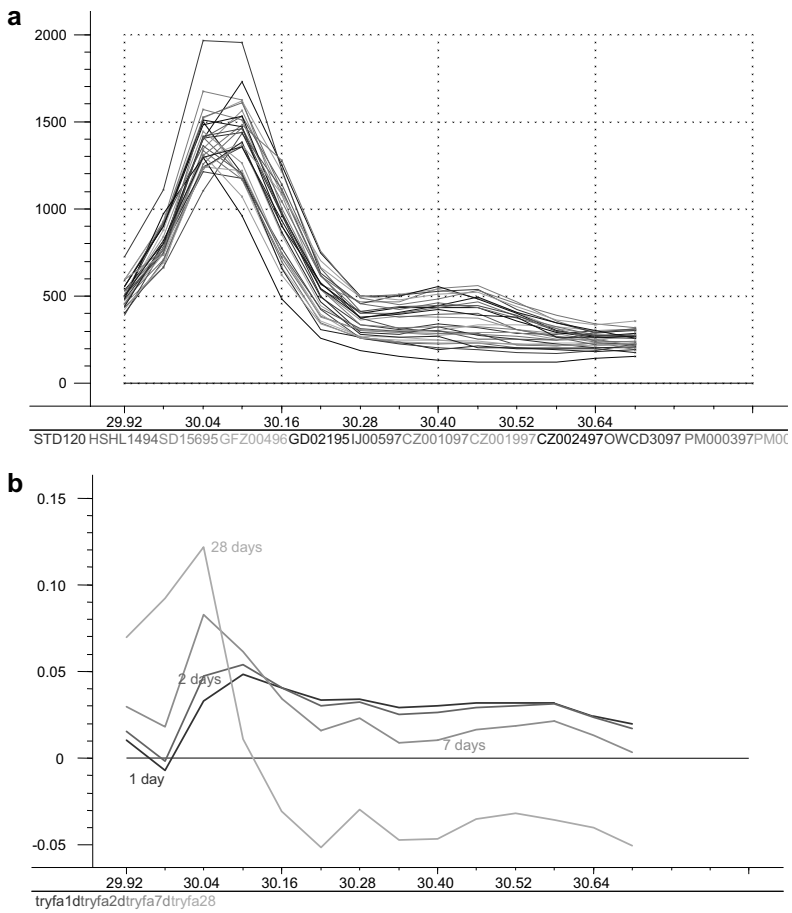

Fig. 10. Results from PLS for prediction of compressive strength at 1, 2, 7 and 28 days from XRD intensities in the 2θ-region 29.92–30.70° (abscissa). (a) Variation in the variables no. 1–14 (ordinate has unit XRD counts). (b) The respective regression coefficients, $\mathbf{b}_w$, for prediction of compressive strengths as ordinate.

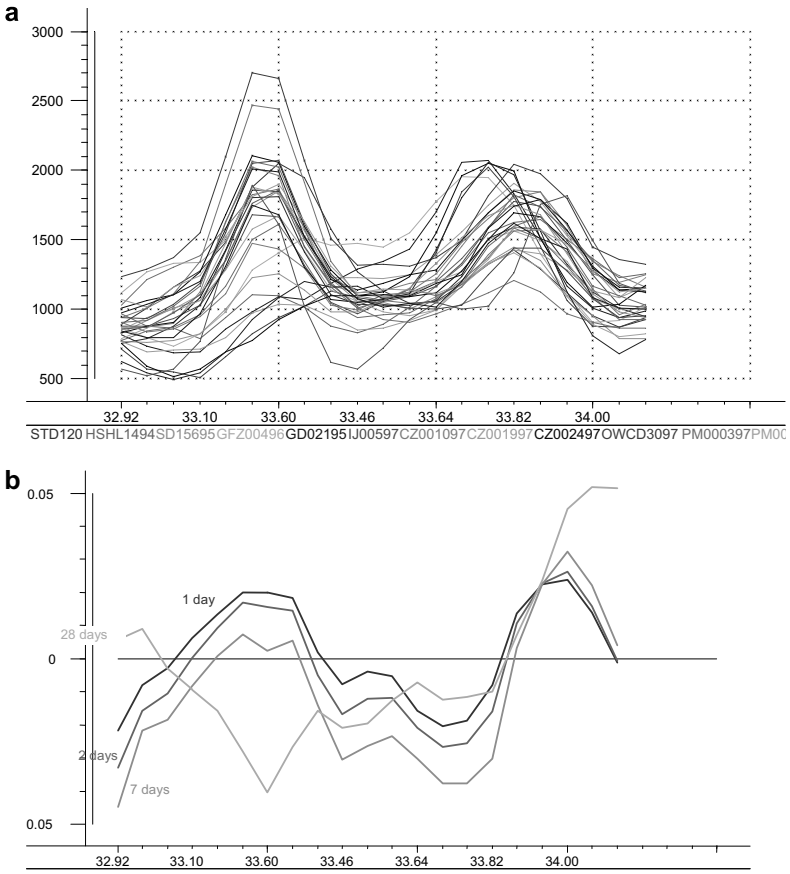

Fig. 11. Results from PLS for prediction of compressive strength at 1, 2, 7 and 28 days from XRD intensities in the 2θ-region 32.92–34.10° (abscissa). (a) Variation in the variables no. 17–37 (ordinate has unit XRD counts). (b) The respective regression coefficients, $\mathbf{b}_w$, for prediction of compressive strengths as ordinate.

The mineral composition could be determined by multi-component Rietveld analyses. Instead of including selected parts of the diffractogram, which requires a lot of variables to describe the profiles, only a few variables giving the whole mineral composition would need to be included in PLS. However, the inaccuracy of the amount of a mineral determined by Rietveld analyses will increase with decreasing amount of the mineral. C_3A could also exist as two polymorphs, cubic and orthorhombic, with different reactivity. Having a total amount of C_3A, as calculated by the Bogue methodology, like for instance 5%, split into polymorphs could lead to fairly high inaccuracy in calculation of the amount of each. The benefits of including the XRD-profile as it has been done here are that (a) no information would be lost, and (b) any change in structure or unit cell dimensions due to foreign ion contamination or interchange would be detected directly by changes in the position of the respective peaks. Such structural changes of the minerals may influence their reactivity towards water leading to changes in properties like compressive strength up to 28 days as shown by Svinning et al. [1]. The minerals giving rise to reflections in the two selected diffraction angle ranges are listed in Tables 3 and 4.

As seen from Table 3, the range $2\theta = 29.88$–$30.70°$ contains information solely on alite and aphthitalite, $K_3Na(SO_4)_2$ (i.e. other known cement minerals have no reflections in this region). Although the intensities of the two overlapping alite reflections are modest, the domination of this mineral in Portland cement secures a good signal to noise ratio for this mineral. Alite is dominating the early strength development, as is well known. One of the strongest reflections of aphthitalite is in the high end of this first XRD region, and it can give valuable information on this easily soluble alkali sulphate. In spite of its low content, aphthitalite can dominate the early pore water chemistry and strongly influence for instance setting time. Note that calcite interground in some cements has its strongest reflection at 29.4°. This means that the tail of the main

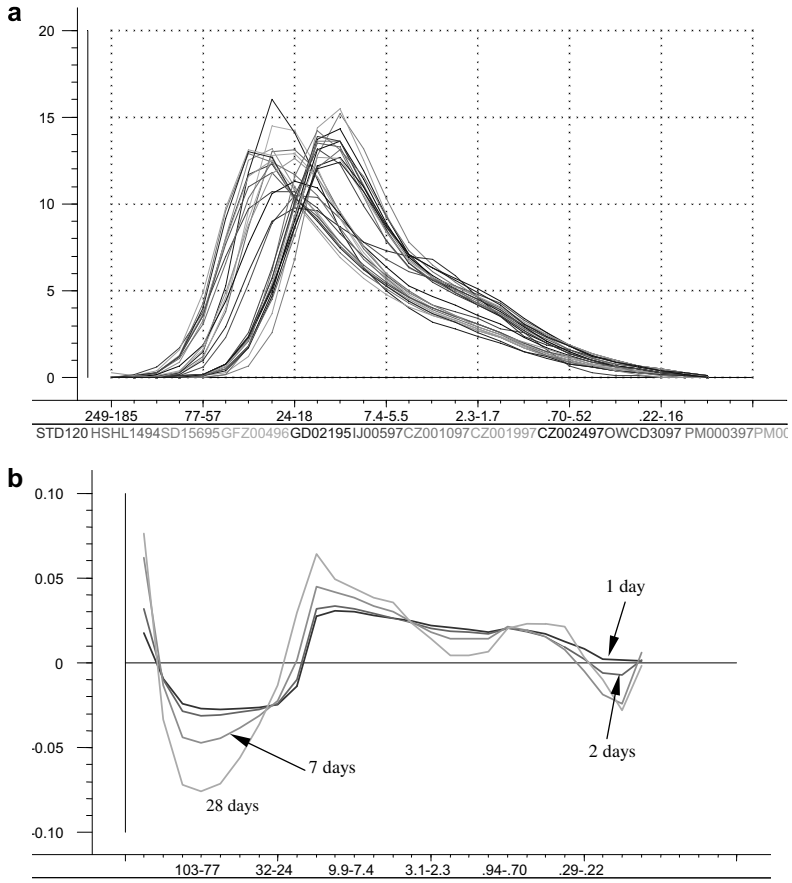

Fig. 12. Results from PLS for prediction of compressive strength at 1, 2, 7 and 28 days from volume fractions of cement in 27 size classes between 249 and 0.09 μm (abscissa). (a) Variation in the variables no. 110–136 (ordinate is volume fraction). (b) The respective regression coefficients, $\mathbf{b}_w$, for prediction of compressive strengths as ordinate.

calcite peak may reach into the 29.88–30.70 2θ range. Table 4 lists the only cement minerals contributing to the reflections in the range $2\theta = 32.90$–$34.10°$. This second XRD region is not only dominated by reflections of C_3A and C_4AF, but it also contains the dominating reflection of the more seldom clinker minerals α'-C_2S and mayenite, $C_{12}A_7$. The common clinker phase belite, β-C_2S, also has a modest reflection in the low end of this region. However, since alite and belite are the only silicate phases, an increase in alite content will lead to a decrease in belite content, so an independent control of the latter is not required. For cement analysis, it is also of interest that gypsum has a medium reflection in the high end of this second XRD region. Thus, the two selected XRD regions cover the responses for all the important cement minerals, and are a more direct measure of the actual content of each mineral since the simple Bogue calculation (see Table 2) at best is an indication of the cement composition.

According to general experiences, the superficial microstructure should influence compressive strength at one day more than the strength at 28 days. $\mathbf{b}_w$ shown in Fig. 13b and Fig. 14b could indicate the opposite. $\mathbf{b}_w$ for predicting compressive strength at 28 days from some of the variables is surprisingly high taking into account the variations of the variables depicted in Fig. 13a and Fig. 14a. To examine the significance of the influence of **x** on **y,** uncertainty testing on $\mathbf{b}_w$ giving confidence interval of each $\mathbf{b}_w$ was performed. Figs. 15 and 16 show $\mathbf{b}_w$ inclusive confidence interval of 95% for prediction of compressive strength at 1 and 28 days, respectively, from the variables presented in Fig. 14a. Evaluation of the significance of the influence of a variable x_k from Jack knifing estimation could be defined significant if the uncertainty level is less than $2|\mathbf{b}_{wk}|$. From this criterion, the influence of the actual variables on the compressive strength at 28 days can be considered to be less significant than the analogues influence on compressive

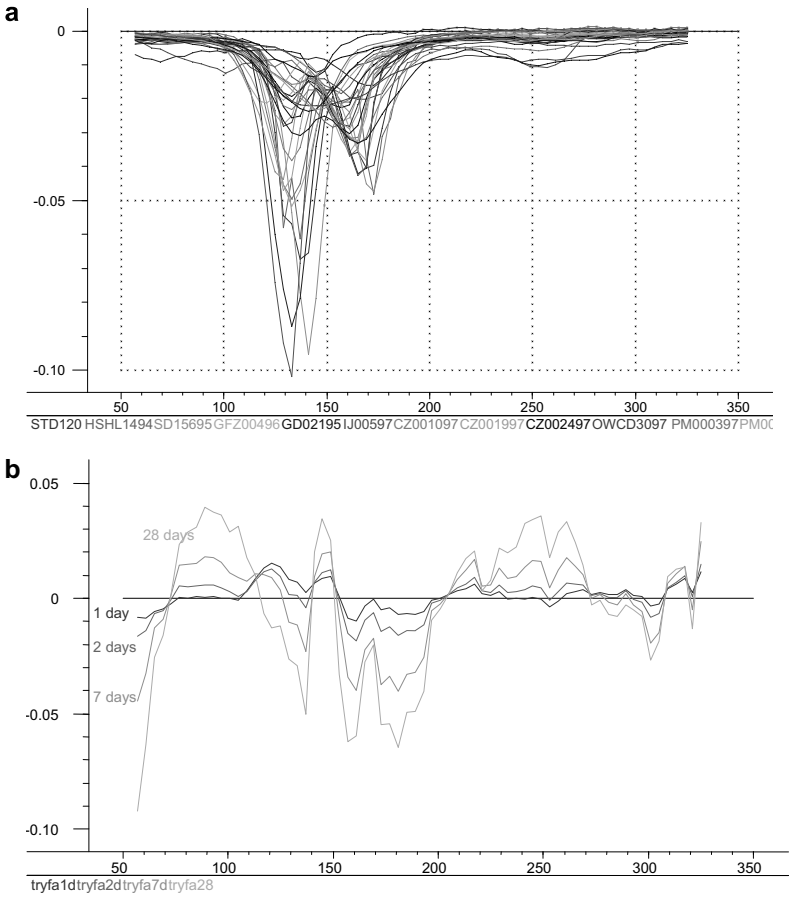

Fig. 13. Results from PLS for prediction of compressive strength at 1, 2, 7 and 28 days from mass loss per 4 °C from DTG in the temperature range 57–325 °C (abscissa). (a) Variation in the variables no. 38–106 (DTG values are ordinate). (b) The respective regression coefficients, $\mathbf{b}_w$, for prediction of compressive strengths as ordinate.

strength at one day. The same consideration can be made for the variables presented in Fig. 13. In general, the variables describing the superficial microstructure can be considered to influence the compressive strength at 28 days less than the compressive strength at one day.

Examples of influence of the structure of minerals on the strength development, as well as influence of the amount the minerals, can be discovered comparing Fig. 10a and b and Fig. 11a and b, respectively. The variation of the position of the XRD-peak of C_3S shown in Fig. 10b indicates variations in the contaminants of C_3S (i.e. the structure is the same, but the unit cell axes may vary). The form and threshold of the curves of $\mathbf{b}_w$ indicate that the structure of C_3S has an great impact on compressive strength at both 1 and 28 days. A C_3S-peak at $2\theta < 30.04°$ will give a low compressive strength at one day and high strength at 28 days. For C_3S having an XRD-peak at $2\theta > 30.04°$ the opposite will be the result. However, note that since limestone has its strongest peak at 29.4°, the tail of this peak for cements with 4% interground filler may make it appear as the C_3S-peak has shifted to a lower value. By comparing Fig. 11a and b a variation in the structure of C_3A is indicated giving variation mostly in compressive strength at one day. The variation in the structure of C_3A is according to Taylor [14] a shift from orthorhombic to cubic structure due to a decrease in amount of sodium. The variation in the structure of C_3S is more difficult to explain (may be due to limestone influence).

Instead of including spectral variables as those describing XRD- and DTGA-curves, fewer variables presenting the interpretation of the curves could be included. A classical example of interpretation is determination of the amount of di- and hemihydrate of $CaSO_4$ from differential scanning calorimetry (DSC) analysis. A successful determination is conditional on having well separated peaks describing the dehydration of $CaSO_4 \cdot 2H_2O$ in two steps.

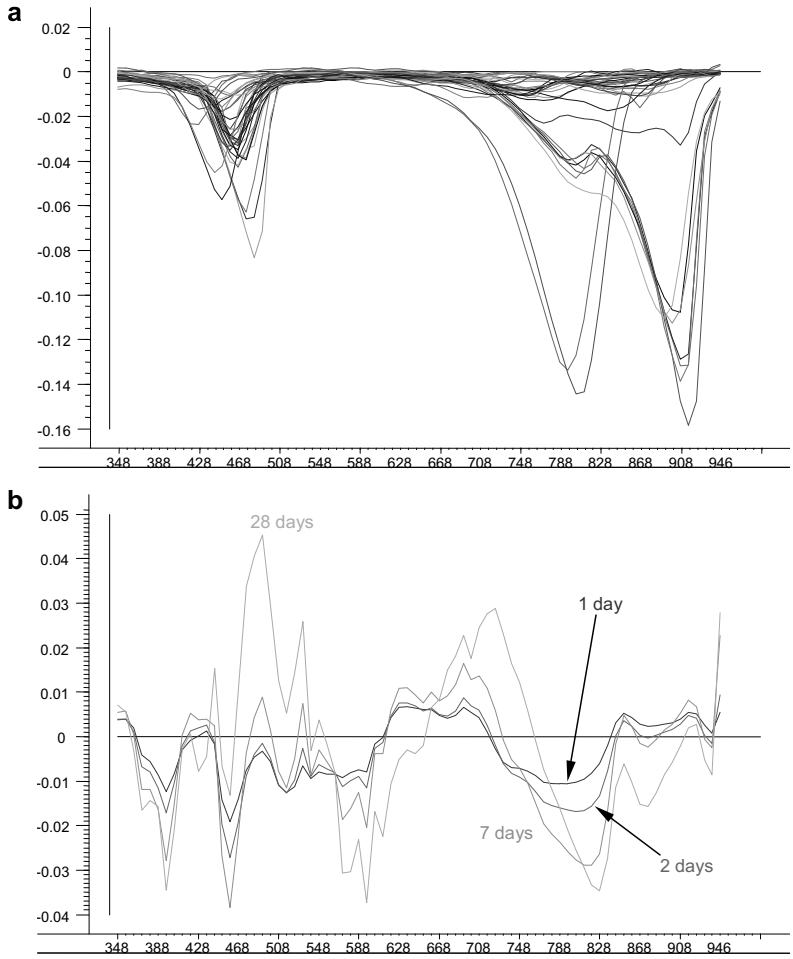

Fig. 14. Results from PLS for prediction of compressive strength at 1, 2, 7 and 28 days from mass loss per 8 °C from DTGA in the temperature range 348–950 °C (abscissa). (a) Variation in the variables no. 137–213 (DTG values are ordinate). (b) The respective regression coefficients, $\mathbf{b}_w$, for prediction of compressive strength as ordinate.

Table 3
Major phases within the XRD range $2\theta = 29.88$–$30.70°$

Phase	2θ (°)	d (nm)	Indices $\langle hkl \rangle$	Intensity (rel)
Alite (M3)	30.04	0.2975	⟨804⟩	10
	30.09	0.2970	⟨620⟩	20
Aphthitalite	30.38	0.2940	⟨102⟩	75

Achievement of such a separation requires less amount of sample and a smaller crucible + lid with an aperture so small that it allows only diffusion controlled transport of vapour of water out of the crucible. In our case the similar two peaks from DTGA are not quite separated. The determination of di- and hemihydrate will be too inaccurate. Instead, the variables describing the DTGA-curves should

Table 4
Major phases within the range $2\theta = 32.90$–$34.10°$

Phase	2θ (°)	d (nm)	Indices $\langle hkl \rangle$	Intensity (rel)
Belite, β-C_2S	32.98	0.2716	⟨121⟩	38
α′-C_2S	33.65	0.2663	⟨260⟩	100
Cubic C_3A	33.26	0.2694	⟨044⟩	100
Orthorhombic C_3A	33.27	0.2693	⟨224⟩	100
	33.04	0.2711	⟨040⟩	25
	32.93	0.2720	⟨400⟩	31
$C_{12}A_7$	33.41	0.2680	⟨420⟩	100
C_4AF	33.84	0.2649	⟨141⟩	100
	33.64	0.2664	⟨002⟩	47
Gypsum	33.35	0.2684	⟨150⟩ and ⟨220⟩	50

therefore be included. Nevertheless, a qualitative interpretation of the curves could be useful to explain the

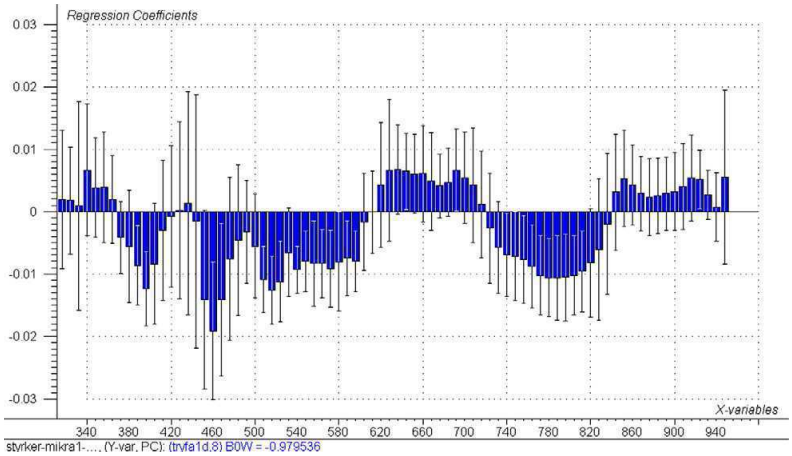

Fig. 15. Results from uncertainty testing on the regression coefficient, $\mathbf{b}_w$ (ordinate), for prediction of compressive strength at one day from the variables presented in Fig. 14 giving confidence intervals of 95%. Abscissa indicates temperature.

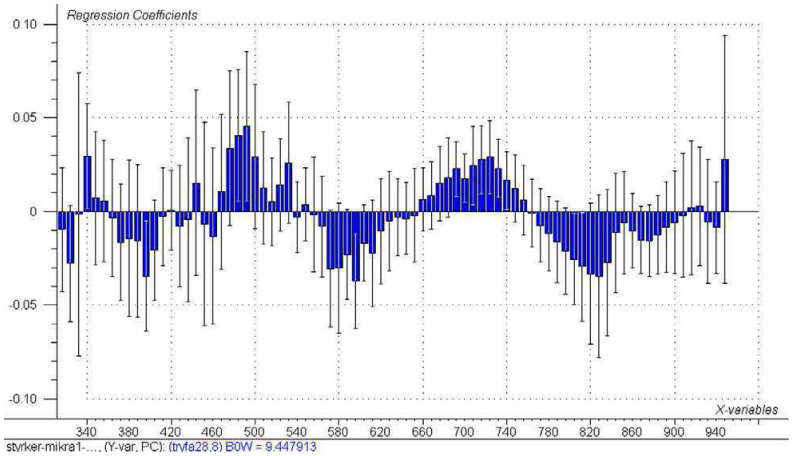

Fig. 16. Results from uncertainty testing on the regression coefficient, $\mathbf{b}_w$ (ordinate), for prediction of compressive strength at 28 days from the variables presented in Fig. 14 giving confidence intervals of 95%. Abscissa indicates temperature.

influences. The same dilemma about what variables to include in the modelling in the case of predicting compressive strength of fly ash cement from the microstructure of the cement could arise. Fig. 17 shows curves from DTGA of four fly ash cements containing about 20% fly ash, EN 197-1-CEM II/A-V 42.5 R. The curve indicates oxidation of perhaps ferrous mineral in the temperature range of approx. 370–550 °C and decarbonisation reaction in the temperature range of approx. 750–920 °C. The DTGA-curves will be difficult interpret quantitatively and accordingly defining variables to present the interpretation will be impossible. In any case the curves might contain some information valuable for giving a good model for prediction of compressive strength. Preliminary work on modelling of the compressive strength shows a high influence of loss on ignition of fly ash on the compressive strength at one day.

By application of sensitive analysis as described by Svinning [8] the influence of the microstructure could be examined more quantitatively. In [8] predictions of variation in compressive strength at 1 and 28 days from variation of latent variables of particle size distribution are shown. By including specific fineness as an additional variable a typical variation in the size distribution while the specific fineness is kept constant was simulated. The influence of a variable or a latent variable on a response variable, which could be a cement property, is significant if the confidence intervals of the predicted values do not overlap.

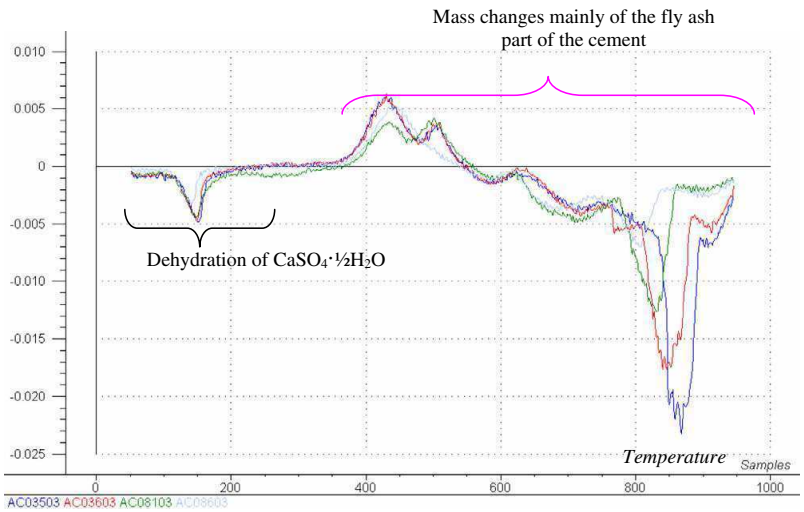

Fig. 17. DTGA of four samples of fly ash cement, EN 197-1-CEM II/A-V 42.5 R.

5. Conclusion

PLS of compressive strength up to 28 days on variables representing the characteristics of Portland cement gave maximum explained variance in compressive strength at 1, 2, 7 and 28 days of 93%, 90%, 79% and 67%, respectively. The high explained variance makes the prediction of the compressive strength up to 28 days from the characteristics reliable. Most of the variance in the compressive strength up to 28 days can be explained from the variances of the variables describing the mineralogy and the particle size distribution. The variables describing the superficial microstructure influenced the compressive strength at 28 days less than the compressive strength at one day.

The prediction ability makes it possible in this case to predict strength from cement characteristics and vice versa. Such a prediction can be utilized to design a cement to achieve target strength performance. By including the *x*-variables presenting the characteristic in the form of spectra no information will be lost and no further interpretation will be necessary to achieve a good prediction model. To achieve good strength prediction of fly ash containing cement, including the fly ash characteristics as spectra could be beneficial since the interpretation of these spectra is difficult.

The methodology demonstrated in the present paper is not limited to strength (which is easy measured directly), but it is also applicable to other more difficult/expensive achievable performance parameters that may beneficially be optimised via prediction from cement characteristics before actually documenting it for the most promising final products.

References

[1] Svinning K, Justnes H, Viggh E, Bremseth SK, Johansson S-E. Examination of clinkers from four Scandinavian Plants with respect to microstructure and cement properties. In: Proceedings of 22nd international conference on cement microscopy, Montreal; 2000. p. 137–153.

[2] Svinning K, Bremseth SK, Justnes H. X-ray diffraction studies on variations in microstructure of Portland clinker correlated with variations in production conditions in the kiln. World Cem 1996:80–6.

[3] Svinning K, Bremseth SK. The influence of microstructure of clinker and cement on setting time and strength development until 28 days. In: Proceedings of 18th international conference on cement microscopy, Houston; 1996. p. 514–513.

[4] Svinning K, Justnes H. Application of partial least square regression analysis in examination of correlations between production conditions, microstructure of clinker and cement properties, In: Proceedings of the 10th international congress on the chemistry of cement, Gothenburg; 1997. li038. p. 8.

[5] Goswani G, Mohapatra BN, Panda JD. Characterisation of burning condition by X-ray diffractometry. Cem Concr Res 1991;21:1176–9.

[6] Brüggemann H, Brentrup L. Correlations between mineralogical clinker parameters and cement strength. In: Proceedings of the 11th international conference on cement microscopy, Richmond; 1994. p. 226–245.

[7] Knöfel D. Interrelation between proportion of clinker phases and compressive strength of Portland cements. In: Proceedings of the 11th international conference on cement microscopy, New Orleans; p. 246–262.

[8] Svinning K. Chemom Intell Lab Syst 2006;84:177–87.

[9] Akkurt S, Tayfur G, Sever C. Fuzzy logic model for the prediction of cement compressive strength. Cem Concr Res 2004;34:1429–33.

[10] Tsivillis S, Parissakis G. A mathematical model for prediction of cement strength. Cem Concr Res 1988;28:9–14.

[11] Akkurt S, Ozdemir S, Tayfur G, Akyol B. The use of GA-ANN in the modelling of compressive strength of cement mortar. Cem Concr Res 2003;33:973–80.

[12] Martens H, Næs T. Multivariate calibration. 2nd ed. Chichester: Wiley; 1989.

[13] Martens H, Martens M. Food Qual Prefer 2000;11:5–16.

[14] Taylor HFW. Cement chemistry. 1st ed. London: Academic Press Ltd.; 1990. p. 24.

Paper V

Cement & Concrete Composites 32 (2010) 300–311

Contents lists available at ScienceDirect

Cement & Concrete Composites

journal homepage: www.elsevier.com/locate/cemconcomp

Prediction of potential compressive strength of Portland clinker from its mineralogy

K. Svinning [a,*], A. Høskuldsson [b], H. Justnes [c]

[a] NORCEM A/S, Process and Environmental Department, Brevik, Norway
[b] Centre for Advanced Data Analysis, Eremitageparken 301, 2800 Kgs Lyngby, Denmark
[c] SINTEF Building and Infrastructure, Concrete, Trondheim, Norway

ARTICLE INFO

Article history:
Received 5 February 2009
Received in revised form 15 December 2009
Accepted 15 December 2009
Available online 28 December 2009

Keywords:
Portland clinker
Potential compressive strength
Mineralogy
XRDA
Prediction
PLS

ABSTRACT

Based on a statistical model first applied for prediction of compressive strength up to 28 d from the microstructure of Portland cement, potential compressive strength of clinker has been predicted from its mineralogy. The prediction model was evaluated by partial least squares regression. The mineralogy was described by patterns from X-ray diffraction analysis in the 2θ-regions 29.88–30.70° and 32.90–34.10° (using CuKα-radiation).

It has been shown that prediction of potential compressive strength of clinker up to 28 d from the observed variation in the mineralogy gave a significant variation of the strength at both 1 and 28 d. Sensitivity analysis based on simulation, optimisation and prediction made it possible to study the influence of the mineralogy on the strength in more detail.

1. Introduction

The influence of the characteristics or the microstructure of Portland cement on compressive strength up to 28 d was investigated statistically by Svinning et al. [1] by application of multivariate data analysis, specifically partial least square regression (PLS) analysis. The main groups of characteristics were mineralogy and superficial microstructure represented by curves from X-ray diffraction analysis (XRDA) and differential thermogravimetric analysis (DTGA), as well as particle size distributions. PLS gave maximum explained variance in compressive strength at 1, 2, 7 and 28 d of 93%, 90%, 79% and 67%, respectively. Most of the variance in the compressive strength up to 28 d was explained from the variances of the variables describing the mineralogy and the particle size distribution. The variables describing the superficial microstructure influenced the compressive strength at 28 d less than the compressive strength at 1 d.

Clinkers from four Scandinavian plants were examined with respect to microstructure and cement properties by Svinning et al. [2]. The development of clinker's potential compressive strength up to 28 d was predicted from its microstructure. Two methods were used to characterise the microstructure of clinker, scanning electron microscopy (SEM) and X-ray diffraction analysis (XRDA). When analysing the process condition in a kiln from the microstructure of clinker, it was found that characterisation of the microstructure by SEM gave more valuable information than characterisation by XRDA. The microstructure characterised by SEM reflected different heating and cooling rates, due to the different size of the kilns and the different types of coolers. XRDA of the cement on the other hand, gives satisfactory characterisation of the mineralogy of the clinker part of the cement concerning the prediction of the compressive strength of cement. The mineralogy of the clinker is described in Refs. [1,2] by XRD-profiles in the 2θ – ranges 29.88–30.70° and 32.90–34.10° (using CuKα-radiation).

The mineral composition could be determined by multi-component Rietveld analyses. Instead of including selected parts of the diffractogram, which requires many variables to describe the profiles, only a few variables giving the whole mineral composition would need to be included in PLS. However, the inaccuracy of the amount of a mineral determined by Rietveld analyses will increase as the amount of the mineral decreases. C_3A could also exist as two polymorphs, cubic and orthorhombic, with different reactivity. A total amount of C_3A, as calculated by the Bogue methodology, like for instance 5%, split into polymorphs could lead to a fairly high inaccuracy in the calculation of the amount of each. The benefits of including the XRD-profile as it has been done here are: (a) no information is lost, and (b) any change in structure or unit cell dimensions due to foreign ion contamination or interchange will be detected directly by changes in the position of the respective peaks. Such structural changes of the minerals may influence their reactivity towards water leading to changes in properties like compressive strength up to 28 d as shown by Svinning et al. [2].

* Corresponding author. Tel.: +47 35572314; fax: +47 35570400.
E-mail address: ketil.svinning@norcem.no (K. Svinning).

0958-9465/$ - see front matter © 2009 Elsevier Ltd. All rights reserved.
doi:10.1016/j.cemconcomp.2009.12.004

As discussed in [1], the range $2\theta = 29.88–30.70°$ contains information solely on alite and aphthitalite, $K_3Na(SO_4)_2$ (i.e. other known cement minerals have no reflections in this region). Although the intensities of the two overlapping alite reflections are modest, the domination of this mineral in Portland cement secures a good signal-to-noise ratio for this mineral. Alite is dominating the early strength development, as is well known. One of the strongest reflections of aphthitalite is in the high end of this first XRD region, and it can give valuable information on this easily soluble alkali sulphate. In spite of its low content, aphthitalite can dominate the early pore water chemistry and strongly influence setting time, for instance. The second XRD region of $2\theta = 32.90–34.10°$ is dominated by reflections of C_3A and C_4AF, but it also contains the dominating reflection of the more seldom clinker minerals α'-C_2S and mayenite, $C_{12}A_7$. The common clinker phase belite, β-C_2S, also has a modest reflection in the low end of this region. However, since alite and belite are the only silicate phases, an increase in alite content will lead to a decrease in belite content so an independent control of the latter is not required. Thus, the two selected XRD regions cover the responses for all the important clinker minerals, and they measure more directly the actual content of each mineral since the simple Bogue calculation is at best an indication of the mineral composition.

Knöfel [3] established a formula for predicting compressive strength at 28 d as a function of clinker phases. The strength increased most with the portions of alite and less by the portions of belite and aluminate. The strength decreased with an increase in the portion of ferrite. Lawrence [4] has established a formula for predicting compressive strength at 1 d. The predicted strength increased with the amount of C_3S and decreased with decreasing amounts of C_3A and C_4AF. According to Aldridge [5], the influence of C_3S decreases with increasing age of curing while the influence of C_2S increases. Odler and Wonnemann [6,7] have studied the effect of alkalis on Portland cement hydration. In [6] the effect of alkali oxides incorporated into the crystalline lattice of clinker minerals was studied and in [7] the effect of alkalis present in form of sulfates.

Ono developed methods to interpret kiln conditions and formulae to predict 28-d mortar-cube strength (F28d). Ono's latest formula [8] express *F28d* as a function of alite size, alite birefringence, belite size and belite color. The equation should be modified in case of magnesia content higher than 1.8% and lower than 1.2%. According to Ono [9] the alite birefringence will vary with lattice constants of alite, which again will vary with the amount of SO_3 and magnesia as well as with the burning temperature and hydraulic activity. From this, he concluded that the X-ray powder diffraction analysis may be an alternative method to microscopy with respect to characterising and controlling the quality of clinker. Tricalcium silicate exhibits seven polymorphs depending on the impurities and the temperature: T_1, T_2, T_3 for the three triclinic forms, M_1, M_2, M_3 for the three monoclinic forms and R for the rhombohedral one [10]. The most common modifications are M_1 and M_3. The formation temperature for M_3 is higher than for M_1. Maki and Chromy [11] have shown that M_1 and M_3 can be distinguished by means of birefringence measurements.

Portions of XRD powder patterns of the different modifications of C_3S were presented by Maki and Kato [12]. The 2θ ranges of the patterns being focused were 32–33° and 51–52°. The peak at approximately 32.6° could contribute much for explaining the change in compressive strength from the change in the birefringence of alite. The profile of the peak rather than its position is changing with the modification from M_3 to M_1. The peak position seems, however, to move slightly to a lower 2θ angle with an increase in M_3 and a decrease in M_1. In a XRD powder pattern of cement, the C_3S-peak at 32.6° will overlap a peak of belite, which will make interpretation of the XRD pattern even more complicated. The positions at 2θ angles 30.04° and 32.6° are reported to change simultaneously and similarly [13]. The ranges of 2θ angle 29.92–30.70° and 32.90–34.10° could therefore be defined to contain sufficient information about the structure of alite for predicting potential compressive strength.

Besides ordinary multivariable regression, fuzzy logic [14], stepwise regression [15], genetics algorithms–artificial neural networks (GAs–ANNs) [16], gene expression programming (GEP) and neural networks (NNs) [17] and PLS [2,18–21] have been applied in the evaluation of the model for prediction of cement strength. GAs–ANNs and PLS represent different types of multivariate calibration or modelling with hidden layer or latent variables. In [21], the latent variables were taken into consideration in the sensitivity analysis while in [16] the hidden layers were not. In [21], examples of sensitivity analysis in the form of a simulated variation of a latent variable from which cement properties are predicted are shown. In the [14–17], only variables presenting chemical component composition not the mineralogy of clinker were included in the modelling.

The prediction of potential compressive strength of clinker from the mineralogy was in this work based on a PLS model evaluated for prediction of compressive strength by Svinning et al. [1] from the whole microstructure of the cement. The observation **X**-matrix could be partitioned into the sub-matrices: $\mathbf{X}_{\text{mineralogy}}$, $\mathbf{X}_{\text{part distr}}$, $\mathbf{X}_{\text{superficial micr LT}}$ and $\mathbf{X}_{\text{superficial micr HT}}$ (LT and HT refer to the low and high temperature range differential thermogravimetric analysis (DTGA)) .The potential compressive strength was predicted from an artificial observation matrix where all the variables, except $\mathbf{x}_{\text{mineralogy}}$ presented as the XRD intensities in the two 2θ ranges, were kept constant and equal to their mean values. The number of observations was the same as in the original observation matrix.

The influence of the mineralogy on the potential compressive strength was examined by simulation, optimisation and prediction. The latent structure of XRD intensities is found by evaluating a new PLS model for predicting potential strength from the XRD intensities only. Variation in the intensities was simulated by model-based optimisations of $\mathbf{x}_{\text{mineralogy}}$ to achieve compressive min and max strength at either 1 or 28 d. It was concluded in [21] that the influence of a latent variable on y was much more significant than that of a single x-variable. Optimisation of y constrained by PLS-components will therefore give a more realistic and better solution for implementation in the design of cement and the quality control during production.

Finally, the potential compressive strengths at 1, 2, 7 and 28 d was predicted from the simulated variation in the intensities being a part of a full x-variables observation matrix where all the other x-variables were kept constant and equal to their mean values. This type of sensitivity analysis has been presented by Svinning and Høskuldsson [21,22]. The amounts of Na_2O and K_2O and the ratio Al_2O_3/Fe_2O_3 were included as supplementary variables from the interest of studying the influence of these variables on the structure of the clinker minerals.

2. Methods

2.1. Characterisation of mineralogy of clinker

The XRD analysis was performed on ground clinker. The XRD-profiles consisted of intensities at every 0.02°. The scaling of the intensities and adjustment of the 2θ-position of the diffraction peaks were based on normalisation of the area and adjusting the 2θ-axis to match the diffraction peak at $d = 3.52$ Å for anatase (TiO_2), which was intermixed in an amount of 10 wt.% of the total sample. Examples of diffractograms including the peak of the reference are shown in Fig. 1. To reduce the number of intensities (and

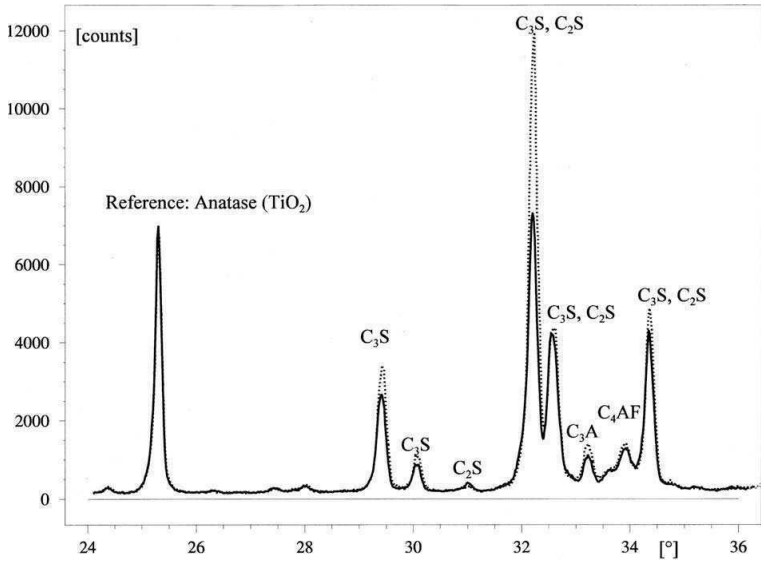

Fig. 1. Examples of X-ray diffractograms of two neat cements in the 2θ range 24–36° (from Ref. [1]).

the number of variables) and simultaneously increase the signal-to-noise ratio, one variable was made out of three by averaging three adjacent variables in the diffraction profile before including the variables in PLS. The number of variables was further decreased by selecting two small regions (2θ) of diffractogram, 29.88–30.70° and 32.90–34.10° (using CuKα-radiation), to be included in the modelling.

The brand of the diffractometer used was Philips X'pert. The TG apparatus applied was a Netzsch STA – Apparatur 409 V/3/C®.

2.2. Evaluation of the prediction model

In cases where the number of variables is large relative to the number of observations or objects, data compression by expressing the original x-variables by fewer latent variables or factors could be necessary. Partial least square regression (PLS) performs calculation and optimisation of a number of factors for maximum explanation of variance in the y-variables. In addition, model parameters are calculated for prediction of y for new values of the x-variables. In this work PLS was performed on several y-variables combined expressed as a vector. The models which relate the PLS model terms are given by the two expressions in the equations below:

$$\mathbf{X} = \mathbf{T}\mathbf{P}^T + \mathbf{E} \tag{1}$$

$$\mathbf{Y} = \mathbf{U}\mathbf{Q}^T + \mathbf{F} \tag{2}$$

T and **U** are factor scores, **P** and **Q** are x and y-variables loadings and **E** and **F** are the residuals in **X** and **Y**, respectively. Alternatively, Eq. (1) could be expressed in the form:

$$\mathbf{X} = \mathbf{t}_1\mathbf{p}_1^T + \mathbf{t}_2\mathbf{p}_2^T + \cdots + \mathbf{t}_a\mathbf{p}_a^T + \cdots + \mathbf{t}_A\mathbf{p}_A^T + \mathbf{E} \tag{3}$$

A is equal to the maximum number of latent variables for maximum explanation of variance in **Y**.

By scaling the variables, unreasonable domination of variables with dominating standard deviations, s(x), on the model can be avoided. The weighting of $x_{i,k}$ by centering and scaling is performed according to the following formula:

$$x_{ik,w} = \frac{x_{ik} - \bar{x}_k}{s(x_k)} \tag{4}$$

The iterative algorithms for calibration, validation and prediction are described in detail in Martens and Næs [23].

2.3. Sensitivity analysis

The type of sensitivity analysis to be applied for examining the influence of x on y depends greatly on the type of modelling applied. In multivariate data analysis like for example PLS, y is correlated to the latent variables which are linear combinations of the x-variables (Eq. (3)). In [3] the variation in y is predicted from simulated variation of a latent variable. The latent variable may be a combination of several original latent variables.

The influence of x-variables on the y-variable(s) may be evaluated by predicting variation in y or y from variation of one latent variable at a time from one 'observed' extreme to the other. By varying the a'th latent variable $\Delta t\ \mathbf{p}_a$ the variation in Δx_k in its original form, i.e. not scaled, can be calculated in the following way:

$$\Delta x_k = (\Delta t p_{ka}) s(x_k) \tag{5}$$

Similar to a type of sensitivity analysis with variation of only one x-variable, the score, t, is varied in one direction and in equal steps, Δt. Calculation of x_j, neither centered nor scaled, will be as follows:

$$x_k = (t p_{ka}) s(x_k) + \bar{x}_k \tag{6}$$

Variation in the whole observation **X**-matrix was usually simulated prior to the prediction by constructing an artificial observation **X**-matrix. In some cases, sensitivity analysis in the form of prediction from simulated variation of a selection or a group of variables could be appropriate.

An influence of one or several x-variables on a y-variable is defined in this work as being significant if there is no overlap of confidence intervals of $\hat{y} \pm 1s(\hat{y}_k)$ of predicted maximum and minimum y, respectively.

The simulation of the variation of the mineralogy, by varying XRD intensities in selected 2θ – ranges, could be based on variation

of one or several latent variables of the XRD intensities. The examination of the influence was carried out in the following way:

In an overall model

$$y = \mathbf{b}^T \left(\mathbf{x}_{\text{mineralogy}} \,|\, \mathbf{x}_{\text{part distr}} \,|\, \mathbf{x}_{\text{superficial micr LT}} \,|\, \mathbf{x}_{\text{superficial micr HT}} \right) + b_0 \tag{7}$$

where the sub-matrices represent the different parts of the microstructure, the examination of the influence of $\mathbf{x}_{\text{mineralogy}}$ on y is carried out by the following procedure:

1. Prediction of $\hat{y}$ from

$$\left(\mathbf{X}_{\text{mineralogy}} (M \times K_{\text{mineralogy}}) \;\middle|\; \begin{matrix} (\bar{\mathbf{x}}_{\text{part distr}})_1 \\ \vdots \\ (\bar{\mathbf{x}}_{\text{part distr}})_M \end{matrix} \;\middle|\; \begin{matrix} (\bar{\mathbf{x}}_{\text{superficial micr LT}})_1 \\ \vdots \\ (\bar{\mathbf{x}}_{\text{superficial micr LT}})_M \end{matrix} \;\middle|\; \begin{matrix} (\bar{\mathbf{x}}_{\text{superficial micr HT}})_1 \\ \vdots \\ (\bar{\mathbf{x}}_{\text{superficial micr HT}})_M \end{matrix} \right)$$

where M is the number of rows in the observation **X**-matrix

2. Revealing the latent structure of $\mathbf{x}_{\text{mineralogy}}$ can be done by evaluating a new model $y = \hat{y} = \mathbf{b}^T (\mathbf{x}_{\text{mineralogy}} \quad \mathbf{x}_{\text{suppl var}}) + b_0$ using PLS. $\mathbf{x}_{\text{suppl var}}$ may contain a few supplementary variables relevant for interpretation of variation in $\mathbf{x}_{\text{mineralogy}}$.
3. Simulation of variation in $\mathbf{x}_{\text{mineralogy}}$ by varying one or several latent variables and establishing an artificial observation matrix $\mathbf{X}_{\text{mineralogy}}(M, \text{art} \times K_{\text{mineralogy}})$ with M, art rows where $M, \text{art} < M$ and $M-1$, art is the number of changes in equal steps of $\mathbf{x}_{\text{mineralogy}}$
4. Prediction of $\hat{y}$ from

$$\left(\mathbf{X}_{\text{mineralogy}} (M, \text{art} \times K_{\text{mineralogy}}) \;\middle|\; \begin{matrix} (\bar{\mathbf{x}}_{\text{part distr}})_1 \\ \vdots \\ (\bar{\mathbf{x}}_{\text{part distr}})_{M,\text{art}} \end{matrix} \;\middle|\; \begin{matrix} (\bar{\mathbf{x}}_{\text{superficial micr LT}})_1 \\ \vdots \\ (\bar{\mathbf{x}}_{\text{superficial micr LT}})_{M,\text{art}} \end{matrix} \;\middle|\; \begin{matrix} (\bar{\mathbf{x}}_{\text{superficial micr HT}})_1 \\ \vdots \\ (\bar{\mathbf{x}}_{\text{superficial micr HT}})_{M,\text{art}} \end{matrix} \right)$$

The simulation was performed by minimizing and maximizing y by application of linear programming. The constraints were given by a latent variable or principal component and lower and upper limits of total variation of **x**. In the simulation above M, art was set equal to 2.

In order to achieve the most optimal solution, several PLS-components could be involved in the optimisation. The "loadings" in the new constraints are linear combinations of the original ones and could be expressed as follows:

$$\mathbf{p}_{\text{combination of several PLS-components}} = \sum_{a=1}^{A} n_a \mathbf{p}_a \tag{8}$$

where $\sum_{a=1}^{A} n_a = 1$ and $0 < n_a < 1$.

The latter constraint prevents absolute values of the scores, |t|, of optimal $\mathbf{x} = (x_1\, x_2 \cdots x_K)$ to be unreasonably high. The model-based optimisation is described in more detail by Svinning et al. [22].

3. Experimental

The types of clinker included in the investigation are applied in the production of the following cements, with reference to European (EN) and in addition Norwegian standards (NS) where they differ by national addendum:

1. Low alkali, sulphate resistant cement, EN 197-1-CEM I 42.5 R, NS 3086-CEM I R-SR-LA
2. Low alkali, high strength cement, EN 197–1-CEM I 52.5 N, NS 3086-CEM I 52.5 N-LA
3. Standard Portland cement, EN 197-1-CEM I 42.5 R
4. Rapid Portland cement, EN 197-1-CEM I 42.5 R, NS 3086-CEM I 42.5 RR.

Table 1 contains the typical mineral composition (calculated from the chemical composition by Bogue's formula) in the clinker used in the different types of cement presented above.

Some of the samples of standard Portland cement, EN 197–1-CEM I 42.5 R, contained limestone filler.

The original observation **X**-matrix consisted of 146 observations and 210 variables. The x-variables were divided into the following groups or categories:

1. Mineralogy of the clinker part of the cement described by X-ray diffractogram sequences (2θ-angle) 29.88–30.70° and 32.90–34.10° (using CuKα-radiation) were taken as variables no. 1–14 and 17–32.
2. Variables no 38–106 and 137–213 were the superficial microstructure of the cement as described by thermograms from DTGA
3. Particle size distribution of the cement were taken into account by variables no. 110–136
4. Variable no. 15–16 consisted of the amount of SO_3 and free lime
5. Variables not included in basic modelling but later included in the sensitivity analysis. These variables were the amounts of K_2O and Na_2O, respectively, and the ratio Al_2O_3/Fe_2O_3.

Table 1
Typical mineral composition of the clinker used in the different types of cement presented above.

Mineral and chemical comp. [%]	Sulphate resistant	High strength	Standard Portland	Rapid Portland
C_2S	16	12	13	12
C_3S	60	66	65	66
C_3A	0.5	6.1	7.7	6.1
C_4AF	15.8	11.0	10.0	11.0
Free lime	0.8	1.1	1.3	1.4
Na_2O-equiv.	0.53	0.55	1.05	1.15

The original y-variables: Compressive strengths at 1, 2, 7 and 28 d, were measured according to EN 196-10. For predicting potential strength of clinker, only the variables describing the mineralogy were varied. The intensity defined to be measured at $2\theta = 29.92^{\circ}$ was the average of the intensities measured at $2\theta = 29.88$, 29.90 and 29.92, the intensity defined to be measured at $2\theta = 29.98^{\circ}$ was the average of the intensities measured at $2\theta = 29.88$, 29.90 and 29.92 and so forth.

The software applied for PLS was Unscrambler version 9.7 and for optimisation OptPilot [22].

4. . Results and discussion

4.1. Prediction of potential compressive strength of clinker from observed mineralogy of the clinker part of the cement

Prior to the investigation of the influence of the mineralogy of the clinker on the compressive strength by sensitivity analysis, the variation of potential compressive strength was predicted from the observed variation in the mineralogy of the clinker part of cement. The significance of the variation of the predictive strength can be studied by comparing the variation in the predicted strength with the standard deviation of each of the predicted strengths. Fig. 2 shows the mean values of the variables describing the particle size distribution of the cement, and Figs. 3 and 4 show the mean values of the variables describing the superficial microstructure. Giving a simpler overview of the variation in the XRD-profiles, every fifth observation is depicted in Fig. 5. To predict the potential compressive strength, the values of the variables describing the other parts of the microstructure were defined and fixed. In this case the values are set constant and equal to their mean values. Fig. 6 shows the regression coefficients **b**: $b_1, b_2, \cdots b_K$ used in the prediction model $y = b_0 + \sum_{k=1}^{K} b_k x_k$ for prediction of the four y-variables for prediction of compressive strength from the XRD-profiles in Fig. 5. Figs. 7 and 8 show the predicted compressive strength at 1 and 28 d, respectively, including confidence intervals of $\hat{\mathbf{y}}_i \pm s(\hat{\mathbf{y}}_i)$.

The confidence intervals of the predicted potential compressive strength of clinker at 28 d are larger than the confidence intervals of the predicted potential strength at 1 d, and also larger relative to the range of variation of the predicted potential compressive strength. This is in accordance with the results in [1] which show that the predicted versus measured compressive strength at 1 d fits the target line (predicted equal to measured) better than the compressive strength at 28 d. There is no overlap of the confidence intervals of minimum and maximum of strengths at either 1 or

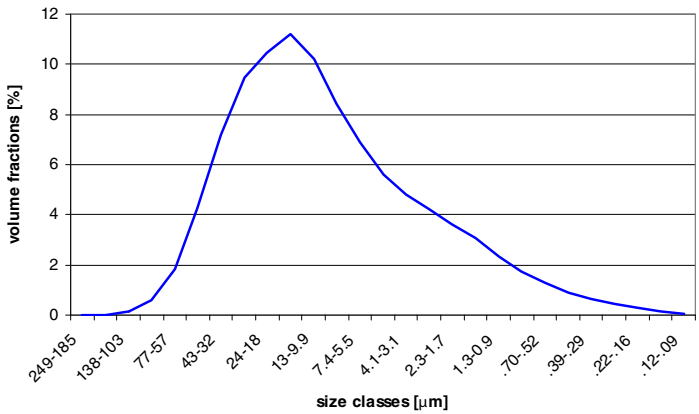

Fig. 2. Mean values of the variables describing the particle size distribution.

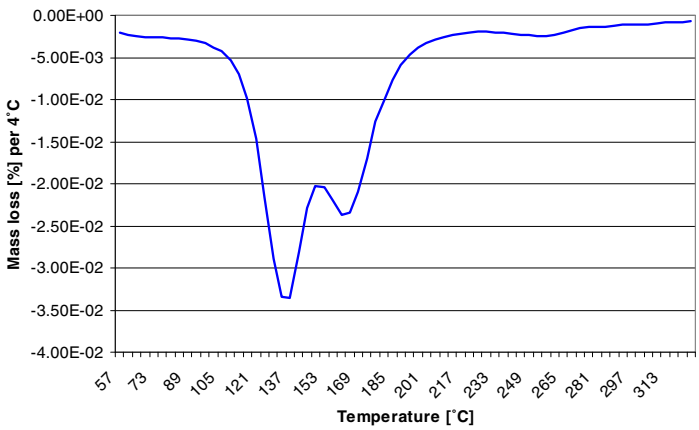

Fig. 3. The mean values of the variables from DTGA, describing the superficial microstructure; the degree of dehydration of gypsum and prehydration of the clinker minerals.

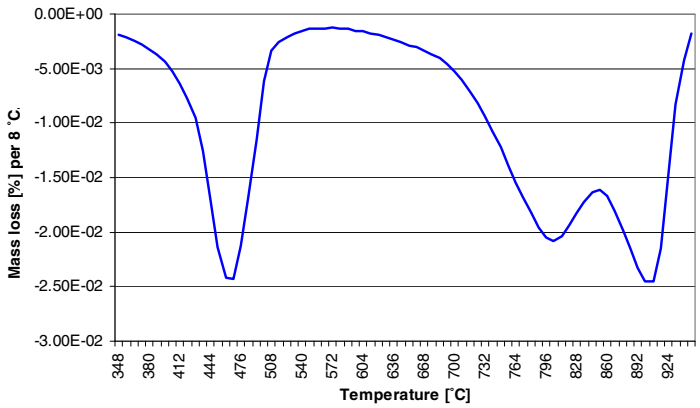

Fig. 4. The mean values of the variables from DTGA, describing the superficial microstructure; the degree of prehydration of free lime, carbonation of $Ca(OH)_2$ and the amount of limestone filler.

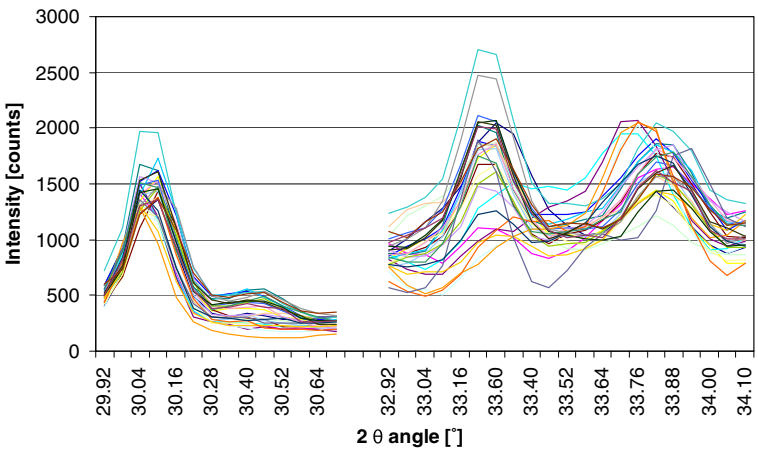

Fig. 5. The mineralogy of clinker described by XRD-profiles in the 2θ – ranges 29.88–30.70° and 32.90–34.10° of every fifth observation of totally 146 observations.

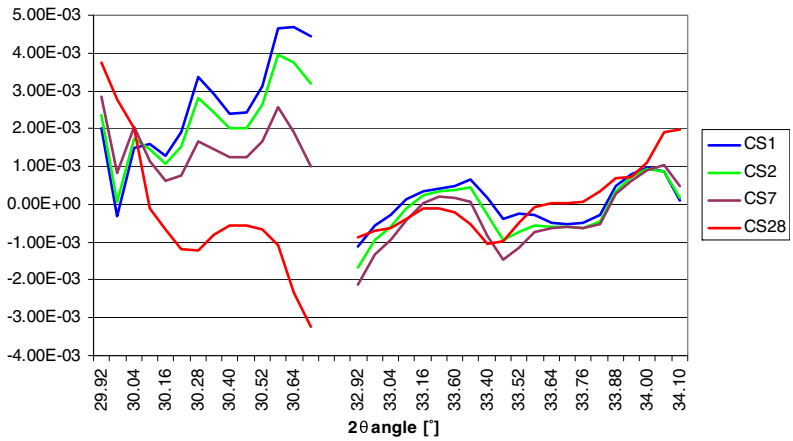

Fig. 6. The regression coefficients for prediction of compressive strength [MPa] at 1, 2, 7 and 28 d from the mineralogy of clinker described by XRD-profiles in the 2θ – ranges 29.88–30.70° and 32.90–34.10°.

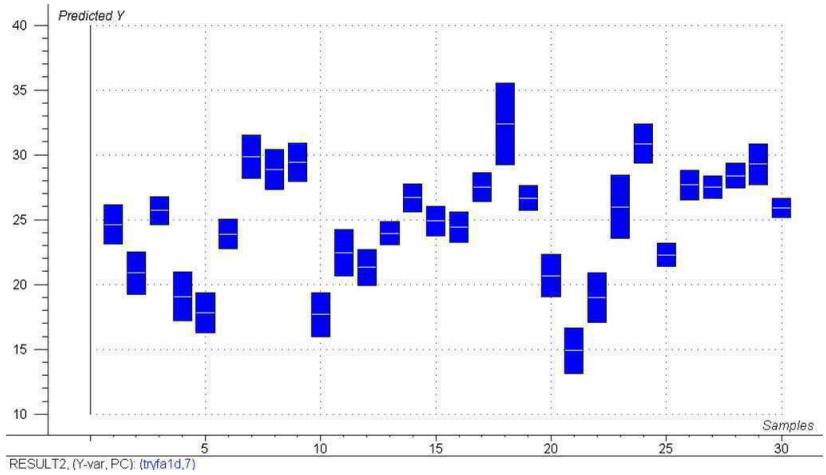

Fig. 7. Potential compressive strength [MPa] of clinker at one day predicted from the XRD-profiles in Fig 4. The confidence intervals of each y_j shown in figure is $\hat{y}_i \pm s(\hat{y}_i)$.

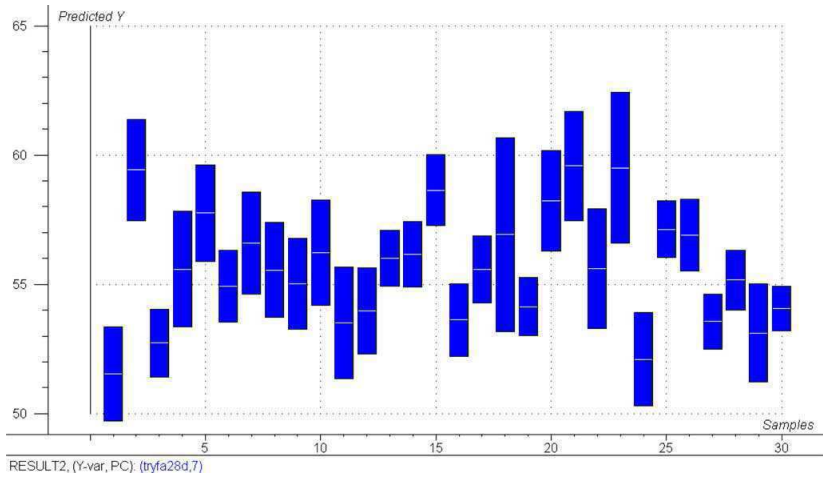

Fig. 8. Potential compressive strength [MPa] of clinker at 28 d predicted from the XRD-profiles in Fig 4. The confidence intervals of each y_j shown in figure is $\hat{y}_i \pm s(\hat{y}_i)$.

28 d, hence the variation in the two strengths predicted from the mineralogy can be said to be significant.

4.2. Examination of the influence of the mineralogy on the potential compressive strength of clinker

Including spectral variables directly in the PLS with no prior quantitative interpretation of the spectra, makes it necessary to base the sensitivity analysis on the variation of latent variables or PLS-components. The varying degree of symmetry in the shapes of the XRD-peaks and the continuity of the XRD-profile should be taken into consideration in the simulation of the variation of the *x*-variables. The fact that the mineralogy of the clinker part in the cement samples can be classified into three or four main groups, constrains the free variation of each clinker mineral. The mineralogy of about 30 out of 146 observations differed from the mineralogy of the main groups. To find the latent structure of the variables $\mathbf{x}_{\text{mineralogy}}$, a new model $y = \hat{y} = \mathbf{b}^T(\mathbf{x}_{\text{mineralogy}} \quad \mathbf{x}_{\text{suppl var}}) + b_0$ was evaluated by PLS2. $\hat{y}$ represent the predicted potential compressive strengths at 1, 2, 7 and 28 d. Some of the predicted potential compressive strengths at 1 and 28 d are presented in Figs. 7 and 8, respectively. $\mathbf{x}_{\text{mineralogy}}$ represents the XRD intensities in the 2θ – ranges 29.88–30.70° and 32.90–34.10° and $\mathbf{x}_{\text{suppl var}}$ contains the supplementary variables, the amounts of Na_2O and K_2O and the ratio Al_2O_3/Fe_2O_3. Fig. 9 shows explained variances in compressive strength at the different ages versus the number of PLS-components included in PLS2. By including predicted values of *y*, the explained variance in compressive strength at all ages was, as expected, close to 100%, in this case by including 5 PLS-components.

The simulation of the variation of the latent variables were carried out by minimizing and maximizing the potential strength at the various ages for an optimum combination of the latent variables, and in other cases the combination of the latent variables were fixed in advance. Out of the four *y*-variables included in the optimisations, one *y*-variable was selected for minimizing and

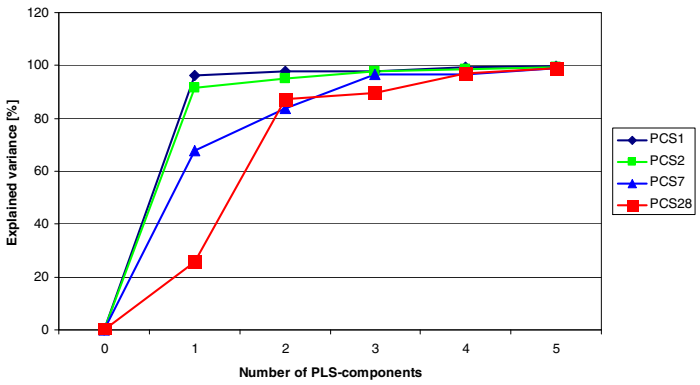

Fig. 9. Explained variances in potential compressive strength of clinker at 1, 2, 7 and 28 d from PLS2 on $\mathbf{X}_{mineralogy}$ and the supplementary variables the amounts of Na_2O, K_2O and the ratio Al_2O_3/Fe_2O_3 versus the number of PLS-components included in PLS2.

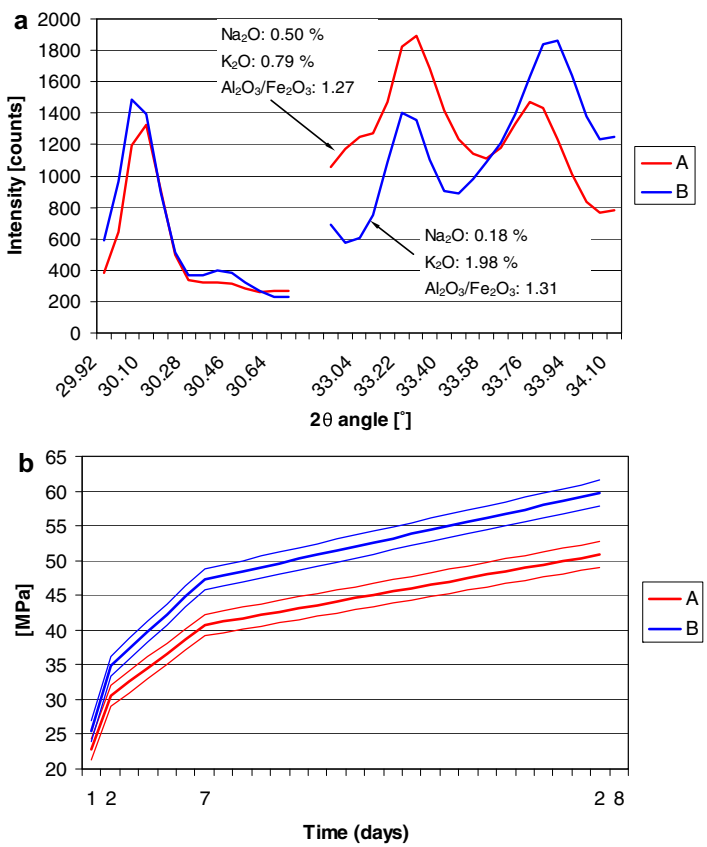

Fig. 10. Minimizing and maximizing potential compressive strength of clinker at 28 d (PCS28). (a) Optimisation of mineralogy of clinker described by the XRD-profiles in the 2θ – ranges 29.88–30.70° and 32.90–34.10° with respect to achieving min (A) and max PCS28 (B). $(n_1, n_2, n_3, n_4, n_5) = (0.001, 0.710, 0.152, 0.098, 0.004)$. (b) PCS at 1, 2, 7 and 28 d predicted from the XRD-profiles in (a). The confidence intervals of $\hat{\mathbf{y}}_i$ is $\hat{\mathbf{y}}_i \pm 1s(\hat{\mathbf{y}}_i)$.

maximizing. The other *y*-variables were predicted from the values of the *x*-variables calculated from the actual combinations of the latent variables.

Studying the explained variance in each of the four *y*-variables versus the number of latent variables included in Fig. 8, most of the explained variance in the potential compressive strengths at 1, 2

and 7 d appear to be explained by three latent variables. Explaining the potential compressive strength at 28 d, the fourth latent variable should be taken into consideration. To be sure that the absolute optimum was obtained, all five latent variables were included in the minimizing and maximizing the strength up to 28 d.

Figs. 10–13a and Fig. 13b show four cases of minimizing and maximizing potential compressive strength of clinker up to 28 d. Limits of variation of the intensities and supplementary variables, x_j, unless constrained by the latent variables, were $\bar{x}_j \pm 1.5\, s(x_j)$. The optimal combination of latent variables (n_1, n_2, n_3, n_4, n_5) is given in each case of optimisation in the respective figures. As a basis for discussing the influence of the mineralogy on the potential compressive strength of clinker in the four cases of optimisation, reflections of the actual minerals in the two selected diffraction angle ranges are presented in Tables 2 and 3.

Maximizing and minimizing the potential compressive strength of clinker at 28 d (Fig. 10b) by varying the mineralogy as shown in Fig. 10a give the least change in the strength at one day. The change in strength will increase gradually up to 28 d. The change in the strength at 28 d is explained to a large extent by the shift in the C_3S-peak from 30.10° to 30.26°, indicating an increase in the amount of polymorph M_3 and a decrease in the polymorph of M_1 of C_3S [6]. M_3 has a higher birefringence than M_1 and by increasing M_3 the birefringence of alite will increase. Ono [8] has predicted the 28 d strength to increase with increasing birefringence. According to Knöfel [3] the 28 d strength increases with increasing amount of C_3S and C_3A. In accordance with [1], a decrease in the amount of C_3A ($2\theta = 33.30°$) and an increase in the amount of C_4AF contribute to an increase in the strength at 28 d. A change in the structure of the C_4AF indicated by a shift in the peak of the mineral from 33.82° to 33.94° will give an increase in the compressive strength at all the actual ages, but the highest increase in the strength occurs at 28 d. A classical example of the change in the structure of C_4AF is the one due to the change in the A/F ratio which can vary over a wide range due to a solid solution of A and F with composition C_2F as an end-point. In Fig. 10a and b, the A/F ratio is nearly constant while Na_2O decreases and K_2O increases when C_3A is decreasing. What impact do K_2O or Na_2O have on the structure of C_4AF? An increase in the amount of K_2O with a simultaneous decrease in Na_2O gives almost no change in the amount of aphthitalite, $K_3Na(SO_4)_2$ ($2\theta = 30.38°$). According to Taylor [24], a decrease in the amount of sodium could change the structure of C_3A from orthorhombic to cubic, giving a shift in the C_3A peak ($2\theta = 33.30°$) to the right. In the case depicted in Fig. 10a and b, the C_3A peak shifts slightly to the left and broadens a little when increasing Na_2O from 0.18% to 0.50%. According to

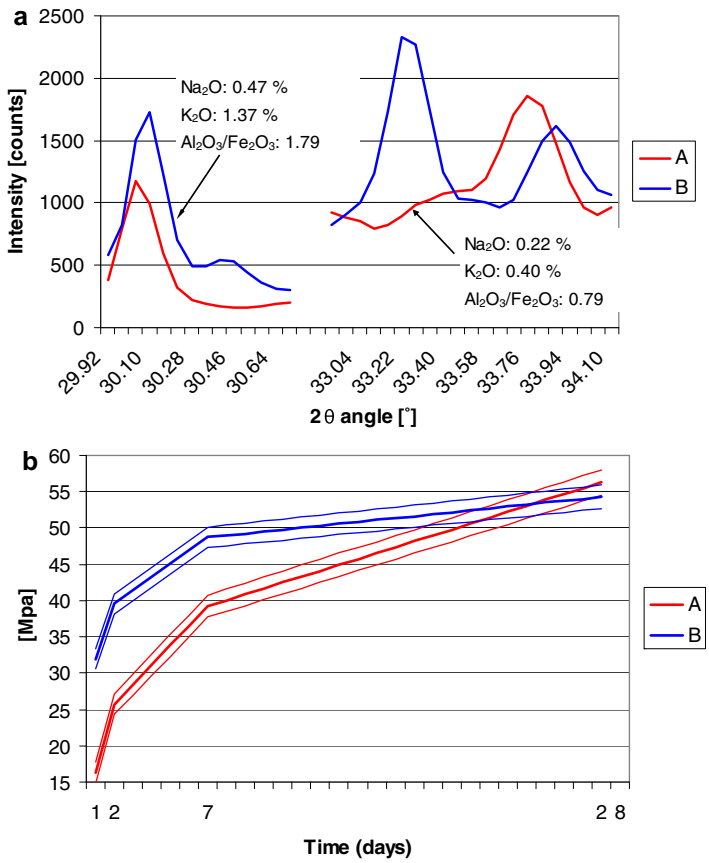

Fig. 11. Minimizing and maximizing potential compressive strength of clinker at 1 d (PCS1). (a) Optimisation of mineralogy of clinker described by the XRD-profiles in the 2θ – ranges 29.88–30.70° and 32.90–34.10° with respect to achieving min (A) and max PCS1 (B). (n_1, n_2, n_3, n_4, n_5) = (0.717, 0.054, 0.090, 0, 0.138). (b) PCS at 1, 2, 7 and 28 d predicted from the XRD-profiles in (a). The confidence intervals of $\hat{\mathbf{y}}_i$ is $\hat{\mathbf{y}}_i \pm 1s(\hat{\mathbf{y}}_i)$.

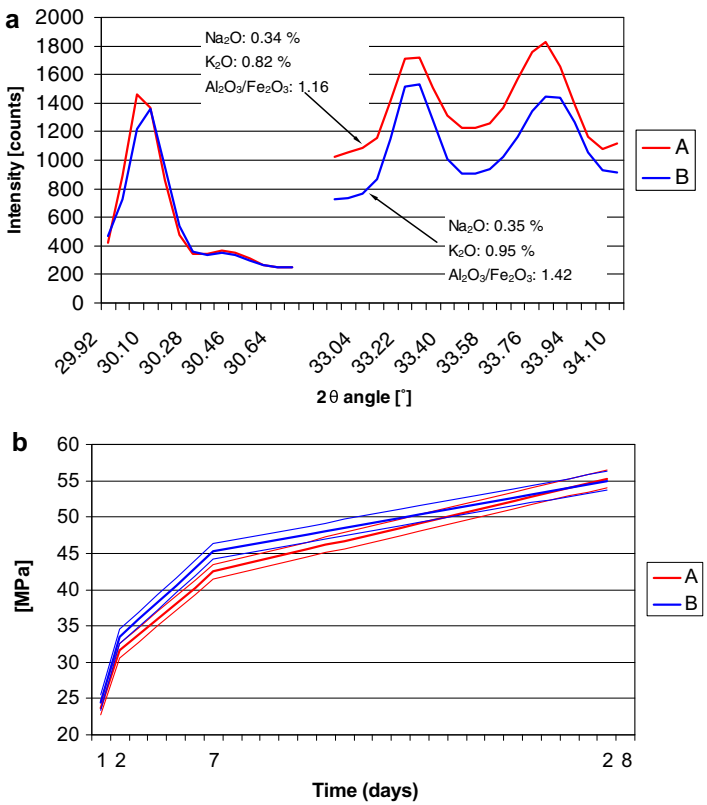

Fig. 12. Minimizing and maximizing potential compressive strength of clinker at 7 d (PCS7). (a) Optimisation of mineralogy of clinker described by the XRD-profiles in the 2θ – ranges 29.88–30.70° and 32.90–34.10° with respect to achieving min (A) and max PCS7 (B). $(n_1, n_2, n_3, n_4, n_5) = (0, 0, 1, 0, 0)$. (b) PCS at 1, 2, 7 and 28 d predicted from the XRD-profiles in (a). The confidence intervals of $\hat{\mathbf{y}}_i$ is $\hat{\mathbf{y}}_i \pm 1s(\hat{\mathbf{y}}_i)$.

Odler and Wonnemann [6] the development of strength is not altered significantly due alkali oxides being incorporated into the crystalline lattice of clinker minerals.

Maximizing and minimizing potential compressive strength of clinker at 1 d (Fig. 11a) by varying the mineralogy as shown in Fig. 11b, give the highest change in the strength at 1 d and no change in the strength at 28 d. Comparing the change in the microstructure described by XRD-profiles with the regression coefficients, $\mathbf{b}_w$, in [1] shows that the increase in compressive strength at one day can be explained by:

- An increase in the amount of and also the shift in the structure of C_3S.
- An increase in the amount of aphthitalite.
- An increase in the amount of C_3A.
- A change in the structure of C_4AF indicated by a shift in the peak to the left.

Lawrence [4] has predicted the strength at 1 d to increase with increasing C_3S but decrease with increasing C_3A. The increase in strength at 1 d with increasing amount of aphtitalite predicted in this work contradicts what is observed by Odler and Wonnemann [7]; a decrease in strength with increases in the amounts of Na_2SO_4 and K_2SO_4 in cement. The change in the mineralogy described by the XRD-profile in the 2θ – ranges 32.90–34.10° is to a large extent identical to the difference in the mineralogy between standard Portland cement and low alkali, sulphate resistant cement [2]. The change in the structure of C_4AF by increasing A/F ratio is evident.

In the case of the optimisation presented in Fig. 12a and b) the combination of latent variables was fixed in advance to $(n_1, n_2, n_3, n_4, n_5) = (0, 0, 1, 0, 0)$. An interesting result is the variation in the potential compressive strength of clinker at 2 and 7 d while no significant change in the potential compressive strengths was found at 1 and 28 d. The change in strength at 2 and 7 d can only be explained by a change in the structure of C_3S and a decrease of C_3A and C_4AF. Aldridge [5] has predicted the strength at 7 d to increase with increases in both C_3S and C_3A. The influence of C_3A on the strength at 7 d is higher than influences on strengths at earlier ages.

In the last case of optimisation (Fig. 13a and b), the amount of Na_2O was kept constant. The optimisation from state A to B gave significant increase in compressive strength at all the ages, but highest increase in the strength at 2 and 7 d. The change in the strength can best be explained by changes in the amount of C_3S, aphthitalite and C_3A. Optimisation by keeping the amount of K_2O and A/F ratio constant gave no change in the mineralogy and consequently no change in the compressive strength at any of the ages.

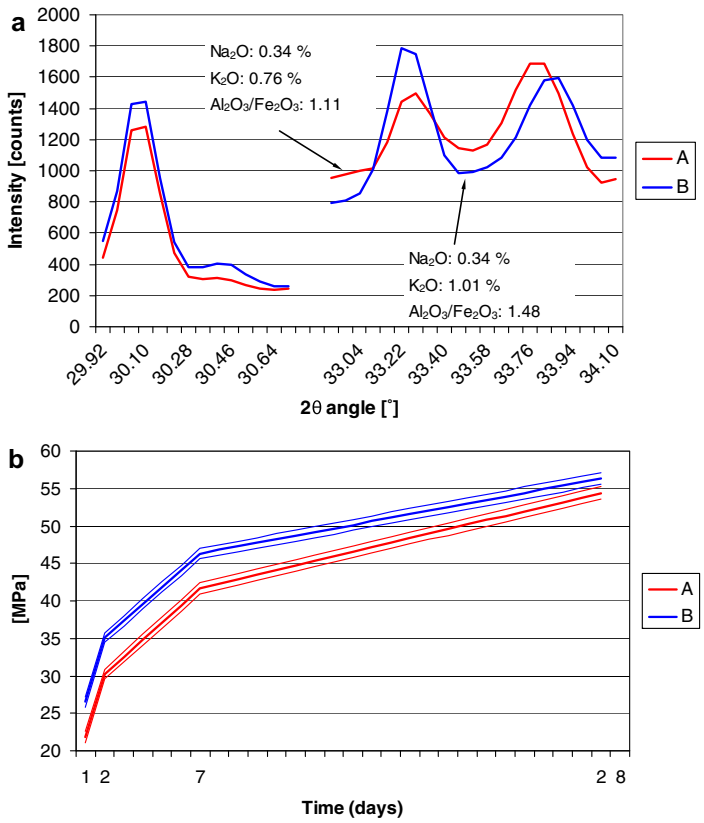

Fig. 13. Minimizing and maximizing potential compressive strength of clinker at 28 d (PCS28), keeping the amount of Na_2O constant. (a) Optimisation of mineralogy of clinker described by the XRD-profiles in the 2θ – ranges 29.88–30.70° and 32.90–34.10° with respect to achieving min (A) and max PCS7 (B). Na_2O was kept constant and equal to 0.34%. $(n_1, n_2, n_3, n_4, n_5) = (0.309, 0.255, 0.167, 0.134, 0.134)$. (b) PCS at 1, 2, 7 and 28 d predicted from the XRD-profiles in (a). The confidence intervals of $\dot{\mathbf{y}}_i$ is $\dot{\mathbf{y}}_i \pm 1s(\dot{\mathbf{y}}_i)$.

Table 2
Major phases within the XRD range $2\theta = 29.88–30.70°$.

Phase	2θ (°)	d (nm)	Indices ⟨hkl⟩	Intensity (rel)
Alite (M_3)	30.04	0.2975	⟨804⟩	10
	30.09	0.2970	⟨620⟩	20
Aphthitalite	30.38	0.2940	⟨102⟩	75

Table 3
Major phases within the range $2\theta = 32.90–34.10°$.

Phase	2θ (°)	d (nm)	Indices ⟨hkl⟩	Intensity (rel)
Belite, β-C_2S	32.98	0.2716	⟨121⟩	38
α′- C_2S	33.65	0.2663	⟨260⟩	100
Cubic C_3A	33.26	0.2694	⟨044⟩	100
Orthorhombic C_3A	33.27	0.2693	⟨224⟩	100
	33.04	0.2711	⟨040⟩	25
	32.93	0.2720	⟨400⟩	31
$C_{12}A_7$	33.41	0.2680	⟨420⟩	100
C_4AF	33.84	0.2649	⟨141⟩	100
	33.64	0.2664	⟨002⟩	47
Gypsum	33.35	0.2684	⟨150⟩ and ⟨220⟩	50

Applying experimental design in the build-up of the observation matrix could reveal to a greater extent the impact of the separate clinker phases on the compressive strength development.

5. Conclusions

Potential compressive strength of clinker can be predicted from the mineralogy of clinker on the basis of a statistical model for prediction of compressive strength up to 28 d from the microstructure of cement.

It has been shown that prediction of potential compressive strength of clinker up to 28 d from the observed variation in the mineralogy gave significant variation of the strength at both 1 and 28 d.

Sensitivity analysis based on simulation, optimisation and prediction made it possible to study the influence of the mineralogy on the strength in more detail.

In minimizing and maximizing the potential compressive strength at one day, the variables describing the amounts of C_3S and aphthitalite were found to be the most influential.

Change in the structure of C_3S indicated by a shift in its XRD-peak in the selected 2θ – ranges influenced the potential compressive strength at 28 d significantly.

References

[1] Svinning K, Høskuldsson A, Justnes H. Prediction of compressive strength up to 28 d from microstructure of Portland cement. Cem. Concr Compos 2008;30:138–51.
[2] Svinning K, Justnes H, Viggh E, Bremseth SK, Johansson S-E. Examination of clinkers from four Scandinavian plants with respect to microstructure and cement properties. In: Proceedings of the 22nd international conference on cement microscopy, Montreal; 2000. p. 137–53.
[3] Knöfel D. Interrelation between proportion of clinker phases and compressive strength of Portland cements. In: Proceedings of the 11th international conference on cement microscopy, New Orleans; 1989. p. 246–62.
[4] Lawrence CD. A study of the microstructure of hardened cement paste by nitrogen and butane sorbtion, PhD thesis, Brunel University; 1981.
[5] Aldridge LP. Estimating strength from cement composition. In: Proceedings of the 7th international congress on the chemistry of cement, Paris; 1980 (Communication: vol. III, VI-83-6).
[6] Odler I, Wonnemann R. Effects of alkalis on Portland cement hydration I. Alkali oxides incorporated into the crystalline lattice of clinker minerals. Cem Concr Res 1983;13:477–82.
[7] Odler I, Wonnemann R. Effects of alkalis on Portland cement hydration. II. Alkalis present in forms of sulfates. Cem Concr Res 1983;13:771–7.
[8] Ono Y. 1995, Presented in Campbell DH, microscopical examination and interpretation of Portland cement and clinker. 2nd ed. Skokie: Portland Cement Association; 1999.
[9] Ono Y. Lattice Constants of alite in plant clinker. In: Review of the 38th general meeting, technical session. Tokyo: The Cement Association of Japan; 1984. p. 28–31.
[10] Dunstetter F, de Noirfontaine M-N, Courtial M. Polymorphism of tricalcium silicate, the major compound of Portland cement clinker, 1. Structural data: review and unified analysis. Cem Concr Res 2006;36:39–53.
[11] Maki I, Chromy S. Characterization of the alite phase in Portland cement clinker by microscopy. Il Cemento 1978;3:301–8.
[12] Maki I, Kato K. Phase identification of alit in Portland cement clinker. Cem Concr Res 1982;12:93–100.
[13] Svinning K, Høskuldsson A. Prediction of potential compressive strength of Portland clinker from production condition cement kiln. J ASTM Int., submitted for publication.
[14] Akkurt S, Tayfur G, Sever C. Fuzzy logic model for the prediction of cement compressive strength. Cem Concr Res 2004;34:1429–33.
[15] Tsivillis S, Parissakis G. A mathematical model for prediction of cement strength. Cem Concr Res 1988;28:9–14.
[16] Akkurt S, Ozdemir S, Tayfur G, Akyol B. The use of GA-ANN in the modelling of compressive strength of cement mortar. Cem Concr Res 2003;33:973–80.
[17] Baykasoglu A, Türkay D, Serkan T. Prediction of cement strength using soft computing techniques. Cem Concr Res 2004;34:2083–90.
[18] Svinning K, Bremseth SK, Justnes H. X-ray diffraction studies on variations in microstructure of Portland clinker correlated with variations in production conditions in the kiln. World Cem 1996:80–6.
[19] Svinning K, Bremseth SK. The influence of microstructure of clinker and cement on setting time and strength development until 28 d. In: Proceedings of 18th international conference on cement microscopy, Houston; 1996. p. 514–13.
[20] Svinning K, Justnes H. Application of partial least square regression analysis in examination of correlations between production conditions, microstructure of clinker and cement and cement properties. In: Proceedings of the 10th international congress on the chemistry of cement, Gothenburg; 1997, li038. p. 8.
[21] Svinning K. Design and manufacture of Portland cement – application of sensitivity analysis in exploration and optimization. Part I: Exploration. J Chemometr Intell Lab Sys 2006;84:177–87.
[22] Svinning K, Høskuldsson A. Design and manufacture of Portland cement – application of sensitivity analysis in exploration and optimization. Part II: Optimization. J Chemometr Intell Lab Sys 2006;84:188–94.
[23] Martens H, Næs T. Multivariate calibration. 2nd ed. Chichester: Wiley; 1989.
[24] Taylor HFW. Cement chemistry. 1st ed. London: Academic Press; 1990. p. 24.

Paper VI

Is not included due to copyright

Paper VII

Is not included due to copyright

Paper VIII

Is not included due to copyright

Paper IX

Is not included due to copyright

Appendix II: A User's Guide to OptPilot

NORCEM
HEIDELBERGCEMENT Group

VEILEDNING I BRUK AV
OPTPILOT

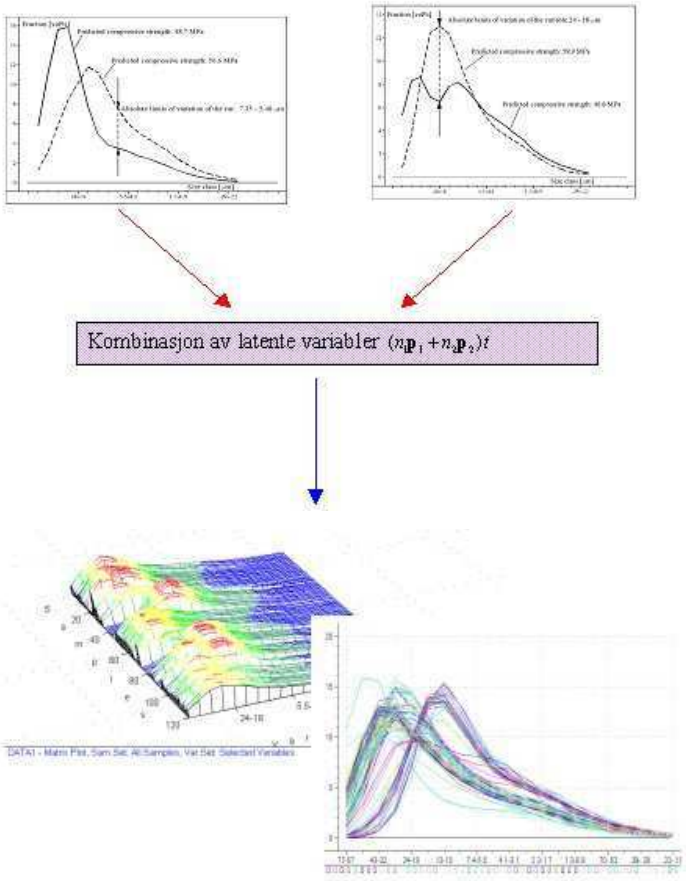

Ketil Svinning

FORORD

Programmet Optpilot er et resultat av arbeidet i delprosjekt: Prosessoptimalisering under hovedprosjektet: Produksjonsforhold / sementegenskaper (P635). Deltakere fra Norcem har vært Øystein Ingerøyen og undertegnede. Vår faste eksterne konsulent og programmerer har vært Kjell Dalsveen. Professor Terje Hertzberg, NTNU, og Agnar Høskuldson, DTU, har bidratt med programkode / program for utførelse av henholdsvis optimalisering ved hjelp av simpleksmetoden og multivariat modellering. Jeg vil takke alle deltakere og bidragsytere for all hjelp i dette arbeidet og den entusiasmen de har vist. Jeg vil også takke prosjektansvarlig Erik Stoltenberg-Hansson og Terje Rønning, leder av Norcem FoU, for deres gode støtte under arbeidet.

Norcem FoU 29.11.02

Ketil Svinning, prosjektleder

INNLEDNING

I forbindelse med produksjon av sement med store kvalitetsvariasjoner er særlig to følgende spørsmål som er aktuelt: Hva er årsaken til kvalitetsvariasjonene? Hvordan skal en finne årsaken til variasjonene, og til slutt hvordan kan vi kontrollere prosessen / produksjonen slik at vi unngår variasjonene? Gjennom tre følgende prosjekter er spørsmålene blitt forsøkt besvart:

- Mikrostruktur, formål: Øke kunnskapen om mikrostruktur i sement før og under hydratasjonen.
- Cemexpo, formål: Basert på kunnskapen fra Mikrostruktur ble sammenhengen mellom produksjonsforhold i ovn, mikrostruktur i klinkerdelen av sementen og sementegenskaper undersøkt. Modellering ble anvendt.
- Produksjonsforhold / sementegenskaper, formål: Hovedmålsetningen med prosjektet er å produsere mer optimale sementer med hensyn til kvalitet og kostnader gjennom en forbedret kontroll av brenselssammensetning og mer aktiv bruk av prosessvariabler.

Det siste prosjektet som avsluttes i løpet av dette året, består av tre delprosjekt: Mølleoptimalisering (Dp1), brenselsoptimalisering (Dp2) og prosessoptimalisering (Dp3). Det dominerende aktiviteten i Dp3 var utvikling av programvare for modellbasert optimalisering, OptPilot.

Modell som anvendes i forbindelse med optimaliseringen, er partiell minste kvadraters regresjon eller på engelsk: Partial least square regression (PLS). I tillegg til å finne sammenhengen mellom y som kan være bindetid, og **x** som kan være prosessvariabler for mølle 5, finner PLS ut hvordan x-variablene varierer i forhold til hverandre. ”Samvariasjon” mellom x-variabler kan utrykkes ved PLS-komponenter eller latente variabler. En mer korrekt betegnelse for det vi ønsker å undersøke ved hjelp av latente variabler, er prinsipale variasjonsretninger i observasjonsmatrisen **X**. Under styring av ovnsprosessen må en operatør ta hensyn til flere ting samtidig for å unngå ustabilitet som for eksempel at ovnen slokner. ”Lovlige” og fornuftige kombinasjoner av endringer av produksjonsvariabler kan utrykkes ved nettopp latente variabler.

OptPilot, optimaliserer y som funksjon av x-variablene. I optimaliseringen tas det hensyn til de latente variablene fra PLS, slik at fornuftige løsninger kan oppnås. Metode som blir benyttet i for optimaliseringen langs en latent variabel er lineærprogrammering, og for å finne den optimale kombinasjonen av latente variabler benyttes en metode som kalles simplex.

De grunnleggende prinsippene for modellering og optimalisering er presentert i Vedlegg 1. Prinsippene er hentet ut fra artikkelen Svinning, K., Ingerøyen, Ø., Dalsveen, K., ”Optimization of a response variable y constrained by principal directions of variations in the observation X-matrix, **J. Chemometrics**, vol.14, 2000, pp.699-709

PRINSIPP

Oppbygging, struktur

Selve programmet for prosessoptimalisering, OptPilot innholder følgende delprogrammer som gjør følgende beregninger / operasjoner:

Mainpilot: Modellbasert optimalisering, minimering eller maksimering av y, langs en utvalgt prinsipal variasjonsretning eller latent variabel. Eksempler på *y*: Bindetid, ett døgns styrke. Eksempler på **x**: Prosessvariabler, variabler som beskriver mikrostruktur i sement som for eksempel partikkelstørrelses-fordeling. Det totale variasjonsområdet for **x** for optimalisering av *y* defineres i dette programmet.

ModelParms: Oppgradering av modell som er lagt som basis for optimalisering langs en prinsipal variasjonsretning.

Optimal: Søk etter den mest optimale kombinasjonen av latente variabler som gir den mest optimale *y*.

Struktur til OptPilot er vist i figur 1.

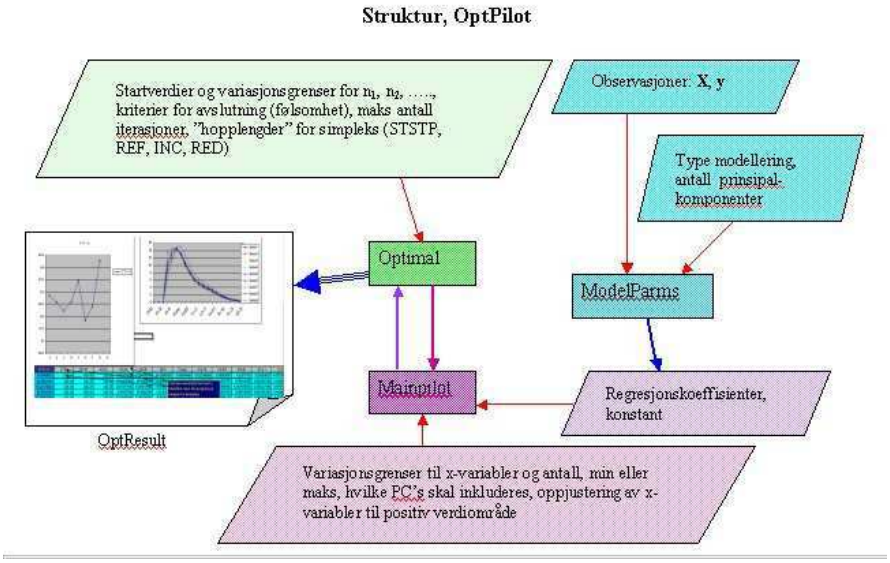

Figur 1.

En mer matematisk versjon er vist i figur 2. Eksemplet i figuren tar utgangspunkt i en modellert sammenheng mellom 28 døgns styrke og partikkelstørrelsesfordelingen. Sammenhengen mellom x-variablene $\mathbf{x} = \{x_1, x_2, \ldots, x_n\}$ og den latente variabelen $n_1\mathbf{p}_1 + n_2\mathbf{p}_2 + \cdots n_l\mathbf{p}_l$ der observasjonsmatrisen **X** i forkant av modelleringen er sentrert og

skalert i henhold til formelen $x_{i\,j,\text{sentrert og skalert}} = \dfrac{x_{i\,j} - \bar{x}_j}{s(x_j)}$ (observasjon nr. i og variabel nr. j), er $\mathbf{x} = (n_1\mathbf{p}_1 + n_2\mathbf{p}_2 + \cdots n_l\mathbf{p}_l)t$. Score, t, er bestemt av tillatt variasjonsområdet for $\mathbf{x}$, i sin opprinnelige form , dvs verken skalert eller sentrert, i optimaliseringen.

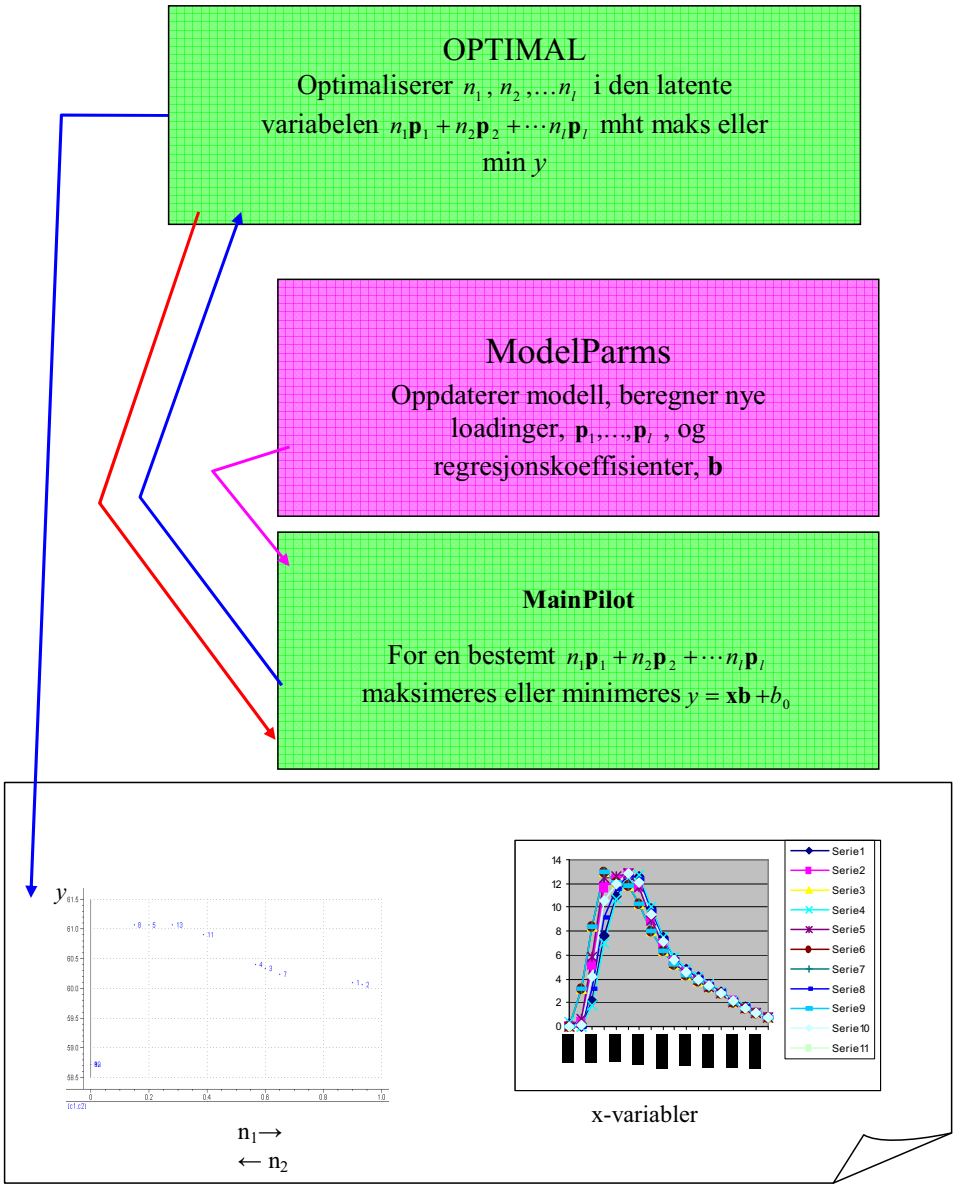

Figur 2.

Tre typer optimalisering er mulig i OPTPILOT

1. Optimalisering langs én prinsipal variasjonsretning eller latent variabel av gangen (nr. 1 og 2 i henholdsvis figur 3 og 4)

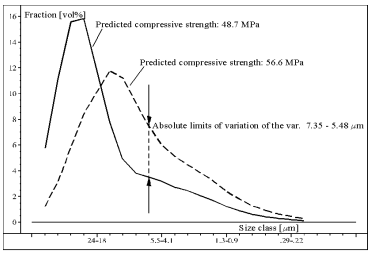

Figur 3.

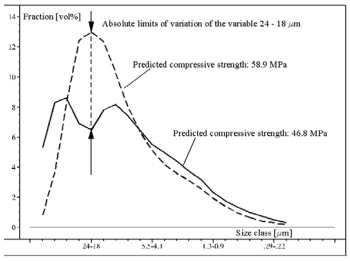

Figur 4.

2. Manuell optimalisering av kombinasjon av prinsipale variasjonsretninger mht å oppnå maksimal styrke

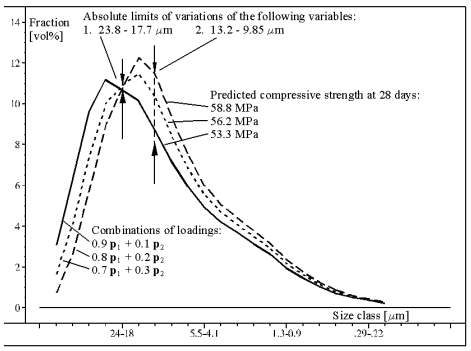

Figur 5.

3. ”Automatisk” optimalisering av kombinasjon av prinsipale variasjonsretning mht å oppnå maksimal styrke

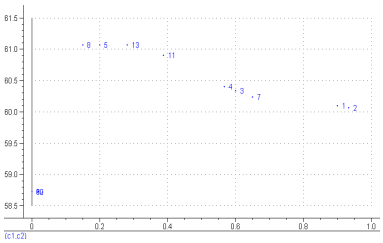

Figur 6.

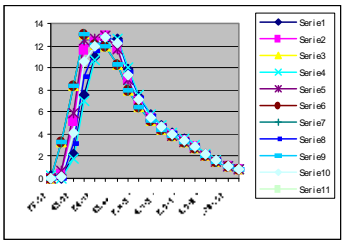

Figur 7.

Beskrankninger

For at optimalisering i *y* skal ha en løsning må tilstrekkelig grenser eller beskrankninger for **x** eller være definert. Et eksempel på optimalisering som kan defineres som et lineær programmeringsproblem i MainPilot er som følger (den engelske teksten er klippet fra /1/):

Having a model $y = b_0 + \sum_{j=1}^{n} b_j x_j$ from PLS on centred and scaled **y** and **X** containing, for example, 4 variables (n = 4), the optimisation of y constrained by one principal component, for example pc 1, could be defined as a following linear program problem:

Find $x_j \geq 0$, j = 1, 2, 3, 4, that will minimise (or maximise)

$$y = b_1 x_1 + b_2 x_2 + b_3 x_3 + b_4 x_4 \qquad \text{Eq. 11}$$

such that

$$\left(\begin{array}{lllll}
p_{2,pc1}s(x_2)x_1 & -p_{1,pc1}s(x_1)x_2 & & = & \bar{x}_1 p_{2,pc1}s(x_2) - \bar{x}_2 p_{1,pc1}s(x_1) \\
p_{3,pc1}s(x_3)x_1 & & -p_{1,pc1}s(x_1)x_3 & = & \bar{x}_1 p_{3,pc1}s(x_3) - \bar{x}_3 p_{1,pc1}s(x_1) \\
p_{4,pc1}s(x_4)x_1 & & -p_{1,pc1}s(x_1)x_4 & = & \bar{x}_1 p_{4,pc1}s(x_4) - \bar{x}_4 p_{1,pc1}s(x_1) \\
\hline
 & x_3 & & \leq & x_{3,upper} \\
 & x_3 & & \geq & x_{3,lower}
\end{array}\right)$$

De tre første beskrankningene begrenser optimaliseringene til langs en rett linje gitt av i dette eksemplet latent variabel nr. 1

De to neste beskrankningene angir hvilken stykke (bare ett (!!)) av linja som det kan optimaliseres langs etter.

$s(x_j)$ is the standard deviation of the variable x_j in its original form, i. e. neither centred nor scaled. The regression coefficient vector $\mathbf{b} = (b_0\ b_1\ \ldots\ b_4)$ is calculated for prediction from the x-variables in their original forms. The constant, b_0, in the model is not included in the optimisation but is added afterwards.

Et eksempel på optimalisering langs en latent variabel er vist i figur 3 og 4. Det bør legges merke til at strengt tatt er beskrankning av kun en x-variabel nødvendig for å få et mulighets-område for optimaliseringen. Dersom det ukritisk settes beskrankning av to variabler eller flere, vil to separate mulighetsområder kunne framkomme i form av to separate stykker på linja. Optimaliseringen vil i så fall ikke ha noen løsning. For å få en mer forståelse kan vi lese videre fra /1/:

To avoid a situation of no solution of the linear programming problem due to an unbounded feasible region at least two other constraints (below the dashed line) should be added to the other. The constraints should give absolute limits of variation (x_{upper}, x_{lower}) for one of the four variables. In this example, the variable x_3 is chosen. If absolute limits of variations of several variables are included as constraints in the optimisation, the constraint for one variable suppresses the variations of the others unless the ranges of the scores, t, of all

$x_j \in (x_{j,\,lower}, x_{j,\,upper})$ are the same. If $(t_{i,\,lower}, t_{i,\,upper}) \cap (t_{j,\,lower}, t_{j,\,upper}) = \emptyset$ for $i \neq j$, the constraints are inconsistent and the linear programming problem has no solution.

Ved "automatisk" optimalisering av kombinasjon av latente variabler, som vist i figur 6, der resultatet ikke er gitt på forhånd, vil det være det være hensiktmessig å operere med generelle grenser for alle variablene. Ved å definere generelle grensene for alle x_j som følger: $\bar{x}_j \pm k\, s(x_j)$ der k er en faktor som kan ha en verdi fra 1 til 2 vil sannsynligheten for inkonsistente beskrankninger, dvs ingen løsning kan oppnås, være liten. En generell begrensning på middelverdi ± 1 eller kanskje opp til 1.5 standardavvik for alle variablene vil i tillegg gi en fornuftig løsning som det er reelt mulig å oppnå. Med utgangspunkt i en modellert sammenheng mellom 28 døgns styrke og partikkelstørrelsesfordelingen i sement er det i figur 8 og 9 vist eksempel på henholdsvis maksimering og minimering av trykkstyrken når x-variablene for lov til å variere ± 1 standardavvik om middelverdi.

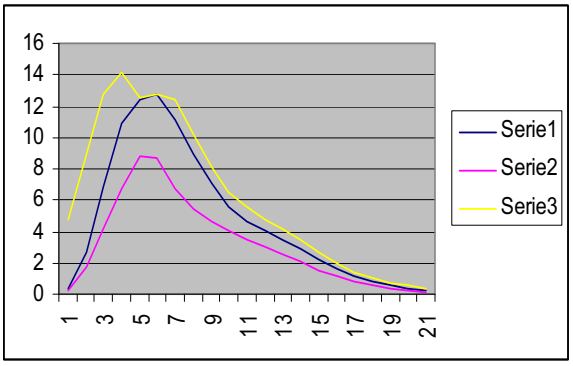

Figur 8. Maksimering av 28 døgns trykkstyrke, y, som funksjon av partikkelstørrelsesfordelingen, **x**, når x-variablene kan variere $\bar{x}_j \pm 1 \cdot s(x_j)$ (mellom gul og rød kurve), Maks trykkstyrke = 59.4 MPa for $n_1 = 0.22$, $n_2 = 0.78$

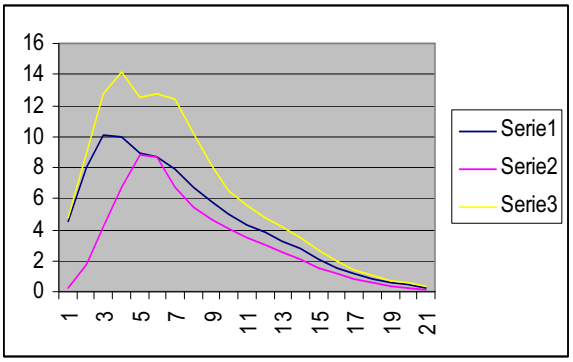

Figur 9. Minimering av 28 døgns trykkstyrke, y, som funksjon av partikkelstørrelsesfordelingen, **x**, når x-variablene kan variere $\bar{x}_j \pm 1 \cdot s(x_j)$ (mellom gul og rød kurve). Min trykkstyrke = 49.6 MPa for $n_1 = 0.22$, $n_2 = 0.78$

Utover en generell beskrankning i x_j på $\bar{x}_j \pm k\, s(x_j)$ kan variasjonsområdet til én variabel knipes inn ytterligere inn uten noen særlig økning i faren for å få inkonsistente beskrankninger. Figur 10 viser et eksempel på optimalisering denne type beskrankninger (sammenlikn figur 10 med figur 8).

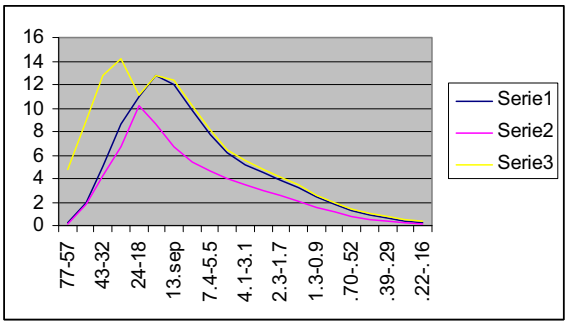

Figur 10. Maksimering av 28 døgns trykkstyrke, y, som funksjon av partikkelstørrelsesfordelingen, **x** (blå kurve) når x-variablene unntatt x_5 kan variere $\bar{x}_j \pm 1 \cdot s(x_j)$ (mellom gul og rød kurve), mens x_5 varierer mellom 10.14 og 11.14 %. Maks trykkstyrke = 58.9 MPa for n_1 = 0.57, n_2 = 0.43.

Optimalisering med negative x-verdier, translasjon av variasjonsområder

I lineær programmering forutsettes det at ingen x_j skal være mindre enn 0. Dette kan være litt upraktisk i tilfeller av prosessvariabler har middelverdi lik null og varierer rundt denne. I eksemplet i figur 11 er de generelle variasjonsgrensene satt lik $\bar{x}_j \pm 2 \cdot s(x_j)$. Selv om nedre grenser er for noen variabler er lavere enn 0 vil x_j aldri bli lavere enn 0.

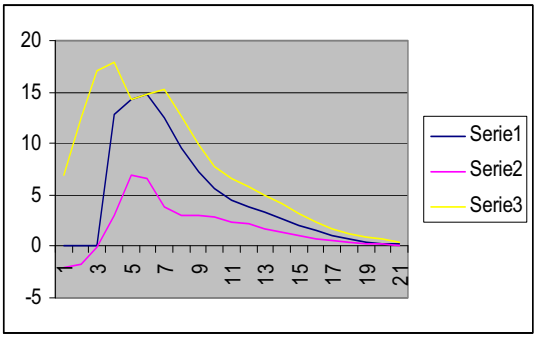

Figur 11. Maks trykkstyrke = 64.3 MPa for n_1 = 0.15, n_2 = 0.85

For å unngå at begrensningen $x_j \geq 0$ skal ha noen innflytelse på resultatene må følgende operasjoner på siden av lineær programmering og som vist i figur 12, utføres:

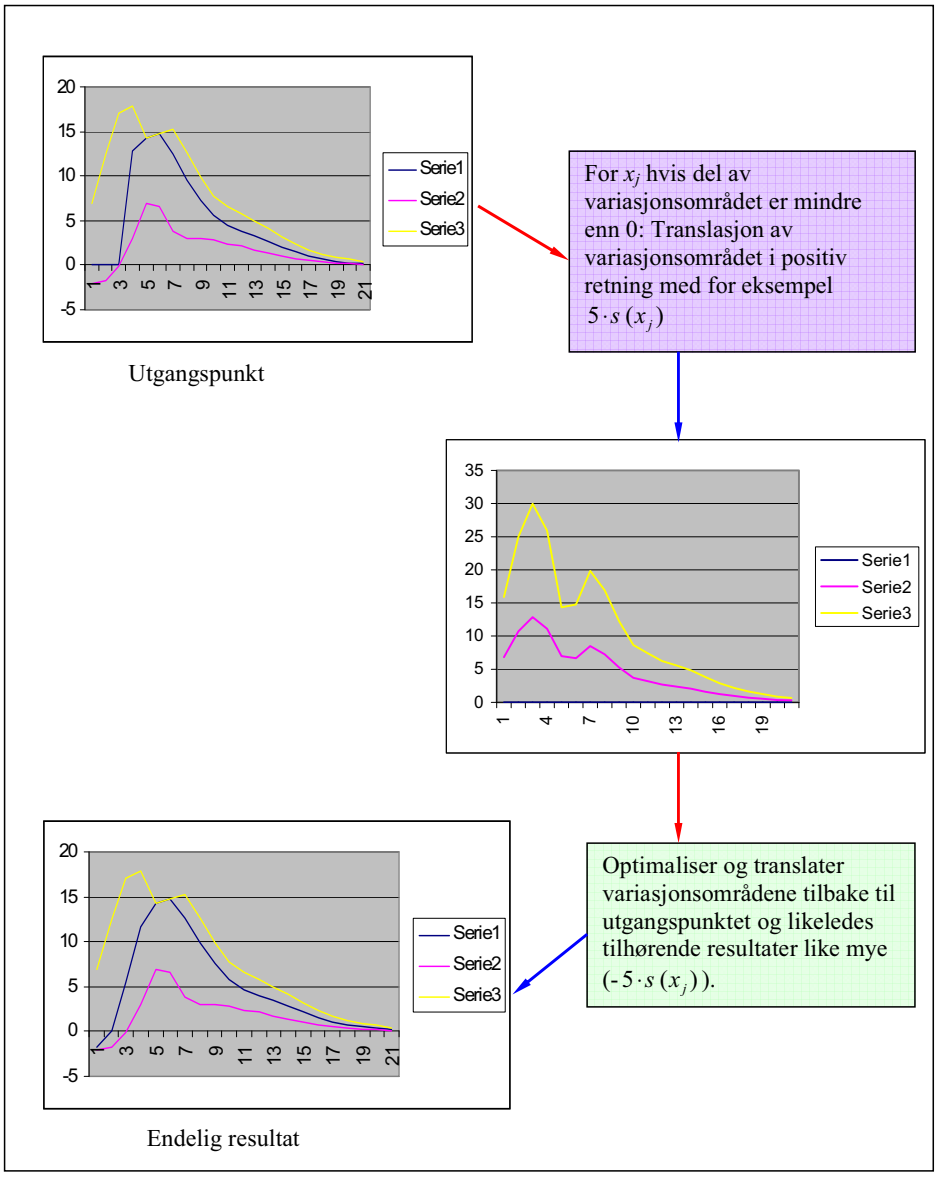

Figur 12

Det må i etterkant gjøres oppmerksom på at optimaliseringen presentert i figur 12 må betraktes som en ren demonstrasjon. Generell fornuft tilsier at ingen størrelsesfraksjon i partikkelstørrelsesfordelingen kan ha en negativ verdi.

Litt om simpleksmetoden for optimalisering

En simpleks er en geometrisk figur med antall hjørner én mer enn antall dimensjoner i det x-rommet det skal optimaliseres i. Simpleks representerer en tangential planar tilnærming til responsflaten til funksjonen $y = f(x_1, \ldots, x_n)$ det optimaliseres på. En ny simpleks kan bli dannet ved å reflektere den forrige simpleks om linja mellom hjørnene som har den høyeste og den nest høyeste verdien (i tilfelle av tre dimensjoner). Operasjonen gjentas til en optimal verdi (minimum eller maksimum y) er funnet. En slik refleksjon kan lett beskrives med figur 13.

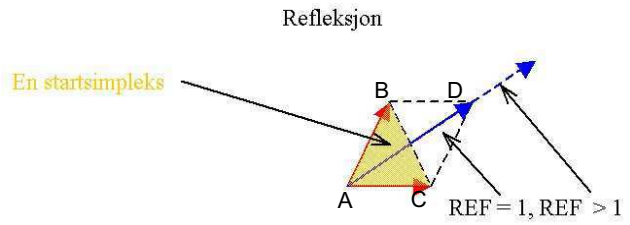

Figur 13.

Ved maksimering har y_A i startsimpleksen lavere verdi enn både y_B og y_C. Vanlig er REF lik 1 ved refleksjon. I Optimal kan REF bestemmes av bruker. Avhengig om y_D er større enn y_B og y_C eller mindre kan refleksjon gjøres <u>om igjen</u> med henholdsvis INC = REF > 1 eller RED = REF < 1. INC og RED legges inn som separate parametrer, i tillegg til REF.

For å visualisere hva som skjer under en slik optimalisering er det vist et eksempel med optimalisering på en responsflate beskrevet med funksjonen
$y = -100 + 4x_1 + 4x_2 + 0.04x_1^2 + 0.04x_2^2$. Grafisk framstilling av funksjon er vist i figur 14.

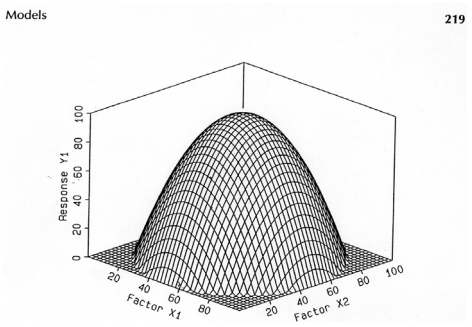

Figur 14.

I figurene under er det vist to eksempler med optimalisering på responsflaten vist i figur 14. I figur 15 er verdier for følgende ”hoppe”-parametre benyttet: REF = 1.0, INC = 0, RED = 0. Dette gir like lange hopplengder. Tilsvarende for figur 16 så er REF = 1.0, INC = 2 og RED = 0.5. I figur 16 brukes det færre steg til for å få en tilnærmet riktig løsning men mange steg til å raffinere løsningen. Antall steg kunne ha vært redusert ved å gi følsomhetsfaktoren EPS som inngår i kriteriet for avbrytelse av optimaliseringen: $|y_{\text{beste}} - y_{\text{nestbeste}}| < \text{EPS} = 0.00001$, en litt større verdi.

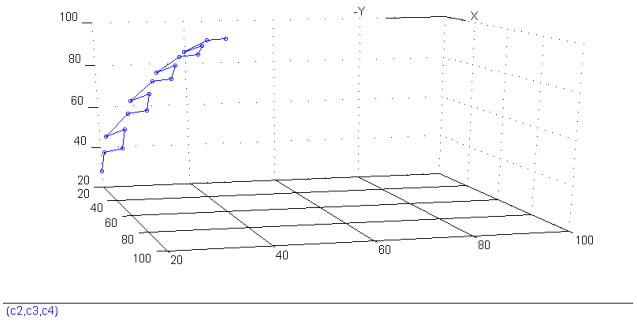

Figur 15.

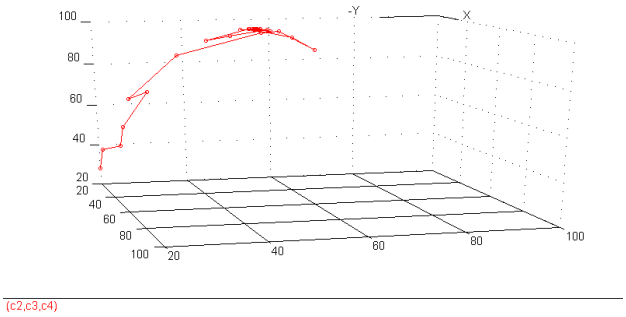

Figur 16.

I OptPilot er funksjon som for eksempel $y = -100 + 4x_1 + 4x_2 + 0.04x_1^2 + 0.04x_2^2$ **erstattet av MainPilot som da ikke er funksjon men en subrutine**. I flere programmeringsspråk håndteres / defineres subrutiner som funksjoner. **I Optimal som kaller opp Mainpilot, er** $x_1, x_2, \ldots$ **erstattet med** $n_1, n_2, \ldots$ **.** Da $\sum_{j=1}^{l} n_j = 1$ reduseres antall dimensjoner i det underrommet av **n** som det optimaliseres i, med 1. *n* er antall latente variabler som inkluderes i optimaliseringen.

PRAKTISK BRUK AV PROGRAMMET. BESKRIVELSER AV SKJERMBILDER.

Mainpilot

Skjermbildet til Mainpilot med forklarende tekstbokser og piler er presentert i figur 18. Plassmangel i figuren gjorde det vanskelig å få med nærmere forklaring om "oppjuster" og manuell optimalisering, kombinasjon av loadings etc. Figur 17 er ment å være et supplement i så måte. Optpilot kan startes fra Mainpilot dersom latent variabel som det optimaliseres langs etter eller en kombinasjon av flere opprinnelige latente variabler er bestemt på forhånd.

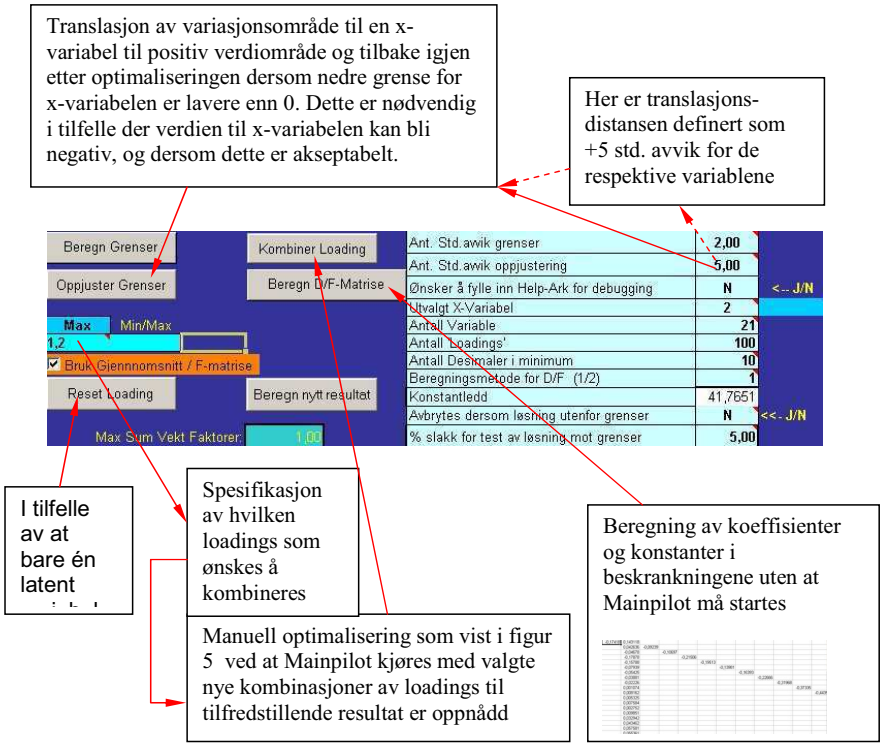

Figur 18. En del av skjermbildet til Mainpilot

Optimal

Øvre del av skjermbildet til Optimal med forklarende tekst og piler er vist i figur 19. Et eksempel på resultat som framkommer på nedre del skjermbildet til Optimal er vist i figur 20. En mer fullstendig presentasjon av resultatene fra Optpilot generert av Optimal finnes på arket Optresult. Et eksempel på Optresult er vist i figur 21.

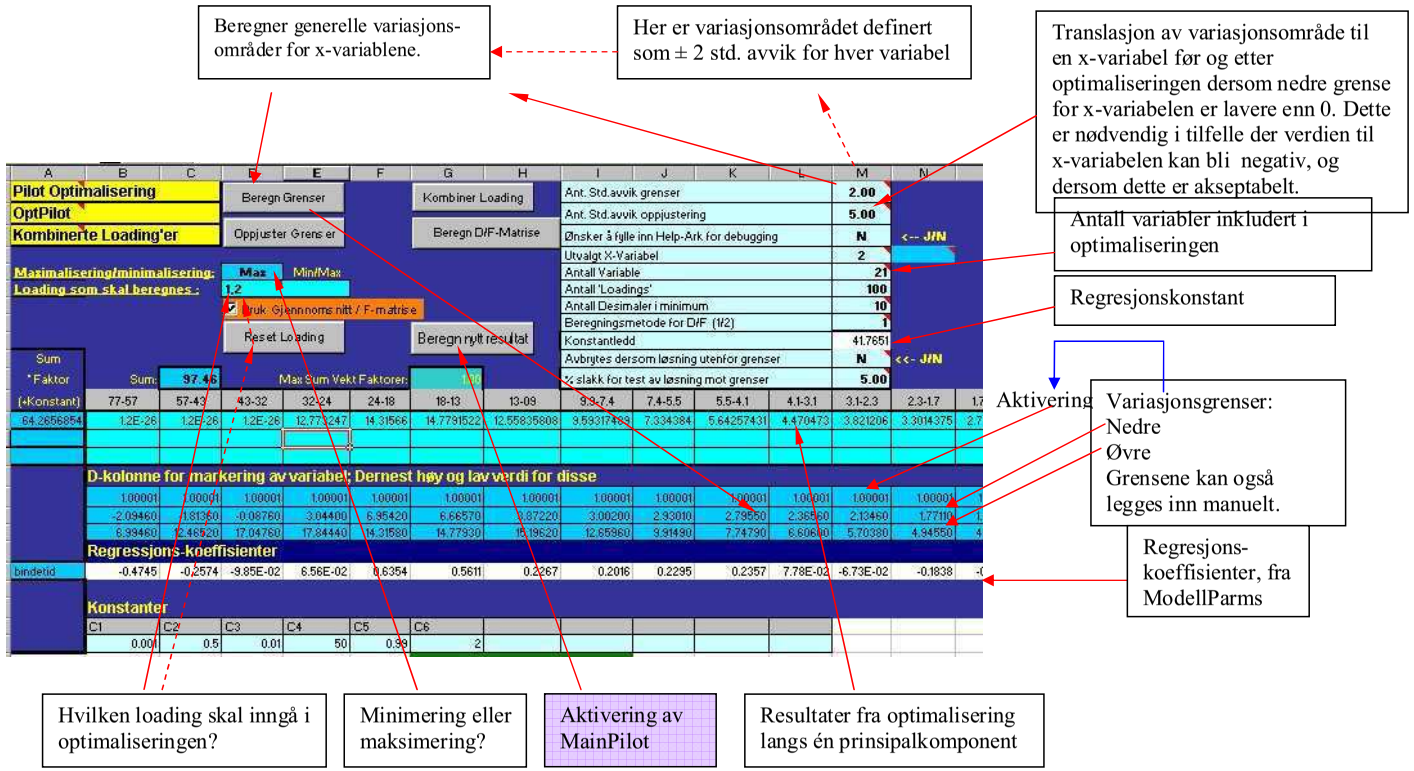

Figur 18. Skjermbildet til Mainpilot

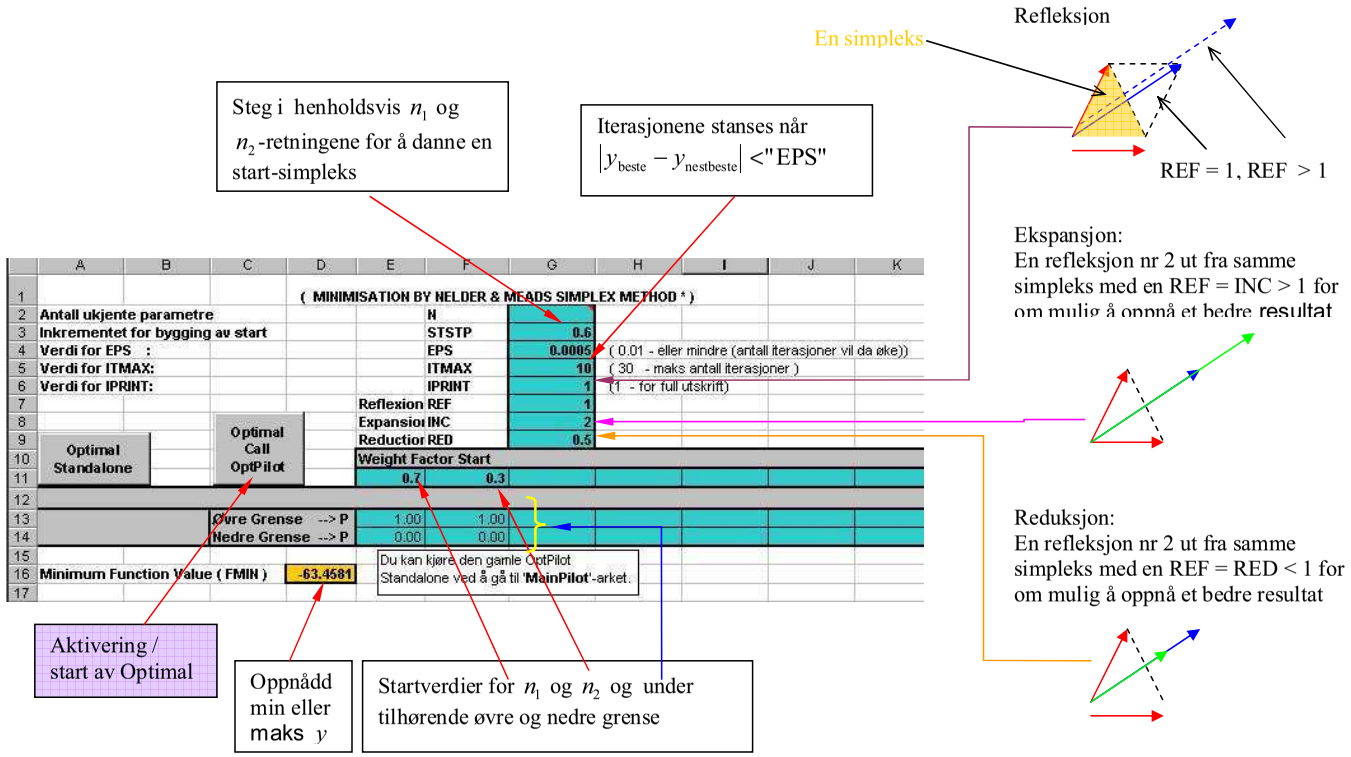

Figur 19. Øvre del av skjermbildet til Optimal

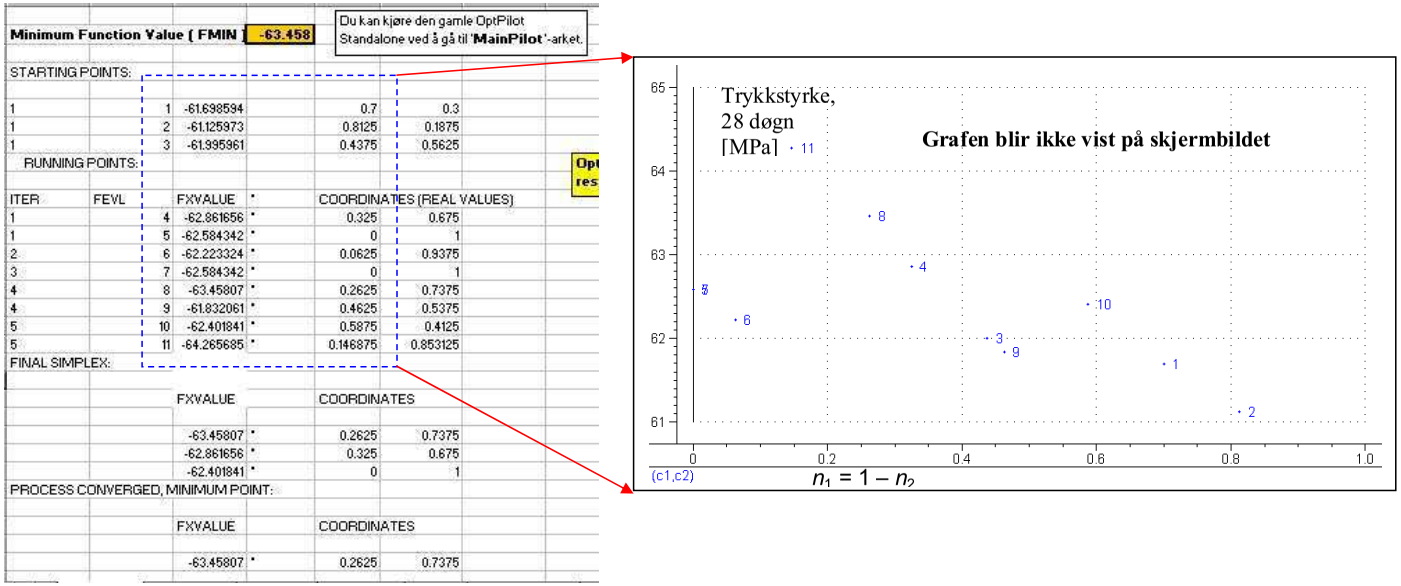

Minimum Function Value (FMIN) -63.458

Du kan kjøre den gamle OptPilot Standalone ved å gå til '**MainPilot**'-arket.

STARTING POINTS:

1	1	-61.698594	0.7	0.3
1	2	-61.125973	0.8125	0.1875
1	3	-61.995961	0.4375	0.5625

RUNNING POINTS:

ITER	FEVL		FXVALUE	*	COORDINATES (REAL VALUES)	
1		4	-62.861656	*	0.325	0.675
1		5	-62.584342	*	0	1
2		6	-62.223324	*	0.0625	0.9375
3		7	-62.584342	*	0	1
4		8	-63.45807	*	0.2625	0.7375
4		9	-61.832061	*	0.4625	0.5375
5		10	-62.401841	*	0.5875	0.4125
5		11	-64.265685	*	0.146875	0.853125

FINAL SIMPLEX:

FXVALUE		COORDINATES	
-63.45807	*	0.2625	0.7375
-62.861656	*	0.325	0.675
-62.401841	*	0	1

PROCESS CONVERGED, MINIMUM POINT:

FXVALUE		COORDINATES	
-63.45807	*	0.2625	0.7375

Figur 20. Nedre del av skjermbildet til Optimal

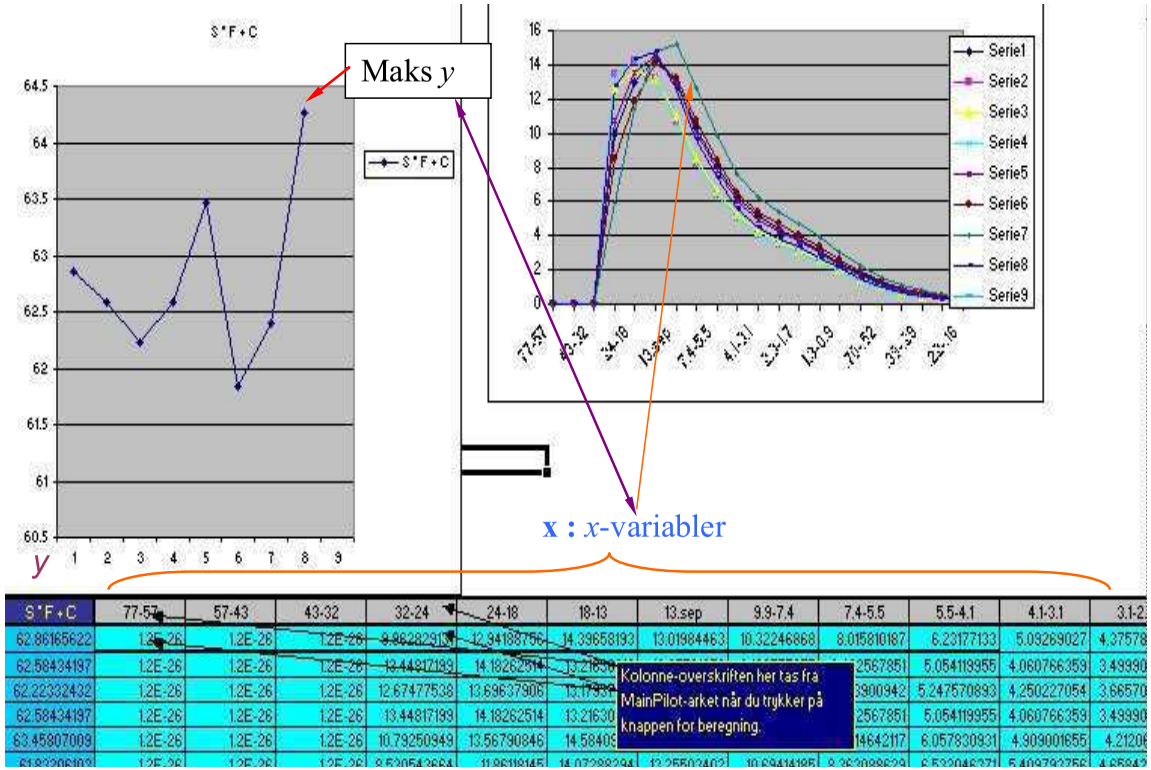

Figur 21. Et eksempel på presentasjon av resultater fra Optpilot på arket Optresult.

Modelparms

Skjermbildet til Modelparms er vist i figur 23. Skjermbildet er mer selvforklarende enn de til MainPilot og Optimal. Noen forklaringer på visse funksjoner er likevel nødvendig. Dataene det modelleres på er lagt på arket partstyrk. Senere vil det bli lagt ut spesielle innlesningsfiler.

Sentrale parameterblokker er "Subset Selection?", "Criterion?", "Select Variables one by one?" og "Specified amount of components to use?". Ved å klikke på hver av blokkene som egentlig står ved siden teksten kommer det opp forklarende tekster. I figur 22 er blokkene tatt ut av figur 23 og koplet sammen med de forklarende tekstene.

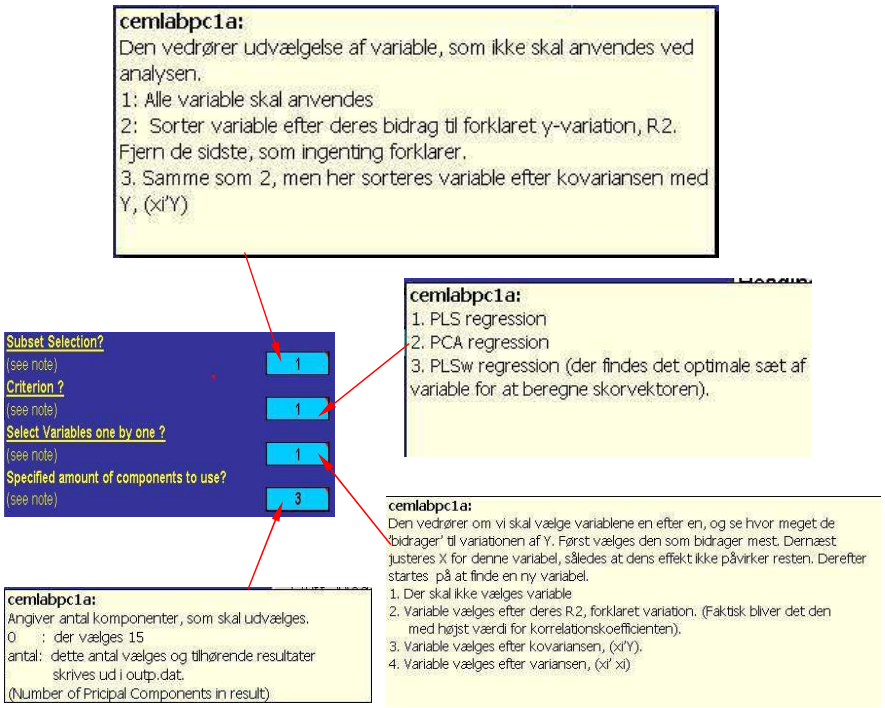

Figur 22.

1 1 1 i de tre første parameterblokkene er et standardoppsett som er brukt hittil. Med hensyn til opplysning som skal legges inn i den fjerde parameterblokken er det viktig at ikke for mange prinsipal komponenter eller latente variabler inkluderes i modelleringen. Modellen i motsatt fall bli nærmest gal med hensyn til prediksjon.

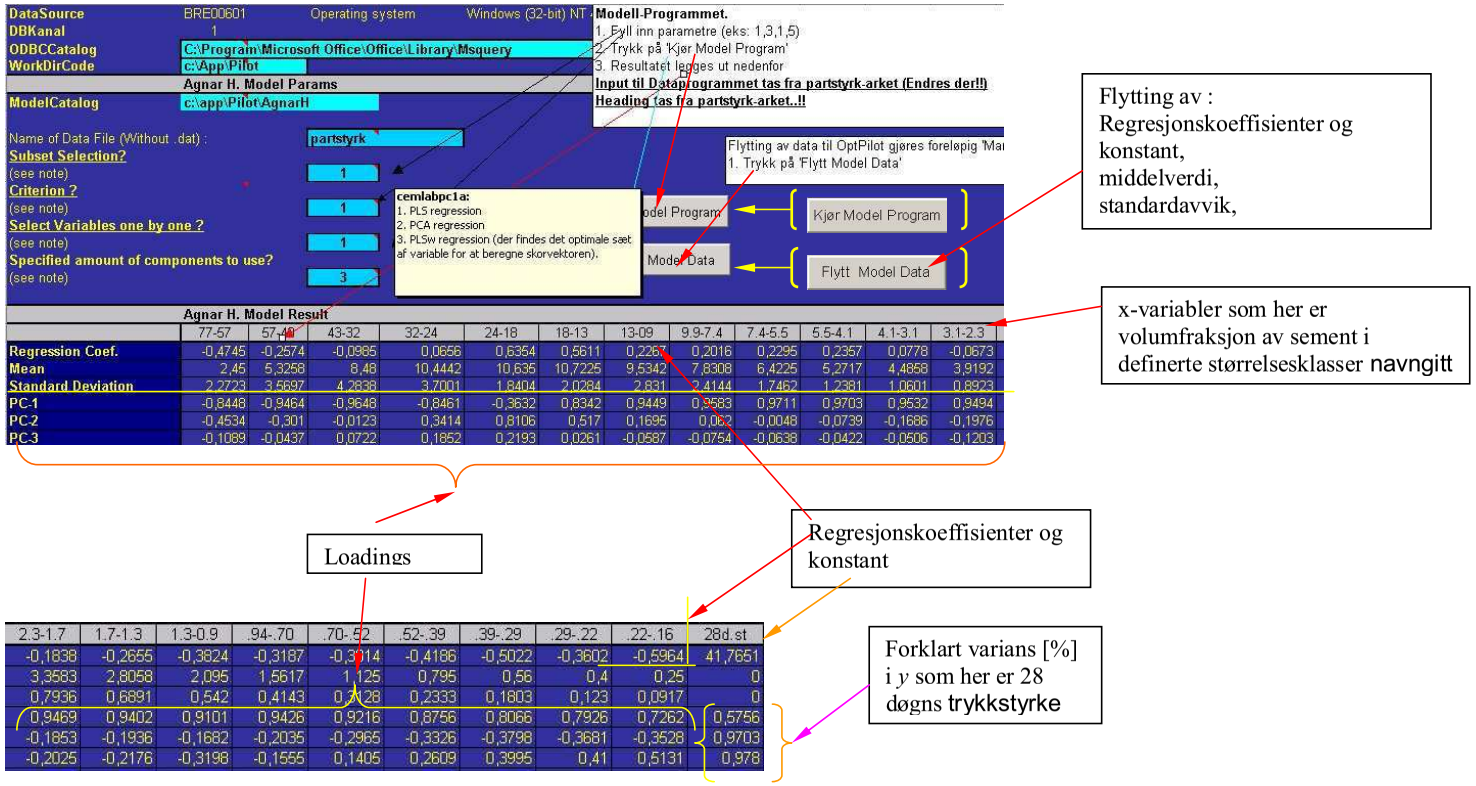

Figur 23. Skjermbildet til Modelparms